Investigations into bioactive natural products from cyanobacteria — a search for drug leads and the discovery of a novel cyanotoxin

Dissertation

zur Erlangung des akademischen Grades
doctor rerum naturalium (Dr. rer. nat.)

der

Naturwissenschaftlichen Fakultät I

Biowissenschaften

der Martin-Luther-Universität
Halle-Wittenberg

vorgelegt

von Steffen Breinlinger

geb. am 10.09.1986 in Tuttlingen

b

Tag der mündlichen Qualifikation: 05.10.2021

Dekan: Prof. Dr. Dietrich Nies

1. Berichterstatter: Prof. Dr. Timo H. J. Niedermeyer

2. Berichterstatter: Prof. Dr. Harald Groß

3. Berichterstatter: Prof. Dr. Peter Imming

Absence of evidence is not evidence of absence.

Summary

Natural products (NPs) have played an important role throughout all of human history. Produced by plants, fungi and bacteria, NPs have been used to treat diseases, improve health and to explore human spirituality. Today, modern drug discovery once again focuses on the vast potential of NPs for new drug leads after pharmaceutical companies briefly shifted their screening campaigns to automated combinatorial chemistry at the end of the 20th century.

Cyanobacteria are among the oldest organisms inhabiting Earth. They occur nearly ubiquitous and thrive successfully in every ecologial niche. However, cyanobacteria have long been neglected by the scientific community in the search for novel NPs and drug leads. In fact, to the general public they are vastly known in the context of harmful algae blooms often producing highly toxic metabolites, threatening wild animals and humans alike. Indeed, cyanobacteria are gifted organisms when it comes to the production of chemically diverse, bioactive metabolites — finally, this has been realized by the scientific community searching for new drug leads in the last 30 years, and the pipeline of clincial and preclinical cyanobacterial compounds is promising!

The vast potential of cyanobacteria for producing bioactive metabolites was the inspiration for the reseach presented in this thesis. It consists of three independent research articles describing the successful isolation and characterization of immunomodulating indole alkaloids (1), several Pan-Assay-Interfering-Compounds (2), and a novel potent neurotoxin responsible for a deadly wildlife disease (3).

(1) A screening campaign of 575 cyanobacterial extracts for immunomodulating agents resulted in the identification, isolation and characterization of 5 hapalindoles from the cyanobacterium *Hapalosiphon* sp. CBT1235 responsible for the immunomodulatory effect observed. For the first time hapalindole A-formamide and hapalindole J-formamide were isolated from a natural source along the known derivatives hapalindoles A, D, and M, providing valuable insight in the structure-

activity relations regarding the immunomodulatory activity (retardation of T-cell proliferation) of hapalindoles: while hapalindole A was the most potent compound and induction of T-cell apoptosis was observed only at 10-fold higher concentrations, the formylated derivatives had a much lower overall activity and less specificity for anti–proliferative over apoptotic effects.

(2) Many bioactive metabolites isolated from cyanobacteria are protease inhibitors. In a similar screening campaign of a cyanobacterial extract library a medium extract of *Nostoc* sp. CBT1153 was found to exhibit a high activity against trypanosomal cystein protease rhodesain, a potential target for the treatment of the human African trypanosomiasis (HAT), also known as sleeping sickness. We identified the homodimeric cyclopentenedione (CPD) nostotrebin 6 and new related monomeric, dimeric, and higher oligomeric compounds as the active substances. Earlier studies found nostotrebin 6 to be active in a variety of different bioassays. However, to us this broad activity was an indication that we are actually dealing with a pan-assay interference compound (PAIN). By comparing the anti–bacterial and cytotoxic activities, as well as the rhodesain inhibition of the newly isolated CPDs we were able to refute the former hypothesis which postulated the chemically reactive CPD substructure to be responsible for the broad bioactivity spectrum. A newly isolated compound with a δ-lactone core structure was equally potent as nostotrebin 6 with its CPD core structure, while a newly isolated monomer displayed a weaker activity. Our findings suggest that the bioactivities rather depend on the number of free phenolic hydroxy groups per molecule. Nostotrebin 6 and its derivatives get actively secreted into the culture medium — based on this fact we discuss possible physiological roles of CPDs including protective functions against bacterial and fungal pathogens, and/or protection against UV irradiation.

(3) Vacuolar Myelinopathy (VM) is fatal neurological wildlife disease that has first been described in 1994 during a mass mortality event among bald eagle populations in Arkansas, US. The mysterious disease has since then spread throughout the southeastern United States and its cause eluded scientists for decades. Earlier studies have linked VM to the cyanobacterium *Aetokthonos hydrillicola* growing on an invasive aquatic plant (*Hydrilla verticillata*) in man-made waterbodies. Laboratory cultures of *A. hydrillicola* did not elicit VM in an avian trial. However, mass spectrometry imaging analysis of colonized *H. verticillata* leaves collected from VM positive reservoirs revealed a polybrominated metabolite co-localizing with

bacterial colonies of *A. hydrillicola*. In this publication we provide the final evidence that VM is caused by a novel cyanobacterial neurotoxin, a pentabrominated biindole alkaloid. After addition of potassium bromide to the cultivation medium, *A. hydrillicola* did produce the elusive toxin which we named Aetokthonotoxin (AETX). After isolation and structure elucidation, a subsequent avian bioassay was conducted and proved the toxin to be the causative agent for VM. In addition, we identified the AETX biosynthetic gene cluster, and provide first mechanistical insights in the biosynthesis. Seasonal environmental conditions, bromide availability and anthropogenic influence, promoting toxin production, are discussed.

In each of the three research articles novel cyanobacterial natural products have been discovered, isolated, their structures elucidated, their toxicity/bioactivity assessed, and their ecological role for the producing organism discussed. State-of-the art technologies in analytical chemistry (e.g. HPLC, (Imaging-)Mass Spectrometry, NMR), preparative isolation techniques, small to large scale cultivation approaches, and functional genomics were used to achieve these results.

Zusammenfassung

Naturstoffe haben seit jeher eine wichtige Rolle für die Menschheit gespielt und Kulturen, wie Gesellschaften nachhaltig geprägt. Produziert von Pflanzen, Pilzen und Bakterien, werden Naturstoffe bis heute verwendet, um Krankheiten zu behandeln, die Gesundheit positiv zu beeinflussen und um spirituelle und außergewöhnliche Bewusstseinszustände zu erforschen. Nachdem die pharmazeutische Industrie beginnend in den 80er Jahren ihre Wirkstoffentwicklung hauptsächlich auf automatisierte chemisch-kombinatorische Synthese ausgerichtet hat, besinnt sich die moderne Arzneimittelentwicklung wieder vermehrt auf das große Potential von Naturstoffen als neue Leitsubstanzen.

Cyanobakterien gelten als die ältesten, die Erde bewohnenden Organismen und haben sich erfolgreich an fast jede ökologische Nische auf diesem Planeten angepasst. Trotzdem wurde Cyanobakterien von der Wissenschaft bei der Suche nach neuen Naturstoffen und Leitsubstanzen lange Zeit keine Aufmerksamkeit geschenkt. Der breiten Öffentlichkeit sind Cyanobakterien hauptsächlich ein Begriff im Zusammenhang mit sich plötzlich stark vermehrende Algenpopulationen (Algenblüten), welche dabei oft für Menschen und Tiere hochgiftige Metabolite produzieren. Cyanobakterien sind talentierte Produzenten von chemisch diversen, bioaktiven Metaboliten — die moderne Wirkstoffentwicklung hat dieses Potential realisiert und die Entwicklungspipeline von Substanzen in (prä-)klinischen Phasen ist vielversprechend. Das große Potential von Cyanobakterien bioaktive Metabolite zu produzieren, stellte die Inspiration für die vorliegende Arbeit dar. Insgesamt drei unabhängige Publikationen beschreiben die erfolgreiche Isolierung und Charakterisierung von immunmodulierenden Indolalkaloiden (1), mehreren Pan-Assay-Interferenz-Substanzen (2), sowie von einem neuartigen, hochtoxischen Nervengift, das für ein Wildtiersterben im Südosten der USA verantwortlich ist (3).

(1) 575 Extrake von Cyanobakterien wurden auf ihren immunmodulierenden Effekt hin analysiert. Aus dem Stammes *Hapalosiphon* sp. CBT1235 konnten 5 Hapalindole isoliert und charakterisiert werden, welche für den beobachteten immunomodulierenden Effekt verantwortlich waren. Zwei dieser Substanzen, Hapalindol A-Formamid und Hapalindol J-Formamid, sind neue Naturstoffderivate der großen Hapalindol-Familie, aus der drei weitere bereists bekannte Derivate isoliert wurden: Hapalindole A, D und M. Die Untersuchung dieser Substanzen

in dem T-Zell-Proliferations-Assay ermöglichte wertvolle Einsichten in Struktur-Wirkungsbeziehungen hinischtlich der immunomodulierenden Eigenschaften von Hapalindolderivaten: Während Hapalindol A die größte Aktivität (Hemmung der T-Zellproliferation) zeigte und erst bei 10-fach höherer Konzentration Apoptose auslöste, wirkten die Formamid-Varianten weniger selektiv (Vergleich anti–proliferierender Effekt und Apoptoseinduktion) und zeigten eine geringere Gesamtaktivität.

(2) Viele cyanobakterielle Metabolite sind Proteaseinhibitoren. Auf der Suche nach neuen Inhibitoren der Cystein-Protease Rhodesain, ein potentielles molekulares Ziel zur Behandlung der afrikanischen Trypanosomiasis, auch bekannt als Schlafkrankheit, konnte ein hoch-aktives Mediumextrakt des Stammes *Nostoc* sp. CBT1153 identifiziert werden. Durch die anschließende Bioaktivitäts-geleitete Isolierung konnten das homodimere Cyclopentendion (CPD) Nostotrebin 6 und neue verwandte monomere, dimere und höher-oligomere Derivate isoliert und charakterisiert werden. Vorherige Studien attestierten Nostotrebin 6 Aktivitäten in mehreren verschiedenen Bioassays. Für uns war diese unspezifische, breite Aktivität allerdings ein Indiz für eine Pan-Assay Interferierende Substanz (PAIN). Durch das Vergleichen der anti–bakteriellen und zytotoxischen Aktivitäten, sowie der Rhodesain Inhibition der neu isolierten CPDs konnten wir die ursprüngliche Hypothese, welche die chemisch reaktive CPD-Substruktur für das breite Aktivitätsspektrum verantworlich machte, widerlegen. Eine neu isolierte Substanz mit einem δ-Lakton-Grundgerüst war gleichermaßen wirksam wie Nostotrebin 6 mit seinem CPD Grundgerüst, wohingegen ein neu isoliertes Monomer eine geringere Aktivität aufwies. Unsere Ergebnisse deuten darauf hin, dass viel eher die Anzahl freier Hydroxygruppen pro Molekül für die unspezifischen Bioaktivitäten verantwortlich sind. Nostotrebin 6 und seine Derivate werden aktiv in das Kulturmedium sekretiert, wir diskutieren deshalb mögliche physiologische Funktionen der CPDs, einschließlich Schutz vor bakteriellen und pilzlichen Pathogenen und/oder UV-Schutz.

(3) Vakuoläre Myelopathie (VM) ist eine tödliche neurologische Erkrankung bei Wildtieren, welche 1994 während eines Massensterbens von Weißkopfseeadler-Populationen in Arkansas, USA, zum ersten Mal beschrieben wurde. Die mysteriöse Erkrankung hat sich während der letzten Jahrzehnte konstant in den südöstlichen Bundesstaaten der USA verbreitet und ihre Ursache Wissenschaftler bis jetzt

vor ein Rätsel gestellt. Frühere Studien haben VM mit dem Cyanobakterium *Aetokthonos hydrillicola* in Verbindung gebracht, welches in künstlichen Seen auf der invasiven Wasserpflanze *Hydrilla verticillata* wächst. *A. hydrillicola* Laborkulturen verursachten keine VM bei Vögeln in einem Tierversuch. Eine Analyse von wild gesammelten, besiedelten *H. vertcillata* Blättern mittels bildgebender Massenspektrometrie offenbarte die Präsenz eines polybrominierten Metaboliten im Bereich der Bakterienkolonien, nicht jedoch auf den unbesiedelten Blattabschnitten. In dieser Publikation liefern wir den abschließenden Beweis, dass VM von einem neuartigen cyanobakteriellen Neurotoxin, einem fünffach-bromierten Biindolalkaloid, verursacht wird. Nach Zugabe von Kaliumbromid zu dem Kultivierungsmedium produzierten die Laborkulturen das erwartete Toxin, welches wir Aetokthonotoxin (AETX) genannt haben. Nach der Isolierung und Strukturaufklärung bestätigte ein anschließender Versuch im Vogelmodell, dass AETX der molekulare Auslöser von VM ist. Zusätzlich, konnten wir das AETX Biosynthesecluster identifizieren, und erste Einsichten in die Biosynthese gewinnen. Wir diskutieren saisonale Umweltbedingungen, Bromidverfügbarkeit und anthropogene Einflüsse auf die Toxinproduktion.

In allen drei Publikationen werden die Entdeckung, die Isolierung, die Strukturaufklärung, die Bioaktivität und die ökologische Rolle von neuen Naturstoffen aus Cyanobakterien beschrieben. Für die Erforschung dieser Ergebnisse wurden modernste Technologien und Methoden in der analytische Chemie (z. B. HPLC, (bildgebende) Massenspektrometrie, NMR), präperative Isolierungsmethoden, diverse Kultivierungstechniken im Labormaßstab, sowie funktionelle Genomik eingesetzt.

Contents

Contents

1. Introduction

1.1. Natural Products

Although, any molecule produced by a living organism could theoretically be considered a Natural Product (NP), the term is usually used when refering to (bioactive) structurally complex metabolites produced by plants, fungi, bacteria. Scientists engaging in the field of natural product research generally search for novel compounds in order to characterize their chemical and biological properties, especially in the context of drug discovery and chemical ecology.[1]

In the past, NPs were usually (de)classified as "secondary metabolites", implying that they are less important because they are non-essential to the immediate survival of the producing organism (which is taken care of by its "primary metabolism"), but rather offer an enhancement in fitness in special environments or under certain conditions.[2–4] Today, the predominant view amongst the majority of natural product scientists is that NPs, which usually are produced via dedicated pathways by the respective organisms, are indeed metabolites valuable for the producing organism, e.g. as part of a chemical arms race with competing organisms or as means for chemical communication, and that they possess an innate bioactivity. This led to the adoption of the new term "specialized metabolites" in the early 2000s.[1,5,6] The Screening Hypothesis is an alternative, more holistic approach to explain why and how so much chemical diversity is generated and retained by organisms. It tries to explain how this diversity is preserved despite an absence of a direct role for a compound, and why maintaining it is actually an advantage under the evolutionary pressure all living organisms inevitably face. Firn and Jones published their hypothesis for the first time in 1991,[7] and then a summarizing review in 2003 with the purpose "to promote a more unified view of natural products [...] based on an evolutionary perspective [...,that] needs to be adopted by those

working on natural products in order to place their own work within a larger, more holistic conceptual framework."[8] In its essence, the model is based on the fact that biological activity is a rare property for any one molecule to possess.[7] Thus, those organisms, which can produce and retain chemical diversity at low expenses, would be evolutionarily favored: the greater the chemical diversity, the more likely the chances of producing the rare molecule with a significant bioactivity — and as a consequence an increased probability of enhanced fitness and survival.[9]
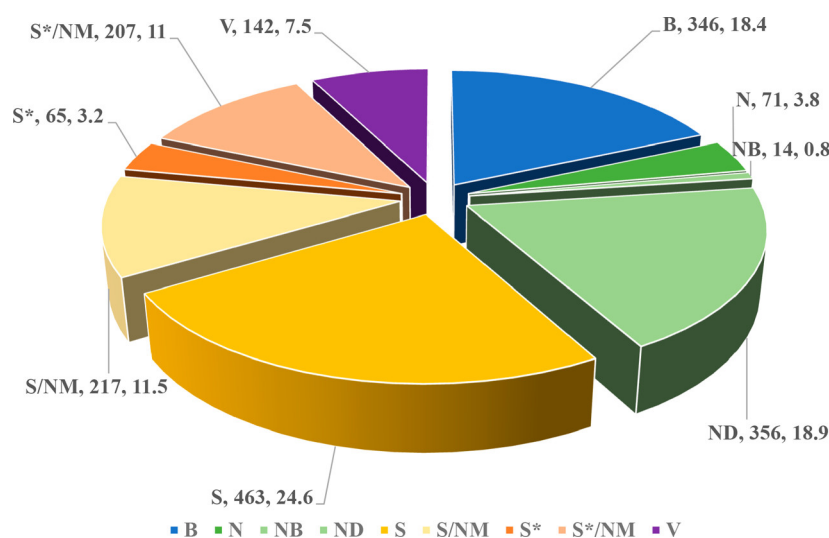
Figure 1.1.: All new approved drugs in the time period from 01.01.1980 to 30.09.2019, categorized by their respective source. B – biological macromolecule, N – unaltered natural product, NB – botanical drug (defined mixture), ND – natural product derivative, S – synthetic drug, S* - synthetic drug (NP derived pharmacophore), V – vaccine, /NM – mimic of natural product. More than 65 % of FDA approved drugs in this time period are natural products (taking into account B, N, NB and ND) or contain a natural product derived pharmacophore. Graphic adopted from the recurring review *Natural Products as Sources of New Drugs* last published by Newman and Cragg in March of 2020.[10]

Since its early days, humanity has realized the immense potential that lies in the usage of NPs (though unaware of singular compounds at that time) to treat diseases, improve health and strength (and even explore human spirituality).[11–13] Still today, throughout modern society we see evidence of traditional (mainly plant based) medicine primarily being used for self-medication.[4,14] Therefore it comes as no surprise that 65 % of novel FDA approved drugs between 1980 and 2019 are

NPs, or contain a NP derived pharmacophore (**Fig. 1.1**).[10] The Golden Age of natural product research started with Fleming's discovery of penicillin in 1945 and reached its peak between the 70s and 80s of the 20th century.[15]

In the 1990s, the development and rise of automated combinatorial chemistry, huge synthetic libraries, and the introduction of high-throughput screening (HTS) led pharmaceutical companies to abandon their NP Research & Development sections (partly due to technical difficulties in applying these novel technologies to NPs).[3,16] However, modern drug discovery has once again realized the vast potential of NPs for new drug leads — evolution simply had a lot more time to refine and select the biological pathways producing bioactive molecules and to conduct its own "screening program".[2,17] Today, it is the selective enhancement of NPs via combinatorial chemistry (and more recently computational molecular design) that leads to the successful identification of new molecular targets and novel bioactive pharmacophores in screening programs.[4,11,18] The ongoing technological innovations in instrumental analytics, molecular target identification and especially the arrival of the genomics era (screening of silent, hidden gene clusters) open up new and promising possibilities to harness nature's treasure box.[19–21]

Many positive aspects and achievements of human society which are taken for granted today, have been made possible by the discovery and dedicated use of NPs. Few examples of this long list include: the use of morphine (opiates) from ancient to modern medicine as a pain reliever,[22] the discovery of penicillin as a revolutionary new anti–bacterial treatment, paclitaxel as the most used breast cancer drug,[23] the use of indigo as dye for more than 6000 years,[24] the use of curare as an arrow poison for hunting in early tribal communities,[25] or the ancient use of psychoactive alkaloids like nicotine, mescaline, dimethyltryptamine and psilocybin within spiritual and religious rituals to induce nonordinary states of consciousness.[26,27] The oldest documented use of NPs in the form of medicinal fungi dates back more than 60,000 years[28] — in Europe the famous Iceman *"Ötzi"* can be considered as one of the earliest proofs of using mushrooms for a therapeutic effect: *Ötzi* carried *Piptoporus betulinus* with him, possibly because of its anti–parasitic activity.[29] The knowledge of finding, identifying, cultivating, and using wild medicinal plants (and fungi) has always played an essential, and almost mythical role in human society and has been carefully passed on to newer generations.[30,31]

Considering all these fascinating aspects, along with the ever increasing need for new (especially anti–infective) treatments, it is not only a necessity, but a privilege to pursue the discovery, widening, and refining of this field as a research scientist.

1.2. Cyanobacteria

Cyanobacteria are Gram-negative oxygenic photoautotrophic bacteria and among the oldest organisms inhabiting Earth. Indirect fossil records (biomarkers) dating 3.3 to 3.5 billion years ago provide evidence for a cyanobacterial origin of oxygenic photosynthesis, the foundation of the world's ecosystem.[32] Cyanobacteria have played the key role in oxygenating Earth's atmosphere during the Great Oxidation Event 2.45 billion years ago.[33] Apart from providing complex life as we know it today its vital atmosphere, the plastids of all plants share a common endosymbiotic cyanobacterial ancestor.[34] This makes cyanobacteria the cornerstone of the development of all complex life forms. Therefore it comes to no surprise that one of the most ancient inhabitants has successfully adapted to nearly every ecological niche on Earth: hot springs, deserts, polar ice, freshwater lakes, oceans, as well as symbiotic associations with invertebrates, plants, and fungi — cyanobacteria flourish ubiquitously.[35,36] They are also sometimes called blue-green algae or cyanophytes. Cyanobacteria owe all the various names to their blue-green colored pigment C-Phycocyanin, which plays a role during photosynthesis. As diverse as their distribution across the earth, their morphology is also encompassing as it varies from unicellular to multicellular filamentous or colonial forms.[33] Certain filamentous strains of the order *Nostocales* can even develop hormogonia, short motile filaments that serve as a way to actively migrate when under stressful environmental conditions, as well as an infection agent in many symbiotic plant-cyanobacteria relationships.[37] Cyanobacteria colonizing nutrient scarce environments developed the ability to fix atmospheric nitrogen via heterocysts.[38] These are specialized cells that separate the nitrogenase enzyme complex from photosynthesis, a necessity due to the inhibition of the complex by oxygen. However, many cyanobacteria that do not possess heterocysts are also capable of fixing nitrogen. They usually perform

photosynthesis during the day and nitrogen fixation during the night, so that the nitrogenase is not inhibited by production of oxygen during photosynthesis.[39]

As an alternative way to cope with harsh environmental conditions (especially low light), some heterocystous strains can develop akinetes, a dormant cell type that can withstand extreme cold and arid conditions for several years before regerminating once living conditions have improved.[38]

1.2.1. Harmful Algae Blooms — HABs

To the general public, cyanobacteria are mostly known in the context of harmful algae blooms (HAB) — algae communities which grow suddenly and exponentially, cyanobacteria being the dominating species especially in brackish and fresh inland water blooms.[40] Cyanobacteria in HABs can often produce a variety of highly toxic metabolites.[41] The neurotoxin anatoxin-a was the first of these so-called cyanotoxins, which has been characterized in 1975 by Carmichael et al.[42] Since then, many cyanotoxins have been discovered in marine and freshwater environments worldwide. Direct consumption of toxins or indirect exposure through the consumption of organisms that have accumulated toxins can not only cause death and illness to wild and domestic animals, but can also be responsible for serious human health issues from mild contact irritation, to gastrointestinal disorders, to acute lethal or chronic poisoning.[43] The primary toxicological effects provide the general classification of cyanotoxins in four major groups: hepatotoxic peptides (often also tumor promoters), neurotoxins, cytotoxins (affecting multiple organs) and contact irritants.[43,44] **Table 1.1** summarizes the molecular structures, properties, and origin of the major known cyanotoxins.[43–46]

Climate change, recent global warming and the even more direct anthropogenic influence on marine and freshwater cyanobacterial habitats in the form of nutrient enrichment have caused an alarming rise in the frequency of HABs.[47] With more frequent algae blooms, the increased risks for human health (due to a massive toxin release) and the economic consequences of cyanobacterial blooms have become the primary aspects focused on by the public.[48]

However, the devastating effects HABs have on ecosystems that are not directly linked to toxin production are often neglected: the massive increase of biomass

in a very short time causes a suppression of other primary producers, disruption in the food web, and the depletion of nutrients. The subsequent dieback and degradation may lead to a mass mortality in fish and other aquatic organisms due to oxygen depletion and a sudden massive release of intracellular cyanotoxins, such as microcystins, into the water. As a consequence, this leads to habitat degradation, diseases, broken community structures, and an overall reduced biodiversity.[43,49]

Table 1.1.: Summary of major known cyanotoxins, their producers, toxicity. The molecular structure of an exemplary compound for the main families is described.[43-46]
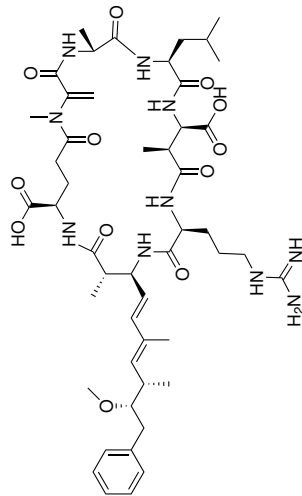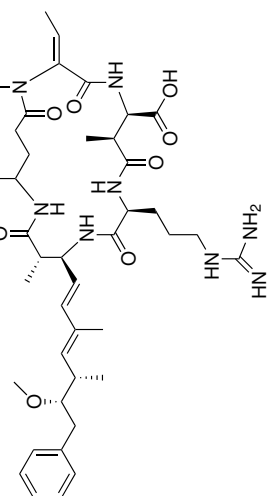
Toxins	Producing genera	Toxicity	Structure of the major congener
		Hepatotoxins	
Microcystins >300 known variants	*Microcystis, Planktothrix, Anabaena, Nostoc, Hapalosiphon, Phormidium*	Inhibition of eukaryotic protein phosphatases 1 and 2A; LD$_{50}$ 25 – >1000 µg kg^{-1}	
Nodularins 10 known variants	*Nodularia*	Inhibition of eukaryotic protein phosphatases 1 and 2A; LD$_{50}$ 30–50 µg g^{-1}	

Table 1.1: Continued.
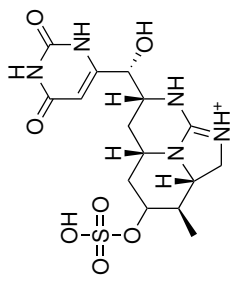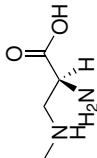
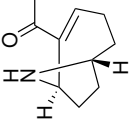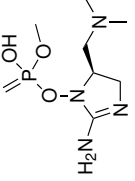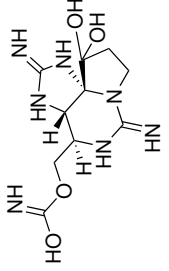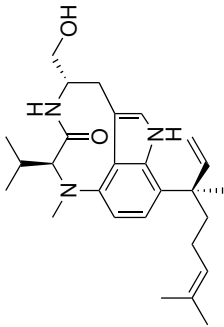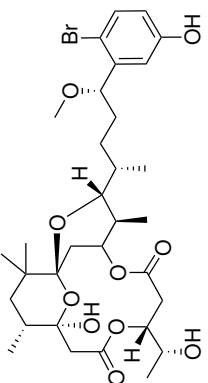| Toxins	Producing genera	Toxicity	Structure of the major congener
Cylindrospermopsin 3 known variants	*Cylindrospermopsis, Dolichospermum, Anabaena, Aphanizomenon, Raphidiopsis, Umezakia, Lyngbya, Oscillatoria*	General cytotoxin inhibiting protein biosynthesis; LD_{50} 2.1 µg kg^{-1} (in 24h)	
		Neurotoxins	
L-β-N-methylamino-L-alanine (BMAA)	Almost all groups of cyanobacteria from freshwater, brackish, and marine environments	Neurotoxic, neurodegenerative, causes hyperexcitation of neurons via increase of intracellular Ca^{2+}; LD_{50} n.d.	

Table 1.1: Continued.

| Toxins	Producing genera	Toxicity	Structure of the major congener
Anatoxin-a 8 known variants	*Anabaena, Arthrospira, Aphanizomenon, Cylindrospermum, Microcoleus, Microcystis, Oscillatoria, Phormidium, Planktothrix, Pseudanabaena*	Neurotoxic, mimics acetylcholine but is not degraded by acetyl-cholinesterase, no known antidot; LD_{50} 200 µg kg^{-1}	
Anatoxin-a(s)	*Anabaena*	Neurotoxic, irreversible acetylcholinesterase in-hibitor; LD_{50} 20–40 µg kg^{-1}	
Paralytic shellfish toxins (saxitoxins) 57 known variants.	*Anabaena, Aphanizomenon, Cylindrospermopsis, Lyngbya, Planktothrix*	Neurotoxic, blocking of Na$^+$-channels leads to respiratory arrest; LD_{50} 10–30 µg STX kg^{-1}	

9

Table 1.1: Continued.

Toxins	Producing genera	Toxicity	Structure of the major congener
		Dermatotoxins	
Lyngbyatoxin A 7 known variants	*Lyngbya (Moorea)*	Strong blister agent, gastrointestinal inflammatory toxin, bioactivity and tumor promoting activity through binding to protein kinase C); LD_{50} 250 µg kg^{-1} (3 weeks old mice)	
Aplysiatoxin 5 known variants	*Lyngbya (Moorea)*	Strong blister agent, gastrointestinal inflammatory toxin, bioactivity and tumor promoting activity through binding to protein kinase C); LD_{50} 107 µg kg^{-1} (3 weeks old mice)	

1.2.2. Cyanobacterial Natural Products

As the manifold spectrum of cyanotoxins illustrates, cyanobacteria are gifted organisms when it comes to the production of chemically diverse, bioactive metabolites. Taking the conceptual framework of the Screening Hypothesis into account and the fact that cyanobacteria are one of the most numerous and ancient organisms in earth's microbial community, this is no wonder. While a vast majority of cyanobacterial bioactive metabolites derive from a combination of non-Ribosomal Peptide Synthetase (NRPS) and Polyketide Synthase (PKS) pathways,[50,51] a closer look into the biochemistry responsible for the biosynthesis of cyanobacterial NPs reveals unique enzymatic pathways not typically described and rarely reported elsewhere in nature.[52] **Figure 1.2** exemplifies the diverse structural classes cyanobacterial NPs can be assigned to (based on the analysis of 670 publications from 1970–2019 by Dermay et al.),[53] and also highlights their chemical diversity and complexity. Recent genomic studies revealed that the metabolic potential known so far seems to be only the tip of the iceberg.[54] Further and more detailed insight into the structural diversity of cyanobacterial NPs is beyond the scope of this work, but can be found in extensive reviews published in the literature.[50,55–59]

Despite their inherent uniqueness, cyanobacteria have long been neglected by the scientific community in the search for novel drug leads. In fact, until the 1980s cyanobacteria were almost exclusively known for their toxin production.[60–62] It was Richard E. Moore who first shed light on the greater biosynthetic potential of cyanobacteria with his discovery of the majusculamides in 1977.[63] Due to a 30-year effort studying their natural product chemistry, Moore is recognized as a pioneer in NP discovery from cyanobacteria. Even with the rising attention and the considerable progress that has been made in the last two decades (a total of 200 cyanobacterial metabolites had been characterized until 1996,[64] whereas an additional 1450 have been characterized in the last 25 years),[55,65] cyanobacteria still remain an underexplored source for novel NPs and drug leads compared to other microorganisms such as actinobacteria.[66,67] Non-trivial culture conditions, slow growing cultures, low isolation yields, difficulties in obtaining pure isolates and in upscaling provide many obstacles and make high throughput screening processes of cyanobacterial NPs challenging[35] — but technological progress in analytics,
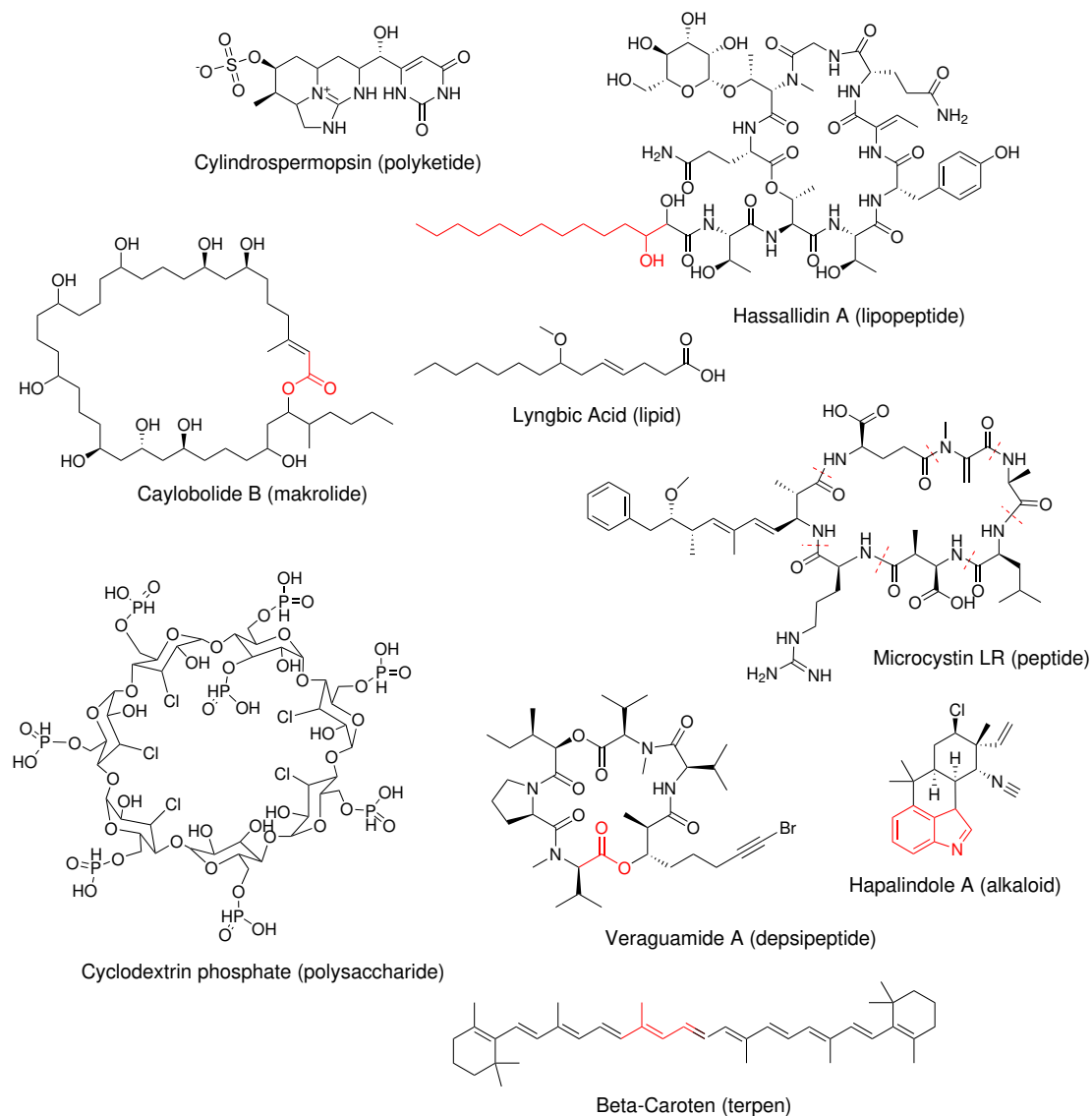
Figure 1.2.: Cyanobacterial metabolite families classified based on their respective structural characteristics. Examples of cyanobacterial natural products for each class (polyketides, lipopeptides, makrolides, lipids, peptides, polysaccharides, depsipeptides, alkaloids, terpens) are illustrated. Main characteristics of each chemical class are highlighted in red, if applicable.

molecular engineering and cultivation techniques, as well as bioinformatic tools and computational approaches provide new promising tools to access this treasure box more easily.[68,69]

The pipeline of clinical and preclinical compounds is rich, and given the reported

bioactivities, the possible applications in biotechnology, agriculture, and medicine are vast.[53,70,71] The final proof for cyanobacteria's role as a prolific source for drug development and new treatment possibilities was the FDA approval of Brentuximab vedotin, an antibody drug conjugate for the treatment of Hodgkin's lymphoma, in 2011.[72] It is the first clinically used anti–cancer drug that has been developed from a cyanobaterial NP. Brentuximab vedotin is an antibody drug conjugate, with its payload based on a synthetic analog of dolastatin 10, which was originally isolated from the sea hare *Dolabella auricularia*, but later attributed to the marine cyanobacterium *Symploca* sp. VP642 forming part of the sea hare's diet — a rather intriguing story itself.[73,74]

(Cyanobacterial) Indole Alkaloids

One of the largest classes of NPs with significant bioactivity are indole alkaloids. Although the majority of these known indole alkaloids are produced by plants, they can also be found throughout the animal, fungal, and bacterial kingdoms.[75] Whereas around 1500 NPs have been isolated from cyanobacteria, cyanobacterial (indole) alkaloids represent a relatively small fraction of this overall number.[55] The majority of bioactive and chemically diverse indole alkaloids have been isolated from phylogenetically closely related, filamentous cyanobacterial species of the order *Nostocales*.[76,77]
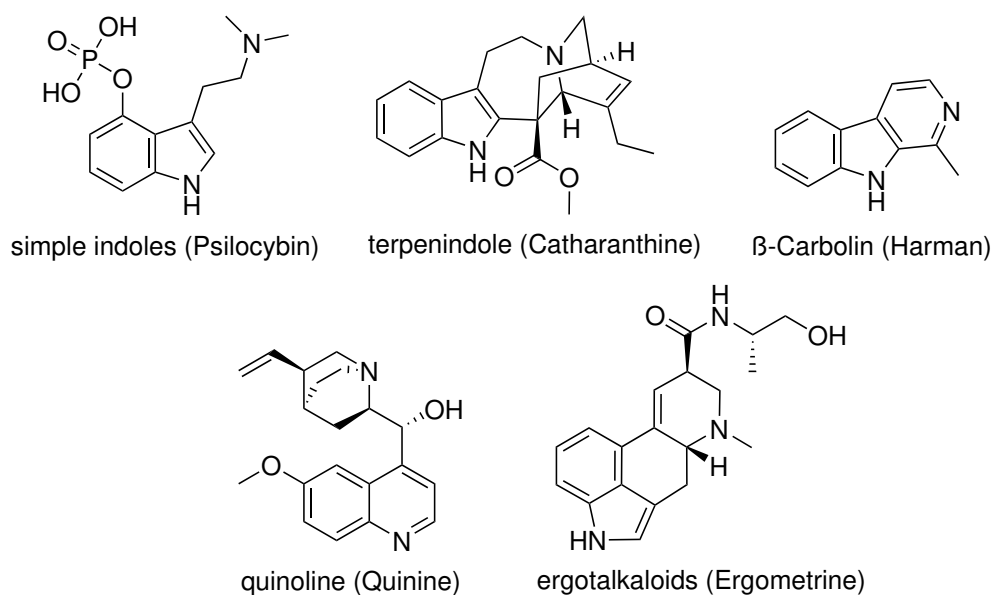
Based on their main scaffold indole alkaloids can further be subdivided into simple indole, β-carboline, terpenoid indole, quinoline, pyrroloindole, and ergot alkaloids (**Fig. 1.3**). Tryptophane acts as the common biosynthetic precursor, originating from the shikimate pathway via anthranilic acid as intermediate. From here, the complexity of the biosynthesis scales with the structural complexity of the final product: the terpenoid indoles (**Fig. 1.3**) possess the most exceptional structures and typically contain a tryptamine portion with a remaining C9 or C10 residue that becomes rearranged in one of three distinct ways, further subdividing the terpenoid indole alkaloids into the *Corynanthe* type, the *Aspidosperma* type, and the *Iboga* type. Many studies that led to an understanding of terpenoid indole alkaloid biosynthesis have been conducted on *Catharanthus roseus*, and have also

been driven by the discovery of the potent anti–cancer activity of vinblastine and vincristine — two bisindole alkaloids isolated from *Catharanthus roseus*, the latter one being extremely effective in the treatment of lymphomas and childhood leukemia.[75]

The biosynthetic formation of simple indoles is straight forward and accomplished via consecutive decarboxylation, methylation, and hydroxylation reactions (in a varying order depending on the final product and the producing organism).

Both C-2 and C-3 positions of the indole system in tryptophan are nucleophilic. However, reactions on C-2 are the most common in indole alkaloid biosynthesis. The β-Carboline biosynthesis illustrates this: an additional six-membered hetero-cyclic ring is formed via an imine intermediate (generated from tryptamine and an aldehyde) that gets attacked by C-2 in a Mannich/Pictet–Spengler-type reaction (see **Fig. 1.4**). The very same pathway is also used for the biosynthesis of complex β-Carbolines: additional carbon atoms and extended scaffolds are supplied by more complex aldehyds or keto acids such as for example secologanin (biosynthesis of ajmalicine) and pyruvate (biosynthesis of harman).[75]

simple indoles (Psilocybin)   terpenindole (Catharanthine)   ß-Carbolin (Harman)

quinoline (Quinine)   ergotalkaloids (Ergometrine)

Figure 1.3.: Subclasses of the indole alkaloid family based on the respective main scaffolds. L-Tryptophan acts as the biosynthetic precursor for indole alkaloids. Extensive decorations and intermediates, derived from other biosynthetic pathways, further extend the chemical diversity within this alkaloid family. Major rearrangement reactions can further convert the indole ring system into a quinoline ring.

Due to the reversibility by which amines can react with aldehydes, ketones and imines in natural processes, the indole scaffold can even be rearranged into a quinoline system, an additional (indole) alkaloid (sub)class.[75,78]

Organisms usually produce a mixture of (indole) alkaloids consisting of major and minor derivatives with the same biosynthetic origin, differing only in their functional groups that decorate a respective core structure. Just like the neurotransmitter serotonin (5-HT), this core structure is derived from tryptophan. Due to this structural resemblance, indole alkaloids can often interact with 5-HT receptors, but they can also target other proteins such as e.g. α-adrenergic, µ-opioid, GABA$_A$-, NMDA-receptors. Thus, they often show a potent neurological bioactivity.[79,80]

Human history has been interwoven with indole alkaloids since its very beginning: the conscious use of indole alkaloids by humans can be traced back to ancient times (see section 1.1) — even a co-evolution is discussed, e.g. to explain the astounding receptor affinity of various psychoactive indoles for the human serotonin receptors compared to other primates,[81,82] or to explain the various selective and highly toxic effects of indole alkaloids, such as strychnine, vincristine to herbivores (including primates). **Table 1.2** gives a short overview of the known indole alkaloid families produced by cyanobacteria, their bioactivity/toxicity, ecological role, and/or possible functions as new drug leads. **Fig. 1.5** shows the scaffolds of selected exemplary compounds from this table and highlights the astounding chemical diversity within the indole alkaloid class.
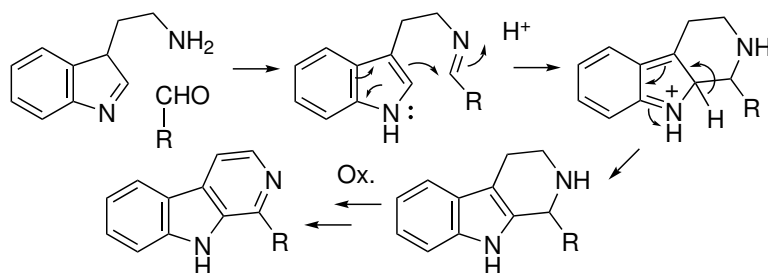
Figure 1.4.: β-carboline biosynthesis. Reactions on the C-2 position of the indole system are the most common due to its nucleophilicity. The biosynthesis of β-carbolines illustrates this: An additional ring is formed via an imine intermediate (generated by an aldehyde and tryptamine) that gets attacked by C-2 in a Mannich/Pictet–Spengler-type reaction. Aromaticity is restored via tautomerism and several additional oxidation steps lead to the final β-carboline scaffold.

Table 1.2.: Overview of indole alkaloid families produced by cyanobacteria. In the case that only singular derivatives with a unique scaffold are known, the individual compound is denoted and also considered a particular indole alkaloid family.

Compound	isolated from	Bioactivity/ecological role	Refs
Bauerines	*Dichotrix baueriana* GO-25-5	anti–viral against Herpes simplex virus 2, cytotoxic against LoVo	83,84
Harmane, Norharmane	*Nodularia harveyana, Noctiluca miliaris*	nephrotoxic at high doses, comutagen, anti–microbial activity, plant growth and enzyme inhibitor.	85–87
Lyngbyatoxins	*Lyngbya majuscula*	carcinogen, blister agent	88–90
Nostocarboline	*Nostoc* 78-12A	Cholinesterase inhibitor	91
Calothrixins	*Calothrix*	anti–bacterial against *P. falciparum*, cytotoxic against HeLa cells	92
Rivularins	*Rivularia firma*	anti–inflammatory agent	93
3,3'-Bi(2,6-dibromoindole)	"	"	94
Nostodione A	*Nostoc commune*	anti–mitotic	95

17

Table 1.2: Continued.

Compound	isolated from	Bioactivity/ecological role	Refs
Scytonemin	all phylogenetic lines of sheathed cyanobacteria incl. *Calothrix* spp., *Lyngbya, Nostoc* spp., *Stigonema* sp.	Pigment from the sheaths of cyanobacteria as protectiosn from UV-radiation, anti–proliferative agent, antioxidant	96–99
Tjipanazoles	*Tolypothrix tjipanasensis, Fischerella ambigua*	anti–fungal, cytotoxic against leukaemia and solid tumor cell lines	100–103
Hapalindoles	mainly *Hapalosiphon fontinalis, Hapalosiphon laingii, Fischerella ambigua, Hapalosiphon welwitschii, Westiella intricata*	anti–fungal activity, algicidal, anti–bacterial, ichthyotoxic, insecticidal	104–115
Fischerindoles	*Fischeralla* sp., *Hapalosiphon welwitschii*	"	116–121
Welwitindolinones	*Hapalosiphon welwitschii, Westiella intricata*	insecticidal	122–124
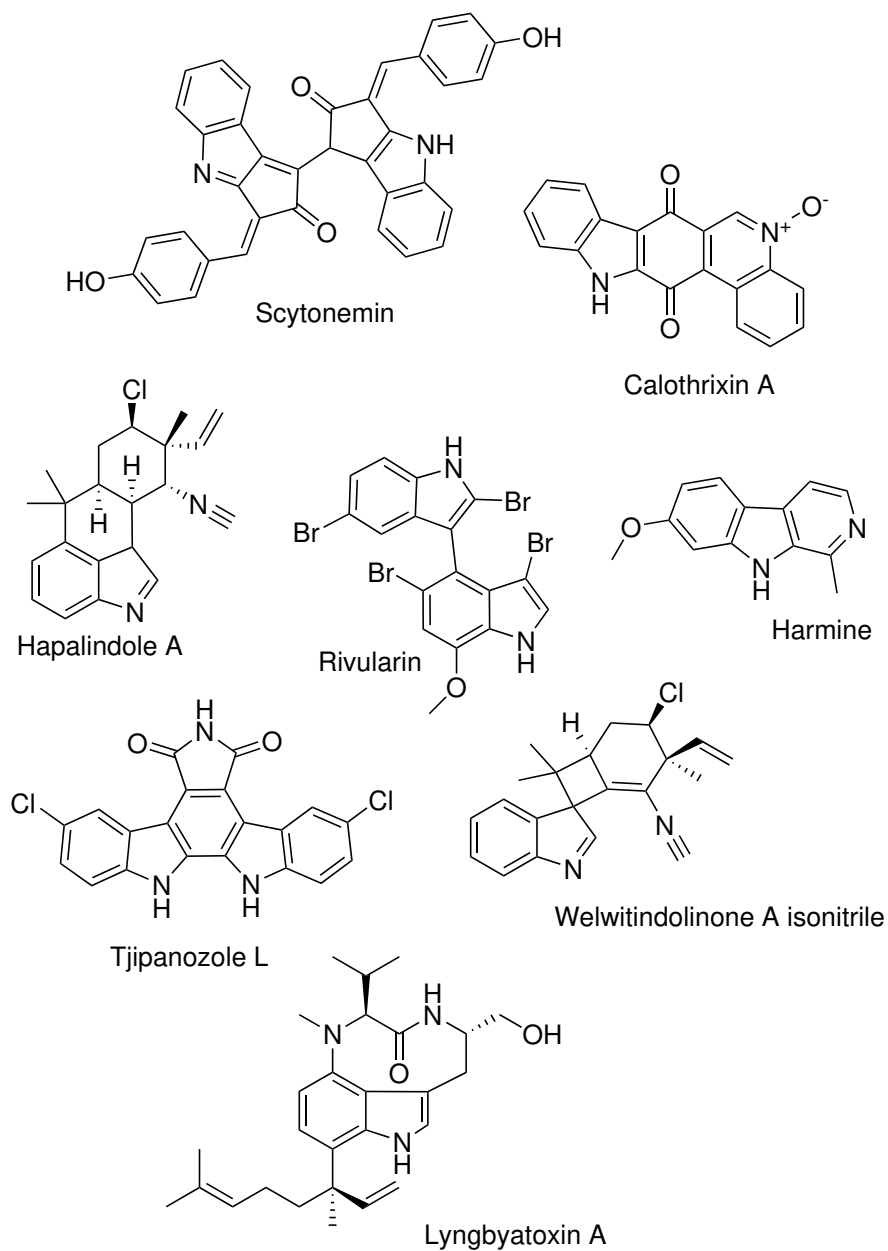
Figure 1.5.: Selected indole alkaloids produced by cyanobacteria. The chemical diversity within this natural product class is mirrored by the diverse bioactivities and ecological roles of these compounds (see **Table 1.2**).

1.3. Objectives and Motivation

Given the importance of NPs for drug development, their historical use throughout human history and an innate curiosity for the unknown, the aim of this thesis was to investigate novel bioactive metabolites, characterize their chemical structures and properties, and to evaluate their biological and ecological roles within the producing organisms. Cyanobacteria have finally been recognized as a rich source for novel bioactive metabolites by drug development programs and natural product scientists alike. Therfore, this thesis focused its research on bioactive metabolites from cyanobacteria. To guarantee an untargeted aproach, state-of-the art technologies in analytical chemistry (e.g. HPLC, (imaging-)mass spectrometry, NMR), preparative isolation techniques (e.g. counter current chromatography, preparative HPLC, solid phase extraction), small to large scale cultivation approaches, bioactivity characterization and functional genomics were applied. The combination of these techniques and approaches led to the successful isolation and characterization of a novel potent neurotoxin responsible for a deadly wildlife disease, several Pan-Assay-Interfering-Compounds, and immunomodulating indole alkaloids. Three original research articles describe the results in detail and are presented and discussed in the following sections.

2. Publications

[1]: Hapalindoles from the Cyanobacterium *Hapalosiphon* sp. Inhibit T Cell Proliferation

T. Chilczuk, C. Steinborn, S. Breinlinger, A. M. Zimmermann-Klemd, R. Huber, H. Enke, D. Enke, T. H. J. Niedermeyer, C. Gründemann, Hapalindoles from the Cyanobacterium Hapalosiphon sp. Inhibit T Cell Proliferation. *Planta Medica* 86, 96–103 (2020), DOI:10.1055/a-1045-5178.

2. Publications

Summary

On the lookout for new immunomodulating agents for the treatment of (rare) autoimmune diseases and cancers, a bioactivity guided screening campaign of 575 cyanobacteria extracts for immunomodulatory effects has been carried out. The following publication describes the successful identification, isolation and characterization of 5 hapalindoles from the cyanobacterium *Hapalosiphon* sp. CBT1235 responsible for the immunomodulatory effect observed for this strain's extract. Hapalindoles have been investigated since the early seventies by Moore et al. and more than 80 variants are known. Although they possess a wide range of different bioactivities (anti–infective, cytotoxic, anti–fungal and others), a modulation of the activity of human immune cells has not yet been described. T-cell proliferation, apoptosis and necrosis induction were determined via flow cytometry measurements and used as parameters to characterize the immunomodulatory activity of the hapalindoles. Two of the five hapalindole derivatives (hapalindole A-formamide and hapalindole J-formamide) were isolated for the first time from a natural source and provided a valuable insight in structure-activity relations regarding the immunomodulatory activity (retardation of T-cell proliferation) of hapalindoles: while hapalindole A was the most potent compound with an IC_{50} of 1.56 µM and induction of T-cell apoptosis only at 10-fold higher concentrations, the formylated derivatives had a much lower overall activity and less specificity for anti–proliferative over apoptotic effects. These findings are in agreement with previous studies where a superior anti–fungal and anti–bacterial activity was reported for the isonitrile and isothiocyanate hapalindole variants compared to their formamide counterparts. Further studies regarding the mode of action in human immune cells are required in order to discriminate between toxicity (hapalindoles are also reported to be neurotoxic metabolites) and immunomodulatory effects. Only then an estimation can be made whether a further development as immunomodulatory drugs would be possible.

Hapalindoles from the Cyanobacterium *Hapalosiphon* sp. Inhibit T Cell Proliferation

Authors

Tomasz Chilczuk[1*], Carmen Steinborn[2*], Steffen Breinlinger[1*], Amy Marisa Zimmermann-Klemd[2], Roman Huber[2], Heike Enke[3], Dan Enke[3], Timo Horst Johannes Niedermeyer[1§], Carsten Gründemann[2§]

Affiliations

1 Department of Pharmaceutical Biology/Pharmacognosy, Institute of Pharmacy, University of Halle-Wittenberg, Halle, Germany

2 Center for Complementary Medicine, Institute for Infection Prevention and Hospital Epidemiology, Faculty of Medicine, University of Freiburg, Freiburg, Germany

3 Cyano Biotech GmbH, Berlin, Germany

Correspondence

PD Dr. Carsten Gründemann
Center for Complementary Medicine, Institute for Infection Prevention and Hospital Epidemiology, Faculty of Medicine
Breisacherstrasse 115B, 79106 Freiburg, Germany
Phone: + 49 (0) 7 61 27 08 31 70, Fax: + 49 (0) 7 61 27 08 32 30
carsten.gruendemann@uniklinik-freiburg.de

Correspondence

Prof. Dr. Timo H. J. Niedermeyer
Department of Pharmaceutical Biology/Pharmacognosy, Institute of Pharmacy
Hoher Weg 8, 06120 Halle (Saale), Germany
Phone: + 49 (0) 34 55 52 57 65, Fax: + 49 (0) 34 55 52 74 07
timo.niedermeyer@pharmazie.uni-halle.de

🌐 Supporting information available online at
http://www.thieme-connect.de/products

ABSTRACT

Novel immunomodulating agents are currently sought after for the treatment of autoimmune diseases and cancers. In this context, a screening campaign of a collection of 575 cyanobacteria extracts for immunomodulatory effects has been conducted. The screening resulted in several active extracts. Here we report the results of subsequent studies on an extract from the cyanobacterium *Hapalosiphon* sp. CBT1235. We identified 5 hapalindoles as the compounds responsible for the observed immunomodulatory effect. These indole alkaloids are produced by several strains of the cyanobacterial family Hapalosiphonaceae. They are known for their anti-infective, cytotoxic, and other bioactivities. Modulation of the activity of human immune cells has not yet been described. The immunomodulatory activity of the hapalindoles was characterized *in vitro* using flow cytometry-based measurements of T cell proliferation after carboxyfluorescein diacetate succinimidyl ester staining, and apoptosis and necrosis induction after annexin V/propidium iodide staining. The most potent compound, hapalindole A, reduced T cell proliferation with an IC_{50} of 1.56 µM, while relevant levels of apoptosis were measurable only at 10-fold higher concentrations. Hapalindole A-formamide and hapalindole J-formamide, isolated for the first time from a natural source, had much lower activity than the nonformylated derivatives while, at the same time, being less selective for antiproliferative over apoptotic effects.

---

* These authors contributed equally to this work.

§ These authors contributed equally to this work.

96

Chilczuk T et al. Hapalindoles from the…   Planta Med 2020; 86: 96–103

23

ABBREVIATIONS	
CFSE	carboxyfluorescein diacetate succinimidyl ester
CPT	camptothecin
CsA	cyclosporine A
PBMC	peripheral blood mononuclear cells

Introduction

Cyanobacteria are an intriguing source for structurally diverse and biologically active natural products. Especially the genera *Microcystis, Nostoc,* and *Lyngbya* or *Moorea* are chemically well-characterized [1–7]. Several strains of the family Hapalosiphonaceae produce indole alkaloids [8]. The major classes of these indole alkaloids include hapalindoles, ambiguines, fischerindoles, and welwitindolinones, of which more than 80 variants have been described in the literature [9–24]. They share several common motifs: an indole or oxindole core, a cyclohexane fused to that core, an isonitrile or isothiocyanate functional group, a chlorine substituent, or an additional ring [25]. The largest group of these alkaloids are the hapalindoles. So far 30 different hapalindoles have been reported [9, 10, 15, 18, 21, 26]. The first hapalindoles, hapalindoles A and B, were discovered in 1984 by Moore et al. from *Hapalosiphon fontinalis* [9]. Since then, diverse hapalindoles have been isolated from various strains of the genera *Hapalosiphon, Fischerella*, and *Westiellopsis* [9, 17, 21, 26].

Hapalindoles have a broad spectrum of biological activities, e. g., activity against bacteria [17, 19, 21, 27], fungi [19, 27], and algae [27]. Studies by Doan et al. suggested inhibition of RNA polymerase and consequently the disturbance of the protein biosynthesis as a possible mode of action for the antibacterial activity [27, 28]. Furthermore, cytotoxic activity against normal mammalian and cancer cell lines has been reported for various hapalindoles [21, 27]. However, no mode of action for this activity has been described yet. Finally, they have been shown to be toxic to insects [18, 29] and vertebrates [23]. The insecticidal activity could be explained by sodium channel modulating activity of the indole alkaloids [30]. Interestingly, inhibition of sodium channels did not lead to any cytotoxicity in neuroblastoma cell lines. Thus, compared to insects, a different mode of action must underlie the cytotoxicity on mammalian cells. Although various bioactivities can be attributed to hapalindoles, modulation of the activity of human immune cells has not yet been described. Immunomodulatory drugs are used as modifiers of the immune system to either enhance the immune response against infectious diseases, tumors, and immunodeficiency, or to suppress the immune reaction in organ transplants or to treat autoimmune responses. Screening of a cyanobacteria extract collection (575 extracts) derived from strains from all cyanobacteria orders for inhibition of T cell proliferation resulted in 35 extracts with an activity at 1 µg/mL or lower. One of the active extracts was derived from a *Hapalosiphon* sp. strain. Bioassay-guided fractionation of the extract led to the isolation of 3 known hapalindoles, hapalindole A (**1**) [9], D (**2**), and M (**3**) [10], as well as 2 formamide-bearing hapalindoles that are reported here for the first time from a natural source, namely hapalindole A-formamide (**4**) [31] and hapalindole J-formamide (**5**) [32]. Here, we report the isolation, structure elucidation, and the investigation of the immunomodulatory properties of the hapalindole derivatives isolated from *Hapalosiphon* sp. CBT1235.

Results and Discussion

Our initial screening of a cyanobacteria extract collection for immunomodulating activity on human immune cells resulted in 35 extracts with an activity at a concentration of 1 µg/mL or lower. Nine out of the 11 most potent extracts were derived from cyanobacteria of the genus *Nostoc*. Dereplication of the natural products in these *Nostoc* strain extracts showed the presence of the well-known cytotoxic compound cryptophycin-1 in most of these strains [33–36], so they were excluded from further investigation. Chromatographic evaluation of the remaining extracts by HPLC-DAD/MS showed that few of them featured prominent peaks. In the HPLC-DAD chromatogram of an *Hapalosiphon* sp. extract, several prominent peaks were observed; thus, this strain was selected for follow-up work. T cell proliferation was inhibited by this extract with an IC_{50} of 0.11 µg/mL (▶ **Fig. 1 a**). At the same time, a trend to an increased amount of apoptotic cells at an extract concentration of 10 µg/mL could be observed (statistically non-significant, ▶ **Fig. 1 b**). No induction of necrosis has been observed (data not shown). Microfractionation of the extract and subsequent bioassays showed that indeed the major compounds observable in the chromatogram were responsible for the bioactivity and led to the significant retardation of T cell proliferation (**Fig. 1S a–c** in the Supporting Information).

Five compounds present in the active micro-fraction were isolated from the extract by semi-preparative HPLC (**1–5**). ^{1}H NMR spectra of the pure compounds displayed typical signals of hapalindoles. The molecular formulas were deduced from HRESIMS data. The structures of **1–5** were elucidated based on 1D and 2D NMR data. NMR and MS spectral data of compounds **1–3** matched the published data for hapalindole A (**1**), hapalindole D (**2**), and hapalindole M (**3**), respectively (structures of all isolated compounds, see ▶ **Fig. 2**). NOESY experiments as well as the determination of specific rotation values confirmed the absolute configuration of compounds **1–3** as originally described in detail by Moore et al. [10]. Hapalindole A (**1**) was the main compound isolated from *Hapalosiphon sp.* CBT1235.

Compounds **4** and **5** were hapalindole derivatives not yet described as natural products. Compound **4** was isolated as a brown oil. HRESIMS showed an [M + H]$^+$ ion with *m/z* 357.1723, corresponding to the molecular formula $C_{21}H_{25}N_2OCl$ (calcd. 357.1728, Δ 1.54 ppm). The ^{1}H-spectrum of **4** was almost identical with the respective spectrum of **1** but with 2 additional peaks in the low-field region (8.04 ppm and 8.57 ppm) and a deshielded H-11 (4.84 ppm) compared to **1** (4.37 ppm), suggesting C-11 to be substituted with a formamide moiety (▶ **Table 1**). Key HMBC and COSY correlations confirmed the planar structure (▶ **Fig. 3**). Evaluation of the NOESY spectrum showed the relative configuration of **4** to be the same as hapalindole A with the formamide group being attached axially to C-11 (strong correlations of the N-formamide proton with H-10, H-13 and H-15) [9]. Comparing the specific rotation
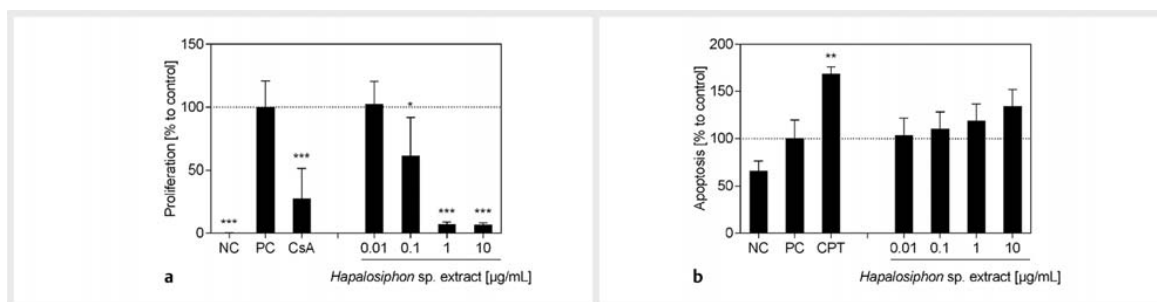
▶ **Fig. 1** Effects of Hapalosiphon sp. CBT1235 extract on T cell proliferation and apoptosis induction. Primary human lymphocytes were cultured in the presence of medium (NC) or were stimulated with anti-human CD3 and anti-human CD28 mAb (PC; 100 ng/mL). Activated T cells were further incubated with cyclosporine A (CsA; 5 µg/mL), camptothecin (CPT; 30 µg/mL), or different concentrations of the *Hapalosiphon* sp. CBT1235 extract. Cell division analysis was carried out using CFSE staining and flow cytometry. Levels of apoptosis were determined using flow-cytometric analysis of annexin V-stained cells. **a** Effects of *Hapalosiphon* sp. CBT1235 extract on lymphocyte proliferation. **b** Induction of apoptosis by *Hapalosiphon* sp. CBT1235 extract. Data of 4 (**a**) or 3 (**b**) independent experiments are presented as mean ± SD in relation to stimulated T cells (PC = 100 %). Asterisks indicate significant differences from PC controls (**p < 0.01, ***p < 0.001).
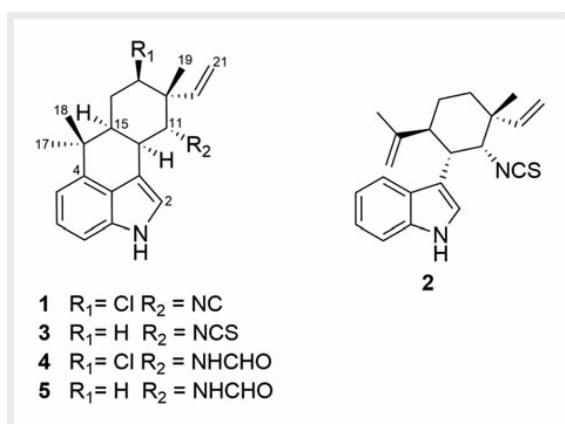
▶ **Fig. 2** Chemical structures of hapalindoles **1**–**5** isolated from *Hapalosiphon* sp. CBT 1235.

values with already published data confirmed our assignment of the absolute configuration of **4** [37]. Therefore, compound **4** was identified as the new natural product hapalindole A-formamide.

The main difference with **5** compared to **1** and **4** was the absence of the chlorine. Compound **5** was also isolated as a brown oil. HRESIMS showed an [M + H]⁺ ion with *m/z* 323.2114, corresponding to the molecular formula $C_{21}H_{26}N_2O$ (calcd. 323.2118, Δ 1.08 ppm). Evaluation of the NMR spectra confirmed the presence of a formamide group at C-11 of the hapalindole backbone, as well (▶ **Fig. 3** and **Table 1**). The absolute configuration of **5** matches the one of hapalindole J, the nonchlorinated variant of hapalindole A (**1**), and has been confirmed by comparing the NOESY correlations and the specific rotation values with those originally published by Moore et al. [10]. Additional NOESY correlations for the axial formamide could be observed (▶ **Fig. 4**). Com-

pound **5** was thus confirmed to be the new natural product hapalindole J-formamide.

Coupling constants between H-22 (NH) and H-23 were found to be 1.37 Hz and 1.45 Hz for hapalindole A-formamide (**4**) and J-formamide (**5**), respectively, indicating a *cis* conformation of the amide bond in both compounds [31].

Hapalindole formamides have been described as intermediates during the total synthesis of hapalindoles, as derivatization products with formic acid, and they can also form during storage in *d*-chloroform [13, 31, 32, 38]. Here, we report for the first time the isolation of 2 hapalindole formamides as natural products from *Hapalosiphon* sp. CBT1235. **4** and **5** could readily be detected by HPLC-MS in a fresh *Hapalosiphon* sp. CBT1235 extract that has not been in contact with formic acid or other acids (**Fig. 2S**, Supporting Information), ruling out the possibility that the isolated formamides are processing or isolation artifacts.

All isolated hapalindoles showed significant effects in the T cell proliferation assay (▶ **Fig. 5**). Hapalindole A (**1**) displayed the highest antiproliferative activity with an IC_{50} of 1.56 µM. Hapalindoles D (**2**) and M (**3**) showed a weaker activity and suppressed proliferation with an IC_{50} value of 27.15 µM for hapalindole D. Hapalindoles A-formamide (**4**) and J-formamide (**5**) again showed lower activity (▶ **Fig. 5**). Except for hapalindole J-formamide, all hapalindoles induced T cell apoptosis at highest concentrations (▶ **Fig. 6**).
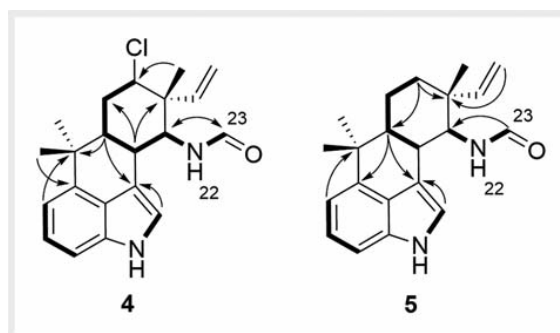
Although relevant amounts of T cell apoptosis were detected, retardation of T cell proliferation was measurable at up to 10-fold lower concentrations. The most potent compound, hapalindole A, was effective at a concentration of 3.0 µM without showing cytotoxic effects. Therefore, potentially a therapeutic range for an application as an anti-inflammatory remedy is given. The isonitrile functional group seems to be crucial for the antiproliferative bioactivity of the hapalindoles, as the formamide derivatives possess a weaker activity. This is in agreement with previous findings, where a reduced antifungal and antibacterial activity of the hapalindole formamides compared to their isonitrile and isothiocyanate counterparts has been reported [31]. Our results, therefore,

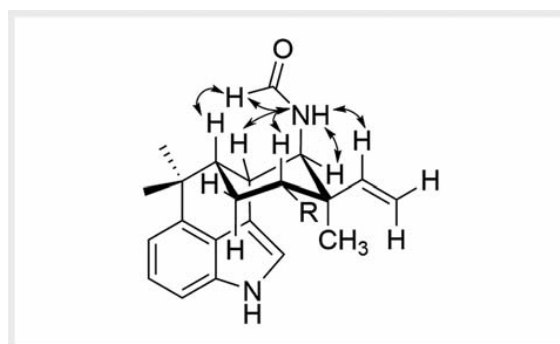98   Chilczuk T et al. Hapalindoles from the… Planta Med 2020; 86: 96–103

25

▶ Table 1 ^{1}H and ^{13}C NMR assignments for **4** and **5** (600 MHz for ^{1}H, 150 MHz for ^{13}C, DMSO-d$_6$). ^{13}C chemical shifts for **5** were extracted from the 2D spectra.

Position	4		5	
	δ$_H$ (J in Hz)	δ$_C$	δ$_H$ (J in Hz)	δ$_C$
1	10.81, s	indole N	10.69, s	indole N
2	7.24, t (1.8)	120.5	7.13, m	119.7
3		110.6		111.8
4		137.1		138.0
5	6.81, d (7.0)	112.3	6.79, br d (7.02)	111.9
6	7.02, t (7.6)	121.9	6.99, t (7.4)	121.5
7	7.14, d (7.9)	108.7	7.10, d (8.0)	108.1
8		133.3		133.4
9		124.0		124.4
10	3.29	36.7	3.30	36.3
11	4.84, m	54.6	4.59, s	51.6
12		44.6		39.1
13 ax	4.61, dd (12.4, 4.0)	65.3	1.74, td (13.2, 3.5)	30.2
13 eq			1.27, m	
14 ax	1.26, m	31.3	0.85, m	19.3
14 eq	1.96, td (13.0, 3.4)		1.60, br d (10.5)	
15	2.11, br td (13.1, 3.8)	44.4	1.87, m	43.4
16		37.4		37.3
17	1.46, s	24.3	1.43, s	24.5
18	1.04, s	31.9	1.06, s	31.5
19	0.85, s	19.6	0.74, s	26.4
20	5.82, dd (17.1, 11.0)	144.2	5.87, m	147.7
21	5.08, m	114.0	4.87, m	109.9
22	8.57, br d (9.9)	N	8.23, br d (9.16)	N
23	8.04, d (1.37)	159.7	8.00, br d (1.45)	159.6

▶ Fig. 3 ^{1}H-^{1}H COSY (bold connections) and selected HMBC correlations (arrows) of **4** and **5**.

▶ Fig. 4 Selected NOESY correlations (arrows) of compounds **4** (R = Cl) and **5** (R = H).
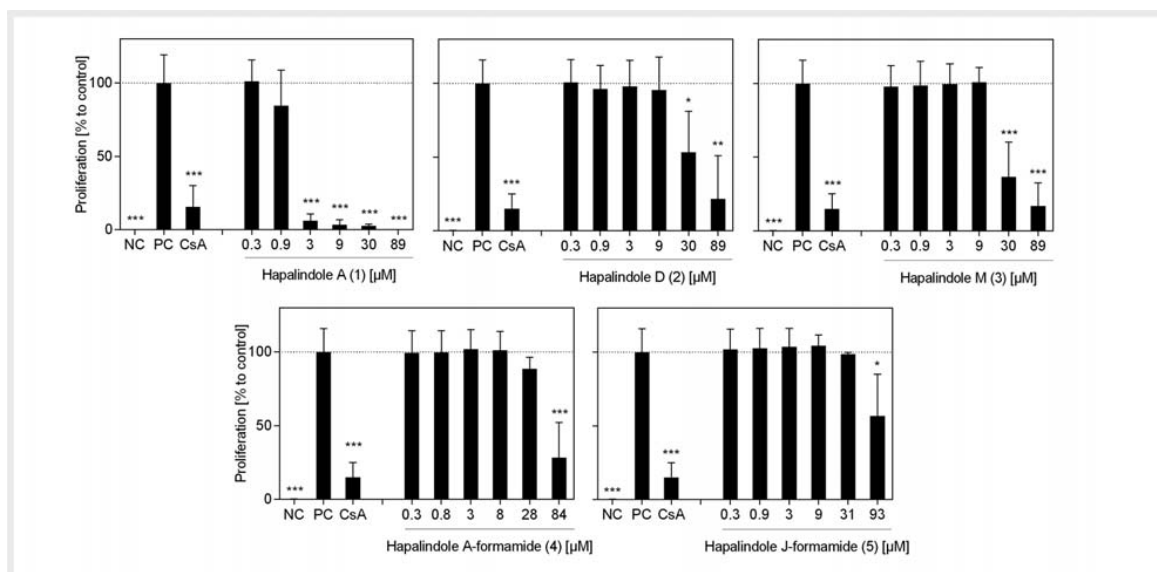
Materials and Methods

General experimental procedures

HRESIMS data were obtained using a Q Exactive Plus mass spectrometer (Thermo Fisher Scientific) coupled to an UltiMate 3000 HPLC system (Thermo Fisher Scientific). Semi-preparative HPLC was conducted on an UltiMate 3000 HPLC system (Thermo Fisher Scientific). NMR spectra were either recorded at 600 MHz (^{1}H frequency) on a Bruker AV-III spectrometer using a cryogenically cooled 5 mm TCI-triple resonance probe equipped with 1-axis self-shielded gradients at 300 K or at 400 MHz (^{1}H frequency) on an Agilent DD2 spectrometer. Spectra were referenced indirectly. If 1D spectra were not separately recorded, ^{13}C chemical shifts were extracted from the 2D spectra (compounds **1–3**, and **5**).

Cyanobacterial material

Hapalosiphon sp. CBT1235 was taxonomically identified as *Hapalosiphon* sp. on the basis of its morphology. The strain has kindly been provided by Algenol Biotech Inc. (USA) as ABCC 804 and is deposited in the culture collection of the Cyano Biotech GmbH

strengthen the key role of this functional group in regard to the bioactivity of members of the hapalindole family. Our work shows that antiproliferative effects on human T cells are more pronounced than toxicity on human T cells, adding this activity to the wide range of reported bioactivities of the hapalindoles. The mode of action in human immune cells remains to be investigated. Moreover, concerning the fact that hapalindoles have been described to be neurotoxic metabolites [30], detailed studies which further discriminate toxicity and immunomodulatory effects need to be carried out in order to estimate whether or not a development as immunomodulatory drugs would be possible.

Chilczuk T et al. Hapalindoles from the … Planta Med 2020; 86: 96–103

99

26

▶ **Fig. 5** Effects of different hapalindoles on T cell proliferation. Primary human lymphocytes were cultured in the presence of medium (NC) or were stimulated with anti-human CD3 and anti-human CD28 mAb (PC; 100 ng/mL). Activated T cells were further incubated with cyclosporine A (CsA; 5 μg/mL) or different concentrations of 1–5. Cell division analysis was carried out using CFSE staining and flow cytometry. Data of 3 independent experiments are presented as mean ± SD in relation to stimulated T cells (PC = 100%). Asterisks indicate significant differences from PC controls (**$p < 0.01$, ***$p < 0.001$).

(Germany) under the accession number CBT 1235. The strain was cultivated in BG11 medium [39] at 28 °C under continuous light (60–80 μmol m^{2}·s^{-1}) in 20 L scale photobioreactors and harvested semi-continuously over a period of several weeks.

Extraction, bioassay-guided fractionation, and isolation of compounds 1–5

Cyanobacterial cells were harvested and lyophilized. Seven grams dry biomass were suspended in 100 mL 50% methanol in water (v/v), treated with an ultrasonication rod (Bandelin), and extracted on a shaker for 30 min at room temperature. After centrifugation (20 min, 10 800 g), the biomass was extracted using 100 mL 80% methanol (v/v). The solutions were combined and dried under reduced pressure, yielding 0.4 g of biomass extract. For micro-fractionation, 4 mg of extract were suspended in 0.1 mL acetonitrile and separated into 23 fractions by HPLC using a C$_{18}$ column (250 × 4.6 mm, 5 μm, 100 Å, Luna, Phenomenex) and 5–100% acetonitrile-water as the mobile phase at 1 mL/min in 23 min. All fractions were tested for inhibitory activity on T cell proliferation.

For preparative isolation of the active compounds, the remaining extract was dissolved in acetonitrile and fractionated by semi-preparative HPLC using a phenyl-hexyl column (250 × 10 mm, 5 μm, 100 Å, Luna, Phenomenex) and 60–80% acetonitrile-water as the mobile phase at 4.7 mL/min in 25 min to afford 11 fractions. Fraction 1 (t$_R$ 6.8 min) was further purified by an additional round of semi-preparative HPLC using a phenyl-hexyl column (250 × 100 mm, 5 μm, 100 Å, Luna, Phenomenex) and 40–47%

acetonitrile-water as the mobile phase at 9.5 mL/min in 20 min to afford hapalindole A-formamide (4, 5.0 mg, t$_R$ 16.5 min) and hapalindole J-formamide (5, 2.0 mg, t$_R$ 15.1 min). Fraction 6 (t$_R$ 15.2 min) was further purified by semi-preparative HPLC using a pentafluorophenyl column (250 × 100 mm, 5 μm, 100 Å, Luna, Phenomenex) and 45–63% acetonitrile-water as mobile phase at 9.5 mL/min in 30 min yielding hapalindole A (1, 16.1 mg, t$_R$ 18.4 min). No further purification was needed for fraction 8 (t$_R$ 19.2 min) and fraction 10 (t$_R$ 22.4 min), which corresponded to hapalindole D (2, 5.3 mg) and hapalindole M (3, 6.4 mg), respectively.

Hapalindole A (1): $[\alpha]_D^{23}$ − 64.2° (CH$_2$Cl$_2$, c 1.2); HRESIMS (positive ion mode): m/z 339.1616 [M + H]$^+$; NMR spectra, see **Fig. 3S, 4S**.

Hapalindole D (2): $[\alpha]_D^{23}$ + 45.2° (CH$_2$Cl$_2$, c 0.31); HRESIMS (positive ion mode): m/z 337.1727 [M + H]$^+$; NMR spectra, see **Fig. 5S, 6S**.

Hapalindole M (3): $[\alpha]_D^{23}$ − 6.7° (CH$_2$Cl$_2$, c 0.45); HRESIMS (positive ion mode): m/z 337.1727 [M + H]$^+$; NMR spectra, see **Fig. 7S, 8S**.

Hapalindole A-formamide (4): brown oil; $[\alpha]_D^{23}$ − 56.2° (CH$_2$Cl$_2$, c 0.45); UV (MeOH) λ$_{max}$ (log ε): 223 (4.38), 282 (3.60), 292 (3.52) nm; HRESIMS (positive ion mode): m/z 357.1723 [M + H]$^+$ (calcd. for C$_{21}$H$_{25}$N$_2$OCl, 357.1728); NMR data, see ▶ **Table 1**; NMR spectra Fig. 9S–14S.

Hapalindole J-formamide (5): brown oil; $[\alpha]_D^{23}$ + 12.2° (CHCl$_3$, c 0.9); UV (MeOH) λ$_{max}$ (log ε): 224 (4.24), 282 (3.50), 292 (3.41) nm; HRESIMS (positive ion mode): m/z 323.2114 [M + H]$^+$ (calcd.

100

Chilczuk T et al. Hapalindoles from the… Planta Med 2020; 86: 96–103

27
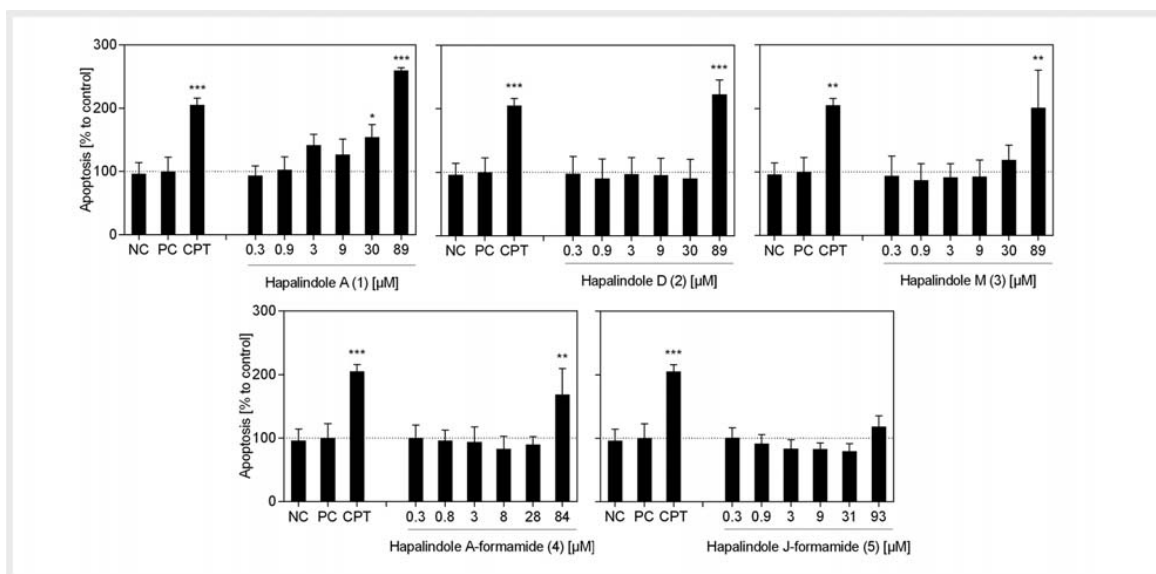
▶ **Fig. 6** Levels of T cell apoptosis after treatment with different hapalindoles. Primary human lymphocytes were cultured in the presence of medium (NC) or were stimulated with anti-human CD3 and anti-human CD28 mAb (PC; 100 ng/mL). Activated T cells were further incubated with camptothecin (CPT; 30 μg/mL) or different concentrations of 1–5. Levels of apoptosis were determined using flow-cytometric analysis of annexin V-stained cells. Data of 3 independent experiments are presented as mean ± SD in relation to stimulated T cells (PC = 100%). Asterisks indicate significant differences from PC controls (**p < 0.01, ***p < 0.001).

for $C_{21}H_{26}N_2O$, 323.2118); NMR data, see ▶ **Table 1**; NMR spectra **Fig. 15S–19S**.

Ethics statement

Written informed consent was obtained from patients prior to blood donation for research purposes. All experiments conducted on human material were approved by the ethics committee of the University Freiburg (55/14; February 11th, 2014).

Preparation and cultivation of human immunocompetent cells

Human PBMC were isolated from the blood of adult donors obtained from the Blood Transfusion Centre (University Medical Center Freiburg). Venous blood was centrifuged on a LymphoPrep gradient (density: 1.077 g/cm³, 20 min, 500 g, 20 °C; Progen). Afterwards, cells were washed twice with medium and cell viability and concentration was determined using the trypan blue exclusion test. Cells were cultured in Roswell Park Memorial Institute (RPMI) 1640 medium (Invitrogen) supplemented with 10% heat-inactivated fetal bovine serum (GE Healthcare), 2 mM L-glutamine, 100 U/mL penicillin and 100 U/mL streptomycin (Invitrogen) at 37 °C in a humidified incubator with a 5% CO_2/95% air atmosphere. PBMC were additionally stimulated with anti-human CD3 (clone OKT3) and anti-human CD28 (clone 28.6) mAb (100 ng/mL; both from eBioscience). Incubation was carried out as indicated in the figure captions in the presence of medium alone, camptothecin (CPT; 30 μg/mL; Tocris), cyclosporine A (CsA, 5 μg/mL, Sandimmun 50 mg/mL, Novartis), or different

concentrations of the *Hapalosiphon* sp. CBT1235 extract (0.01, 0.1, 1, 10 μg/mL), fractions (semi-quantitative using dilutions 1:250, 1:500, 1:1000, 1:2000) or various hapalindoles (0.1, 0.3, 1, 3, 10, 30 μg/mL).

Cell division tracking using CFSE

PBMC were harvested, washed twice in cold PBS (Invitrogen) and resuspended in PBS at a concentration of 5×10^6 cells/mL. CFSE (5 mM; Sigma) was diluted 1/1000 and incubated for 10 min at 37 °C. The staining reaction was stopped by washing twice with complete medium. PBMC were activated as described above and cultured with the *Hapalosiphon* sp. CBT1235 extract, fractions, hapalindoles, or DMSO as a solvent control for 72 h. Cell division progress was analyzed from 3 independent experiments with a BD FACSCalibur flow cytometer using BD CellQuest Pro Software.

Determination of apoptosis and necrosis using annexin V and propidium iodide staining

Cells were cultured as described, and levels of apoptosis and necrosis were determined using annexin V-FITC apoptosis detection kit (eBioscience) according to the manufacturer's instructions. After annexin V and propidium iodide staining, cells were analyzed by flow cytometry. CPT and Triton-X 100 (0.5%; Sigma-Aldrich) were used as positive controls for apoptosis and necrosis, respectively.

Chilczuk T et al. Hapalindoles from the ... Planta Med 2020; 86: 96–103

101

28

Data analysis

For statistical analysis, data were processed with Microsoft Excel and SPSS software (IBM, Version 22.0). Data were adjusted in relation to untreated control cells (= $100\% \pm SD$) and values are presented as mean $\pm SD$. Statistical significance was determined by one-way ANOVA followed by Dunnett's *post hoc* pairwise comparisons. P values < 0.05 were considered as statistically significant (* $p < 0.05$, ** $p < 0.01$, *** $p < 0.001$). IC_{50} and EC_{50} values were determined using GraphPad Prism 6.

Supporting information

^1H, ^{13}C, HSQC, HMBC and NOESY spectra, MS data as well as a chromatogram of the micro-fractionation and the results of the inhibition of T cell proliferation by different *Hapalosiphon* sp. CBT1235 fractions are available as Supporting Information.

Acknowledgements

Conflict of Interest

HE is CSO and co-owner of Cyano Biotech GmbH, DE is CEO and co-owner of Cyano Biotech GmbH. The company does not have any financial interest in the research presented here. The other authors declare no conflicts of interest. The funding sponsors had no role in the design, writing and publishing strategy of the study, nor in collection, analysis or interpretation of the data.

References

[1]   Burja AM, Banaigs B, Abou-Mansour E, Burgess JG, Wright PC. Marine cyanobacteria – a prolific source of natural products. Tetrahedron 2001; 57: 9347–9377

[2]   Dixit RB, Suseela MR. Cyanobacteria: potential candidates for drug discovery. Antonie Van Leeuwenhoek 2013; 103: 947–961

[3]   Welker M, Dittmann E, von Döhren H. Cyanobacteria as a source of natural products. Methods Enzymol 2012; 517: 23–46

[4]   Leao PN, Engene N, Antunes A, Gerwick WH, Vasconcelos V. The chemical ecology of cyanobacteria. Nat Prod Rep 2012; 29: 372–391

[5]   Salvador-Reyes LA, Luesch H. Biological targets and mechanisms of action of natural products from marine cyanobacteria. Nat Prod Rep 2015; 32: 478–503

[6]   Niedermeyer TH. Anti-infective natural products from cyanobacteria. Planta Med 2015; 81: 1309–1325

[7]   Dittmann E, Gugger M, Sivonen K, Fewer DP. Natural product biosynthetic diversity and comparative genomics of the cyanobacteria. Trends Microbiol 2015; 23: 642–652

[8]   Walton K, Berry JP. Indole alkaloids of the stigonematales (cyanophyta): chemical diversity, biosynthesis and biological activity. Mar Drugs 2016; 14: 73

[9]   Moore RE, Cheuk C, Patterson GML. Hapalindoles: new alkaloids from the blue-green alga *Hapalosiphon fontinalis*. J Am Chem Soc 1984; 106: 6456–6457

[10] Moore RE, Cheuk C, Yang XQG, Patterson GML, Bonjouklian R, Smitka TA, Mynderse JS, Foster RS, Jones ND, Swartzendruber JK, Deeter JB. Hapalindoles, antibacterial and antimycotic alkaloids from the cyanophyte *Hapalosiphon fontinalis*. J Org Chem 1987; 291: 1036–1043

[11] Schwartz RE, Hirsch CF, Springer JP, Pettibone DJ, Zink DL. Unusual cyclopropane-containing hapalindolinones from a cultured cyanobacterium. J Org Chem 1987; 52: 3704–3706

[12] Moore RE, Yang XQG, Patterson GML, Bonjouklian R, Smitka TA. Hapalonamides and other oxidized hapalindoles from *Hapalosiphon fontinalis*. Phytochemistry 1989; 28: 1565–1567

[13] Park A, Moore RE, Patterson GML. Fischerindole L, a new isonitrile from the terrestrial blue-green alga *Fischerella muscicola*. Tetrahedron Lett 1992; 33: 3257–3260

[14] Smitka TA, Bonjouklian R, Doolin L, Jones ND, Deeter JB, Yoshida WY, Prinsep MR, Moore RE, Patterson GML. Ambiguine isonitriles, fungicidal hapalindole-type alkaloids from 3 genera of blue-green algae belonging to the Stigonemataceae. J Org Chem 1992; 57: 857–861

[15] Stratmann K, Moore RE, Bonjouklian R, Deeter JB, Patterson GML, Shaffer S, Smith CD, Smitka TA. Welwitindolinones, unusual alkaloids from the blue-green algae *Hapalosiphon welwitschii* and *Westiella intricata*. Relationship to fischerindoles and hapalindoles. J Am Chem Soc 1994; 116: 9935–9942

[16] Huber U, Moore RE, Patterson GML. Isolation of a nitrile-containing indole alkaloid from the terrestrial blue-green alga *Hapalosiphon delicatulus*. J Nat Prod 1998; 61: 1304–1306

[17] Asthana RK, Srivastava A, Singh AP, Singh SP, Nath G, Srivastava R, Srivastava BS. Identification of an antimicrobial entity from the cyanobacterium *Fischerella* sp. isolated from bark of *Azadirachta indica* (Neem) tree. J Appl Phycol 2006; 18: 33–39

[18] Becher PG, Keller S, Jung G, Süssmuth RD, Jüttner F. Insecticidal activity of 12-epi-hapalindole J isonitrile. Phytochemistry 2007; 68: 2493–2497

[19] Mo S, Krunic A, Chlipala G, Orjala J. Antimicrobial ambiguine isonitriles from the cyanobacterium *Fischerella ambigua*. J Nat Prod 2009; 72: 894–899

[20] Mo S, Krunic A, Santarsiero BD, Franzblau SG, Orjala J. Hapalindole-related alkaloids from the cultured cyanobacterium *Fischerella ambigua*. Phytochemistry 2010; 71: 2116–2123

[21] Kim H, Lantvit D, Hwang CH, Kroll DJ, Swanson SM, Franzblau SG, Orjala J. Indole alkaloids from 2 cultured cyanobacteria, *Westiellopsis* sp. and *Fischerella muscicola*. Bioorg Med Chem 2012; 20: 5290–5295

[22] Kim H, Krunic A, Lantvit D, Shen Q, Kroll DJ, Swanson SM, Orjala J. Nitrile-containing fischerindoles from the cultured cyanobacterium *Fischerella* sp. Tetrahedron 2012; 68: 3205–3209

[23] Walton K, Gantar M, Gibbs PDL, Schmale MC, Berry JP. Indole alkaloids from *Fischerella* inhibit vertebrate development in the zebrafish (*Danio rerio*) embryo model. Toxins (Basel) 2014; 6: 3568–3581

[24] Raveh A, Carmeli S. Antimicrobial ambiguines from the cyanobacterium *Fischerella* sp. collected in Israel. J Nat Prod 2007; 70: 196–201

[25] Bhat V, Dave A, MacKay JA, Rawal VH. The chemistry of hapalindoles, fischerindoles, ambiguines, and welwitindolinones. Alkaloids Chem Biol 2014; 73: 65–160

[26] Klein D, Daloze D, Braekman JC, Hoffmann L, Demoulin V. New hapalindoles from the cyanophyte *Hapalosiphon laingii*. J Nat Prod 1995; 58: 1781–1785

[27] Doan NT, Rickards RW, Rothschild JM, Smith GD, Thanh Doan N. Allelopathic actions of the alkaloid 12-epi-hapalindole E isonitrile and calothrixin A from cyanobacteria of the genera *Fischerella* and *Calothrix*. J Appl Phycol 2000; 12: 409–416

[28] Doan NT, Stewart PR, Smith GD. Inhibition of bacterial RNA polymerase by the cyanobacterial metabolites 12-epi-hapalindole E isonitrile and calothrixin A. FEMS Microbiol Lett 2001; 196: 135–139

102   Chilczuk T et al. Hapalindoles from the… Planta Med 2020; 86: 96–103

29

2. Publications

[29] Becher PG, Jüttner F. Insecticidal compounds of the biofilm-forming cyanobacterium *Fischerella* sp. (ATCC 43239). Environ Toxicol 2005; 20: 363–372

[30] Cagide E, Becher PG, Louzao MC, Espiña B, Vieytes MR, Jüttner F, Botana LM. Hapalindoles from the cyanobacterium *Fischerella*: potential sodium channel modulators. Chem Res Toxicol 2014; 27: 1696–1706

[31] Bonjouklian R, Moore RE, Patterson GML. Acid-catalyzed reactions of hapalindoles. J Org Chem 1988; 53: 5866–5870

[32] Muratake H, Natsume M. Synthetic studies of marine alkaloids hapalindoles. Part I Total synthesis of (±)-hapalindoles J and M. Tetrahedron 1990; 46: 6331–6342

[33] Schwartz E, Hirsch CF, Sesin DF, Flor JE, Chartrain M, Fromtling E, Harris GH, Salvatore MJ, Liesch JM, Yudin K. Pharmaceuticals from cultured algae. J Ind Microbiol 1990; 5: 113–124

[34] Wagner MM, Shih C, Jordan A, Williams DC. *In vitro* pharmacology of cryptophycin 52 (LY355703) in human tumor cell lines. Cancer Chemother Pharmacol 1999; 43: 115–125

[35] Eggen M, Georg GI. The cryptophycins: their synthesis and anticancer activity. Med Res Rev 2002; 22: 85–101

[36] Rohr J. Cryptophycin anticancer drugs revisited. ACS Chem Biol 2006; 1: 747–750

[37] Fukuyama T, Chen X. Stereocontrolled synthesis of (−)-hapalindole G. J Am Chem Soc 1994; 116: 3125–3126

[38] Chandra A, Johnston JN. Total synthesis of the chlorine-containing hapalindoles K, A, and G. Angew Chem Int Ed Engl 2011; 50: 7641–7644

[39] Andersen RA. Algal culturing Techniques. Burlington, MA: Elsevier Academic Press; 2005

Chilczuk T et al. Hapalindoles from the … Planta Med 2020; 86: 96–103   **103**

30

[2]: Nostotrebin 6 Related Cyclopentenediones and δ-Lactones with Broad Activity Spectrum Isolated from the Cultivation Medium of the Cyanobacterium *Nostoc* sp. CBT1153

The published work can be retrieved online under the direct link:
https://pubs.acs.org/articlesonrequest/AOR-SAnbhRMG9Gv2UimgNxq3

2. Publications

Summary

Neglected for a long time, the search for novel anti–infective NPs as potential new drug leads has caught a new momentum during the last two decades. Cyanobacteria are a (in)famous source for chemically diverse and potent NPs, especially protease inhibitors. The following publication describes the search for new inhibitors of the trypanosomal cystein protease rhodesain, a potential target for the treatment of the human African trypanosomiasis (HAT), also known as sleeping sickness. A library of 572 cyanobacteria extracts was screened, and a medium extract of *Nostoc* sp. CBT1153 was found to exhibit a high activity against rhodesain. Here, we present the identification of the homodimeric cyclopentenedione (CPD) nostotrebin 6 and new related monomeric, dimeric, and higher oligomeric compounds as the active substances. Two core monomeric structures build the base for the oligomeric compounds: a trisubstituted CPD or a trisubstituted unsaturated δ-lactone. Nostotrebin 6 has been isolated earlier and found to be active in a huge variety of assays, indicating an unspecific bioactivity and possibly that it might be a pan-assay interference compound (PAIN). In order to evaluate this broad suspicious bioactivity, we compared the anti–bacterial and cytotoxic activities, as well as the rhodesain inhibition of the newly isolated CPDs. The compound with the δ-lactone core structure was equally active as nostotrebin 6 in all bioactivity assays. These findings disprove the former hypothesis which postulated the chemically reactive CPD substructure to be responsible for the broad bioactivity spectrum. The newly isolated monomer exhibited a weaker activity than the respective dimers. Hence, our data further suggests that the bioactivities depend on the number of free phenolic hydroxy groups per molecule rather than on the CPD core structure.

We further discuss the potential physiological roles of CPDs which has not yet been studied in detail. Due to their presence in the cultivation medium, possible roles include protective functions against bacterial and fungal pathogens and/or protection against UV irradiation.

Nostotrebin 6 Related Cyclopentenediones and δ-Lactones with Broad Activity Spectrum Isolated from the Cultivation Medium of the Cyanobacterium *Nostoc* sp. CBT1153

Ronja Kossack, Steffen Breinlinger, Trang Nguyen, Julia Moschny, Jan Straetener, Anne Berscheid, Heike Brötz-Oesterhelt, Heike Enke, Tanja Schirmeister, and Timo H. J. Niedermeyer*

ACCESS | Metrics & More | Article Recommendations | Supporting Information

ABSTRACT: Cyanobacteria are an interesting source of biologically active natural products, especially chemically diverse and potent protease inhibitors. On our search for inhibitors of the trypanosomal cysteine protease rhodesain, we identified the homodimeric cyclopentenedione (CPD) nostotrebin 6 (**1**) and new related monomeric, dimeric, and higher oligomeric compounds as the active substances in the medium extract of *Nostoc* sp. CBT1153. The oligomeric compounds are composed of two core monomeric structures, a trisubstituted CPD or a trisubstituted unsaturated δ-lactone. Nostotrebin 6 thus far has been the only known cyanobacterial CPD. It has been found to be active in a broad variety of assays, indicating that it might be a pan-assay interference compound (PAIN). Thus, we compared the antibacterial and cytotoxic activities as well as the rhodesain inhibition of selected compounds. Because a compound with a δ-lactone instead of a CPD core structure was equally active as nostotrebin 6, the bioactivities of these compounds seem to be based on the phenolic substructures rather than the CPD moiety. While the dimers were roughly equally potent, the monomer displayed slightly weaker activity, suggesting that the compounds show unspecific activity depending upon the number of free phenolic hydroxy groups per molecule.
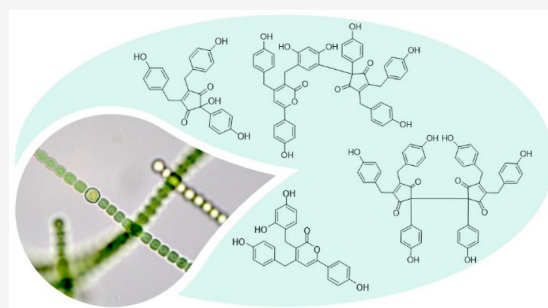
Neglected by natural product researchers for a long time, cyanobacteria are nowadays recognized as a prolific source of structurally diverse and pharmacologically active natural products.[1−6] Several cyanobacterial specialized metabolites have served as potent lead structures inspiring drug development programs, e.g., the dolastatins,[7−9] the cryptophycins,[10−12] the saxitoxins,[13,14] and the anabaenopeptins.[15,16] One of the better studied cyanobacteria genera is *Nostoc*, from which numerous compounds have been isolated.[6,17] These are mainly non-ribosomal peptides and depsipeptides, but a variety of other chemically diverse structures, such as, e.g., polyketides, alkaloids, or terpenoids, were also found.

About 100 natural cyclopentenediones (CPDs) were isolated from various sources, like higher plants,[18,19] fungi,[20,21] and bacteria.[22,23] Most of those CPDs are based on a cyclopent-4-ene-1,3-dione, varying in the side chains. The biosynthesis of CPDs has not yet been explored, but several synthetic routes were described.[24−26] The only cyanobacterial CPD known to date is the *Nostoc* metabolite nostotrebin 6 (**1**), a homodimer built of two identical 4,5-bis(4-hydroxybenzyl)-2-(4-hydroxyphenyl)cyclopent-4-ene-1,3-dione units. Compound **1** was discovered in a *Nostoc* sp. biomass extract as a result of its acetylcholinesterase (AChE) and butyrylcholinesterase (BChE) inhibitory activities.[27,28] In addition, cytotoxicity and pro-

apoptotic activity on mouse fibroblasts as well as antimicrobial activity, especially against Gram-positive bacteria, have been reported for the compound.[29,30]

Often, cyanobacterial specialized metabolites show pronounced cytotoxicity, but another activity that is frequently observed for cyanobacterial non-ribosomal peptides is the inhibition of proteases.[31−36] The cathepsin L-like cysteine protease rhodesain plays an important role during human infection with *Trypanosoma brucei*, known as human African trypanosomiasis (HAT).[37] It is involved in the parasitic crossing of the blood−brain barrier, leading to the late stage of HAT.[38] Furthermore, rhodesain is involved in the synthesis of variant surface glycoproteins (VSGs) of the trypanosomes, enabling *T. brucei* to elude the host immune response.[39] Because of its essential physiological role in the metabolism of the parasite, rhodesain is regarded as a promising target for the development of urgently needed new therapeutics.[37]
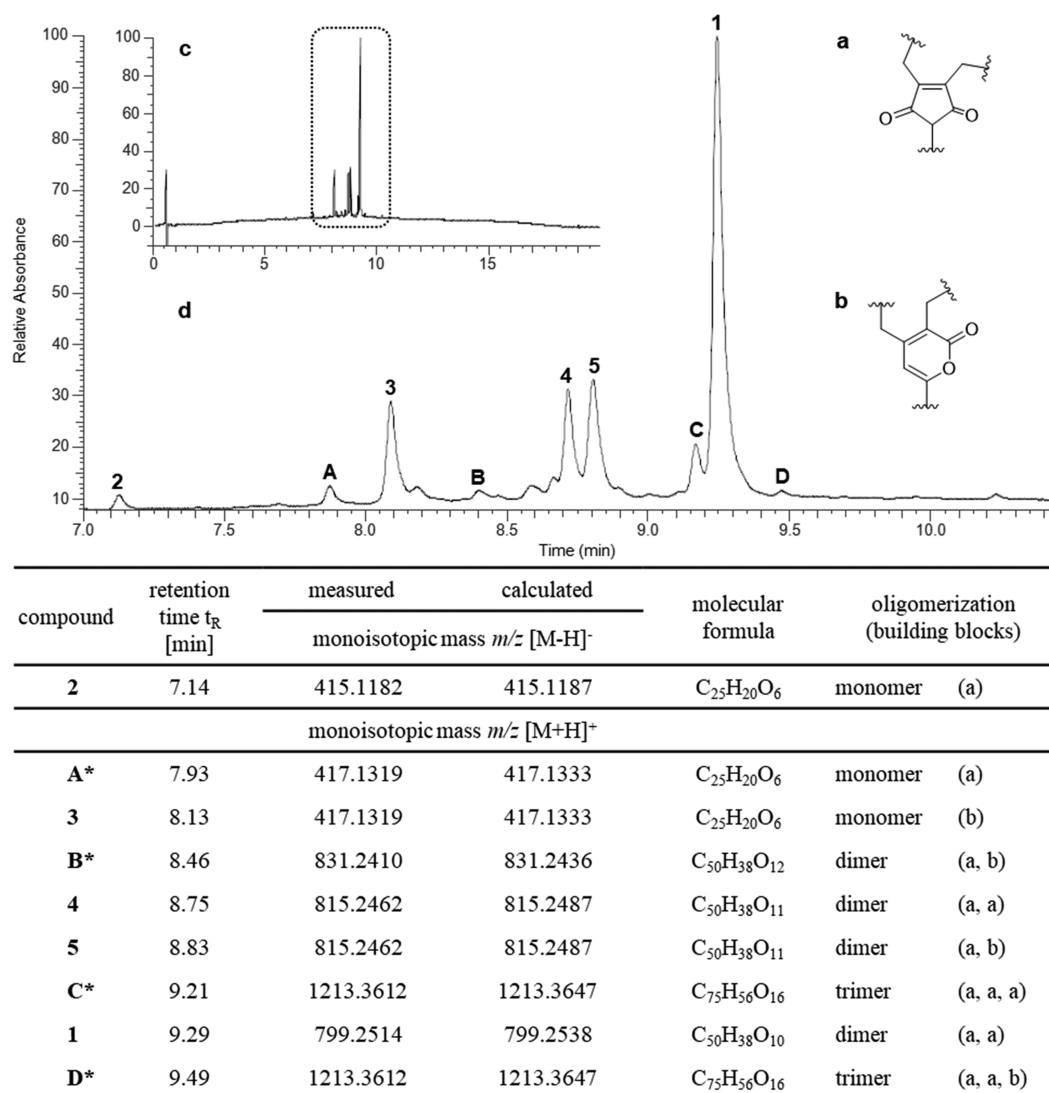
compound	retention time t_R [min]	measured	calculated	molecular formula	oligomerization (building blocks)	
		monoisotopic mass m/z [M-H]$^-$				
2	7.14	415.1182	415.1187	$C_{25}H_{20}O_6$	monomer	(a)
		monoisotopic mass m/z [M+H]$^+$				
A*	7.93	417.1319	417.1333	$C_{25}H_{20}O_6$	monomer	(a)
3	8.13	417.1319	417.1333	$C_{25}H_{20}O_6$	monomer	(b)
B*	8.46	831.2410	831.2436	$C_{50}H_{38}O_{12}$	dimer	(a, b)
4	8.75	815.2462	815.2487	$C_{50}H_{38}O_{11}$	dimer	(a, a)
5	8.83	815.2462	815.2487	$C_{50}H_{38}O_{11}$	dimer	(a, b)
C*	9.21	1213.3612	1213.3647	$C_{75}H_{56}O_{16}$	trimer	(a, a, a)
1	9.29	799.2514	799.2538	$C_{50}H_{38}O_{10}$	dimer	(a, a)
D*	9.49	1213.3612	1213.3647	$C_{75}H_{56}O_{16}$	trimer	(a, a, b)

Figure 1. Nostotrebin 6 (**1**) and derivatives based on a (a) CPD or (b) δ-lactone core structure, biosynthesized by *Nostoc* sp. CBT1153. (c) HPLC−UV chromatogram overview (λ = 230 nm) of the *Nostoc* sp. CBT1153 medium extract. (d) HPLC−UV chromatogram, with t_R of 7.0−10.5 min. (∗) Not fully structure-elucidated compounds; the structures were proposed on the basis of HRMS^2 and UV spectroscopy data.

Our ongoing search for specialized metabolites from cyanobacteria combined with our interest in finding novel anti-infective natural products prompted us to screen a library of 572 cyanobacteria extracts for inhibitors of the trypanosomal protease rhodesain. A medium extract from *Nostoc* sp. CBT1153 revealed not only high biological activity against rhodesain but also a rather simple chemical composition. Until today, most cyanobacterial natural products were isolated from biomass and only few compounds from cyanobacteria cultivation media are known.[40−43] Therefore, we set out to isolate and characterize the rhodesain-inhibiting compounds found in this medium extract, identifying compound **1** and several new biosynthetically related compounds as active substances.
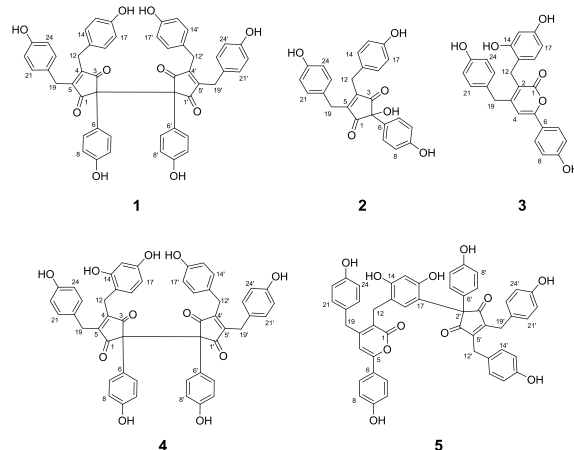
■ RESULTS AND DISCUSSION

Isolation and Structure Elucidation. Our screening of a cyanobacteria extract collection (450 biomass extracts and 122 medium extracts) against the cysteine protease rhodesain resulted in 9 biomass extracts with an inhibitory activity of more than 80% at 0.1 mg/mL and 14 medium extracts with an inhibition higher than 80% at 0.2 mg/mL. With inhibition of >90%, an extract from the culture medium of *Nostoc* sp. CBT1153 revealed prominent activity, while the corresponding biomass extract showed inhibition of 89% at 0.33 mg/mL. This raised our interest, because only few compounds have been isolated from cyanobacteria cultivation media to date. A comparison of the chromatographic profiles showed that the biomass and medium extracts contained the same major compounds (Figure S1 of the Supporting Information). However, because the medium extract did not contain any hydrophilic metabolites or chlorophylls, we decided to proceed with the medium extract. The main substance present in the medium extract as well as in the biomass extract of this *Nostoc* strain could quickly be dereplicated by high-resolution tandem mass spectrometry (HRMS[2]) to the CPD homodimer nostotrebin 6 (**1**), which was first isolated from a *Nostoc* sp. biomass extract by Zelik et al. in 2010.[30] Because we later isolated the compound for comparative bioactivity testing, the dereplication was also confirmed by one-dimensional (1D) and two-dimensional (2D) nuclear magnetic resonance (NMR) data.

Fractionation and subsequent bioactivity testing showed that the inhibitory activity was caused by not only compound **1**, but also the other substances present in the extract. Intriguingly, the molecular masses and the respective calculated sum formulas as well as the tandem mass spectrometry (MS[2]) spectra of these compounds indicated a structural relationship with the homodimeric CPD **1** and hinted at the presence of monomeric, dimeric, and higher oligomeric forms of a common core structure (Figure 1). More detailed evaluation of the high-performance liquid chromatography−mass spectrometry (HPLC−MS) data showed that the extract contained at least four putative monomeric, eight dimeric, and three trimeric compounds (Figure S3 of the Supporting Information). Trace amounts of tetrameric structures could be detected. Four new mono- and dimeric derivatives were isolated in sufficient yield for structure elucidation by 1D and 2D NMR experiments.

Compound **2** was isolated as a yellow amorphous powder. The molecular formula $C_{25}H_{20}O_6$ was calculated from the [M − H]⁻ ion at *m/z* 415.1182. The ¹H NMR spectrum showed only five distinct proton signals, indicating a highly symmetric structure. Four signals were found in the aromatic region (integrals of 4, 4, 2, and 2), and two doublets were observed around δ_H 3.75 (integral of 4). On the basis of the sum formula and the ¹H NMR spectrum, we assumed compound **2** to be related to the monomeric building block of compound **1** (core structure a), with an additional hydroxy group being present. Structure elucidation via 2D NMR experiments was straightforward. Heteronuclear multiple-bond correlations (HMBCs) and the ¹³C chemical shifts were similar to compound **1** (see Figure 2 and Table 1), except C-2 as well as C-6, which were deshielded by more than 15 and 7 ppm, respectively. The NMR data thus confirmed the presence of a hydroxy group at C-2 (instead of the second monomer in compound **1**). Similar intramolecular interactions as in compound **1** can be expected in compound **2** (intramolecular hydrogen bonds and stacking interactions
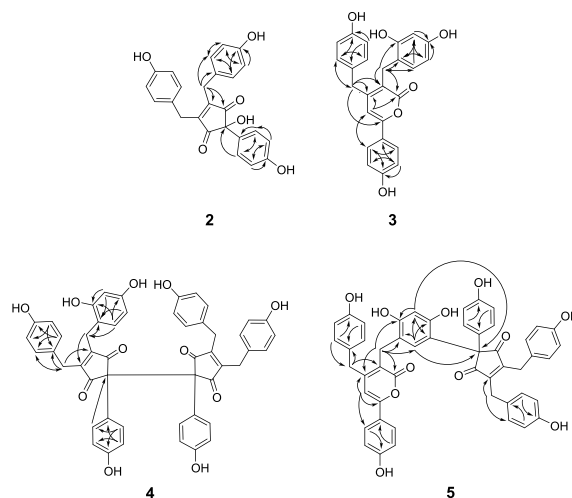
Figure 2. HMBC correlations of compounds **2**, **3**, **4**, and **5**, indicated by arrows.

between the aromatics),[28] resulting in a restricted rotation of the substituents of the CPD. Thus, as in compound **1**, the methylene protons at C-12 and C-19 in compound **2** are magnetically inequivalent, showing geminal coupling. Being the monomer of nostotrebin 6 with an additional hydroxy group, compound **2** was named nostotrebinol 3.

Compound **3** was isolated as a yellow amorphous powder. HRMS analysis resulted in a [M + H]⁺ ion at *m/z* 417.1319 from which the molecular formula $C_{25}H_{20}O_6$ was calculated, suggesting this compound to be composed of just one of the monomers present in compound **1**, carrying an additional hydroxy group. Four singlet signals in the region near δ_H 9 were observed in the ¹H spectrum, and one of these broad singlets was further deshielded, indicating increased acidity. ¹³C chemical shifts were determined via heteronuclear single-quantum correlation (HSQC) and HMBC experiments. The data indicated that compound **3** was not simply a hydroxylated monomer of compound **1**, because the ¹³C signals for the keto groups of the CPD substructure (δ_C >200) were missing. Instead, the ¹³C shift for C-1 (δ_C 170) and HMBCs pointed to a δ-lactone core structure (core structure b). The conjugation of the *p*-hydroxyphenyl group with the lactone via the C-5−C-6 bond accounts for the broad singlet at δ_H ~9.5 (vinylogous phenylogous carboxylic acid). Similar to compound **1**, two hydroxybenzyl substituents are attached to the δ-lactone at C-2 and C-3. Chemical shifts differ slightly as a result of the additional *m*-hydroxy group in one of the hydroxyphenyl substituents but are similar to compound **1** overall (Table 1). HMBC key correlations are depicted in Figure 2. In comparison to compound **1**, the ultraviolet (UV) spectrum of compound **3** features an additional maximum at 360 nm with equal intensity as the maximum at 223 nm (Figure S2 of the Supporting Information). Because compound **3** contains a lactone core structure and four hydroxy groups, it was named nostolactone 4.

Compound **4** was isolated as an orange amorphous solid. The detected protonated molecule [M + H]⁺ at *m/z* 815.2462 suggested a molecular formula of $C_{50}H_{38}O_{11}$, indicating the presence of an additional hydroxy group in comparison to compound **1**. Indeed, the ¹H NMR spectrum of compound **4** showed that the compound is not symmetrical, featuring three

Table 1. ^{1}H (600 MHz) and ^{13}C (150 MHz) NMR Spectroscopic Data of Monomeric Compounds 2 and 3 in DMSO-d_6

position	2 δ_C, type	2 δ_H (J in Hz)	3 δ_C, type	3 δ_H (J in Hz)
1	202.0, C		169.7, C	
2	75.2, C		125.1, C	
3	202.0, C		151.7, C	
4	156.2, C		109.7, CH	6.26, s
5	156.2, C		145.5, C	
6	127.3, C		124.2, C	
7	126.9, CH	6.84, m	131.7, CH	7.55, d (8.8)
8	114.9, CH	6.59, m	115.7, CH	6.80, d (8.8)
9	157.2, C		158.3, C	
10	114.9, CH	6.59, m	115.7, CH	6.80, d (8.8)
11	126.9, CH	6.84, m	131.7, CH	7.55, d (8.8)
12a	28.5, CH$_2$	3.74, d (14.5)	22.6, CH$_2$	3.49 (s)
12b		3.77, d (14.5)		
13	126.4, C		114.4, C	
14	129.7, CH	6.91, d (8.6)	155.3, C	
15	115.3, CH	6.62, m	102.2, CH	6.28, d (1.0)
16	156.2, C		156.5, C	
17	115.3, CH	6.62, m	105.9, CH	6.11, dd (8.2, 2.5)
18	129.7, CH	6.91, d (8.6)	129.8, CH	6.76, d (8.2)
19a	28.5, CH$_2$	3.74, d (14.5)	28.4, CH$_2$	3.86, s
19b		3.77, d (14.5)		
20	126.4, C		128.0, C	
21	129.7, CH	6.91, d (8.6)	129.1, CH	7.01, m
22	115.3, CH	6.62, m	115.2, CH	6.65, m
23	156.2, C		155.8, C	
24	115.3, CH	6.62, m	115.2, CH	6.65, m
25	129.7, CH	6.91, d (8.6)	129.1, CH	7.01, m
OH		OH 9.45, br s		OH 9.07
OH		OH 9.45, br s		OH 9.27
OH		OH 9.45, br s		OH 9.41
OH		OH 9.45, br s		OH 9.92

doublets in the aromatic region with an integral of 1 each. Coupling constants of 8.25 and 2.4 Hz indicated a *m*-dihydroxy-substituted phenyl residue. This substitution pattern was confirmed via correlations in the HMBC spectrum (Figure 2). The remaining proton and carbon signals are in good accordance with the data for compound **1** (Table 2). The UV spectrum of compound **5** is virtually identical to the spectrum of compound **1**. Because the only structural difference between compounds **1** and **4** is the presence of one additional hydroxy group (7 instead of 6), compound **4** was named nostotrebin 7.

Compound **5**, isolated as a yellow amorphous solid, has the same molecular formula as compound **4** ([M + H]$^+$ ion at *m/z* 815.2462). Intriguingly, evaluation of the ^{1}H and ^{13}C NMR spectra revealed that this compound contains both the monomer **3** (core structure b) and the CPD monomer (core structure a) found in compound **1**, forming a heterodimer. Evaluation of the 2D NMR data showed a strong HMBC of H-18 and C-2′ (Figure 2), indicating that the two monomeric building blocks are not, as expected, connected by a covalent bond between the monomer cores but that the CPD monomer is an additional substituent at the dihydroxy-substituted phenyl group of the δ-lactone monomer (covalent bond between C-17 and C-2′). The presence of monomer **3** in compound **5** is confirmed by the UV spectrum of compound **5**, which also shows an absorption maximum at 360 nm. Interestingly, because the dimer **5** only contains one δ-lactone monomer, the maximum at 360 nm is only about half as intense as the

maximum at 230 nm. As a result of its dimeric structure, comprising one lactone and one CPD monomer, with in total seven hydroxy groups, compound **5** was named nostotrebinlactone 7.

Compounds **A**, **B**, **C**, and **D** could not be isolated in sufficient amounts for unambiguous structure elucidation. However, their HRMS^2 and UV spectra clearly showed that they are composed of the basic core structures a and b (Figure 1 and the Supporting Information). Their deduced structural features are discussed in the Supporting Information.

In addition to the compounds discussed above, several additional monomers, dimers, and trimers could be detected by HPLC−MS (Figure S3 of the Supporting Information). These compounds mainly differ in the number of hydroxy groups. Intriguingly, we could also detect minor amounts of two tetramers (C$_{100}$H$_{76}$O$_{22}$ and C$_{100}$H$_{74}$O$_{22}$; Figure S3 of the Supporting Information). We suspect that the oligomerization of the two monomers is not enzyme-catalyzed but due to their general chemical reactivity, resulting in an array of compounds differing mainly in the monomers that reacted and the extent of hydroxylation. This non-enzymatic oligomerization is also supported by the fact that compounds **4** and **5** are not optically active.

Bioactivity Characterization. Nostotrebin 6 (**1**) was first isolated from the extract of *Nostoc* sp. str. Lukešová 27/97, which was highly active in a screening for AChE inhibitors (Table 3).[27] Although HPLC analysis of this extract revealed compound **1** as

Table 2. ^{1}H (600 MHz) and ^{13}C (150 MHz) NMR Spectroscopic Data of Dimeric Compounds 1, 4, and 5 in DMSO-d_6

position	1 δ_C	1 δ_H (J in Hz)	4 δ_C, type	4 δ_C, type	4 δ_H (J in Hz)	4 δ_H (J in Hz)	5 δ_C, type	5 δ_C, type	5 δ_H (J in Hz)	5 δ_H (J in Hz)
1	nd^a		nd	nd			169.6, C	nd		
2	61.2, C		58.1, C	58.1, C			125.0, C	61.2, C		
3	nd		nd	nd			151.5, C	nd		
4	155.0, C		155,^{b} C	155,^{b} C			109.7, CH	152.9, CH	6.13, m	
5	155.0, C		155,^{b} C	155,^{b} C			145.5, C	152.9, C		
6	120.3, C		120.3, C	120.3, C			124.2, C	124.6, C		
7	130.5, CH	6.457, m	130.8, CH	130.8, CH	6.46, m	6.46, m	131.9, CH	129.2, CH	7.52, br d (8.7)	6.85, br d (8.7)
8	113.6, CH	6.46, m	113.9, CH	113.9, CH	6.46, d (1.5)	6.46, d (1.5)	115.8, CH	115.3, CH	6.80, br d (8.9)	6.62, br d (8.7)
9	156.9, C		157.2, C	157.2, C			158.1, C	156.9, C		
10	113.6, CH	6.46, m	113.9, CH	113.9, CH	6.46, d (1.5)	6.46, d (1.5)	115.8, CH	115.3, CH	6.80, br d (8.9)	6.62, br d (8.7)
11	130.5, CH	6.457, m	130.8, CH	130.8, CH	6.46, m	6.46, m	131.9, CH	129.2, CH	7.52, br d (8.7)	6.85, br d (8.7)
12	28.0, CH$_2$	3.56, br d (14.3)	22.4, CH$_2$	28.0, CH$_2$	3.46, br d (3.3)	3.55, m	22.7, CH$_2$	28.0, CH$_2$	3.30, br s	3.62, s
13	126.4, C		112.8, C	126.3, C			113.6, C	126.8, C		
14	129.4, CH	6.72, d (8.4)	156.9, C	129.4, CH		6.72, m	155.0, CH	129.4, CH		6.82, m
15	115.1, CH	6.52, d (8.4)	102.3, CH	115.1, CH	6.22, d (2.4)	6.52, m	101.7, CH	115.1, CH	6.24, s	6.56, m
16	155.7, C		155.7, C	155.8, C			153.7, C	155.7, C		
17	115.1, CH	6.52, d (8.4)	106.0, CH	115.1, CH	5.96, m	6.52, m	117.3, C	115.1, CH		6.56, m
18	129.4, CH	6.72, d (8.4)	129.9, CH	129.4, CH	6.42, d (8.25)	6.72, m	132.6, CH	129.4, CH	6.14, m	6.82, m
19	28.0, CH$_2$	3.56, br d (14.3)	28.0, CH$_2$	28.0, CH$_2$	3.55, m	3.55, m	28.6, CH$_2$	28.0, CH$_2$	3.66, s	3.62, s
20	126.4, C		112.8, C	126.3, C			127.8, C	126.8, C		
21	129.4, CH	6.72, d (8.4)	129.4, CH	129.4, CH	6.72, m	6.72, m	129.2, C	129.4, CH	6.9, br d (8.2)	6.82, m
22	115.1, CH	6.52, d (8.4)	115.1, CH	115.1, CH	6.52, m	6.52, m	115.4, CH	115.1, CH	6.65, br d (8.5)	6.56, m
23	155.7, C		155.8, C	155.8, C			155.8, C	155.7, C		
24	115.1, CH	6.52, d (8.4)	115.1, CH	115.1, CH	6.52, m	6.52, m	115.4, CH	115.1, CH	6.65, br d (8.5)	6.56, m
25	129.4, CH	6.72, d (8.4)	129.4, CH	129.4, CH	6.72, m	6.72, m	129.2, CH	129.4, CH	6.9, br d (8.2)	6.82, m
OH		2×OH 9.47, br s			2×OH 9.0–9.7,^{b} m				2×OH 9.25, br s	
OH		4×OH 9.21, br s			3×OH 9.0–9.7,^{b} m				3×OH 9.46, br s	
OH					OH 9.0–9.7,^{b} m				OH 9.90, br s	
OH					OH 9.0–9.7,^{b} m				OH 10.13, br s	

^{a} nd = not detected. ^{b} Overlapping ^{13}C and ^{1}H resonances.

Table 3. Inhibitory Effects of Compounds 1, 3, and 5[a]

compound	IC$_{50}$ (μM)		MIC (μM)		
	rhodesain	HeLa cells	*B. subtilis* 168	*E. faecium* BM4147-1	*S. aureus* ATCC29213
1	15 ± 2	16 ± 9	13	13	13
5	33 ± 4	33 ± 9	3	13	3
3	63 ± 3	84 ± 13	50	100	50

[a]half maximal inhibitory concentrations (IC$_{50}$) of compounds **1**, **3**, and **5** against rhodesain and HeLa cells (*n* = 3) and minimal inhibitory concentrations (MICs) of compounds **1**, **3**, and **5** against selected Gram-positive bacteria (*n* = 3).

the main compound, several minor peaks were detected as well but not characterized at that time.[28] Compound **1** was also found to be cytotoxic and pro-apoptotic on mouse fibroblasts (BALB/c)[29] as well as antibacterial against Gram-positive bacteria (Table S1 of the Supporting Information)[30] and suggested as lead structure for drug development.[24] However, because compound **1** is a polyphenolic compound, caution might be appropriate. Showing such a broad variety of bioactivities in seemingly unrelated assays, the compound can be suspected to be a pan-assay interference compound (PAIN).[44,45] To either confirm compound **1** and its derivatives are PAINs or to establish structure−activity relationships for this compound family, we performed a comparative activity testing with compound **3** as the monomer, compound **1** as the homodimer, and compound **5** as the heterodimer. Therefore, we assessed the cytotoxicity on HeLa cells, the antibacterial activity against *Bacillus subtilis*, *Enterococcus faecium*, and *Staphylococcus aureus*, and the rhodesain inhibition potency. Results are summarized in Table 3.

The IC$_{50}$ of compound **1** against HeLa cells (16 μM) was comparable to published data,[29] while compounds **5** (IC$_{50}$ = 33 μM) and **3** (IC$_{50}$ = 84 μM) were slightly less active. Our results also confirmed published data concerning the antimicrobial activity of compound **1** against selected Gram-positive bacteria.[30] Compound **1** and the two tested derivatives were active against *B. subtilis* 168, *E. faecium* BM4147-1, and *S. aureus* ATCC29213, with MICs of 13 μM for compound **1**, 3−13 μM for compound **6**, and 50−100 μM for compound **3** (Table 3).

Inhibition of rhodesain was tested in a standard fluorescence assay[46] by measuring the fluorescence increase as a result of the hydrolysis of Cbz-Phe-Arg-AMC in the absence or presence of inhibitor. To investigate the inhibition mechanism (time dependency, unspecific thiol reactivity, and unspecific inhibition by aggregation[46,47]), more detailed experiments were performed with compound **1** as the major representative of this compound family. The residual activity of rhodesain after 5, 10, and 30 min incubation time of enzyme and compound **1** prior to substrate addition ([S] = 10 μM) was measured. The inhibition was found to be not time-dependent.[48] The presence of the low-molecular-weight sulfur nucleophile dithiothreitol (DTT, 4.75 mM) did not have any influence on the inhibition of rhodesain by compound **1** (Figure S5 of the Supporting Information). Therefore, it can be excluded that the compound reacts unspecifically with thiols.[46,49] Unspecific inhibition by aggregation was excluded by the addition of the non-ionic detergent Brij 35 (0.005 and 0.025%; Supporting Information).[46,47] Thus, prominent error sources in fluorometric assays[47] could be discarded. Additionally, the inner filter effects for compounds **1**, **3**, and **5** were calculated and included in the calculations of IC$_{50}$

values, because in fluorometric assays, yellow-colored substances are known to potentially absorb light at the wavelength of interest. Slight differences in the inhibitory activity of compounds became apparent (Table 3). While compound **1** revealed an IC$_{50}$ of 15 μM against rhodesain (comparable to the IC$_{50}$ against BChE and AChE[28]), compound **5** showed a higher IC$_{50}$ value of 33 μM and compound **3** again was less active (IC$_{50}$ = 66 μM). Interestingly, the IC$_{50}$ values against HeLa cells of each compound are in line with their rhodesain inhibitory activity. Hence, despite their structural similarity, the bioactivity seems to vary slightly between the monomeric and dimeric derivatives.

Although all three compounds are active in a comparable concentration range, in all assays, the monomer **3** (3 hydroxy groups; $M_r \sim 400$ Da) is slightly less active than the dimers **5** and **1** (7/6 hydroxy groups; $M_r \sim 800$ Da). This agrees with the observation in other polyphenolic natural products that the bioactivity increases with the number of hydroxy groups per molecule,[50−55] suggesting that the activity of the nostotrebins/nostolactones is indeed due to unspecific, polyphenol-like activity on proteins.

The broad bioactivity spectrum, which has been reported for CPDs in general, was postulated to be based on the chemically reactive CPD substructure.[24] For example, the antifungal activity of coruscanone A was at first attributed to the 2-methoxymethylenecyclopent-4-ene-1,3-dione moiety, assuming an irreversible covalent addition to its target by Michael addition,[18] while the side chain styryl-like moiety was suspected to contribute to target binding. However, subsequent evaluation of synthesized 2-cinnamyliden-1,3-diones related to coruscanone A showed that the CPD core structure was not essential for bioactivity but, instead, highlighted the importance of the styryl side chain.[56] Furthermore, CPDs isolated from *Lindera aggregata*, comprising one or two CPD moieties but no hydroxy groups, were found to be inactive against *B. subtilis*.[57] Compound **1**, containing two CPD subunits, and compound **5**, containing just one CPD substructure, were roughly equally active in our assays. Hence, as discussed above, it is likely that the bioactivities of the nostotrebin compound family are not due to the CPD moiety but the phenolic hydroxy groups.

Although the physiological role of CPDs has not yet been studied in detail, a protective function for the producing organisms, especially against bacterial and fungal pathogens, was assumed.[24] In the case of compound **1**, a protective role against biotic stress was suggested as well.[30] Our study might affirm this reasoning, as the nostotrebins/nostolactones were found to be present in the cultivation medium. Another potential ecological role of the CPDs might be protection against UV irradiation. The structures of the nostotrebins show some resemblance with the structures of the scytonemins, known UV protectants or photon dissipators.[58] However, in contrast to the scytonemins, which absorb strongly over the entire UV range (100−380 nm), the nostotrebins absorb UV light strongly only in the UV-C range (100−280 nm), while their absorption in the UV-B range (280−315 nm) is comparably weaker and low in the UV-A range (315−380 nm).

■ EXPERIMENTAL SECTION

General Experimental Procedures. Optical rotations were obtained on a Jasco P-2000 polarimeter. UV spectra were obtained on a GeneQuant 1300 spectrophotometer (GE Healthcare Bio-Sciences). Infrared−attenuated total reflection (IR−ATR) spectra were obtained on a Bruker FTIR IFS 28 spectrometer, equipped with a

38

deuterated triglycine sulfate (DTGS) detector and a ZnSe crystal (1.3 mm). The incidence angle was 45°. NMR experiments were performed in DMSO-d_6 on a Bruker Avance II spectrometer operating at 600 MHz (^{1}H) or 150 MHz (^{13}C) on an Agilent DD2 spectrometer equipped with a OneNMR probe at 400 MHz (^{1}H) or on a Varian/Agilent VNMRS spectrometer operating at 600 MHz (^{1}H). Chemical shifts were referenced to the residual solvent signals (δ_H 2.49, δ_C 39.5). NMR data were analyzed with ACD/Structure Elucidator Suite 2018.2. High-resolution electrospray ionization mass spectrometry (HRESIMS) data were acquired on a Q Exactive Plus mass spectrometer (Thermo Fisher Scientific) equipped with a heated ESI interface coupled to an UltiMate 3000 HPLC system (Thermo Fisher Scientific). The following parameters were used for the data acquisition: positive ion mode, ESI spray voltage of 3.5 kV, and scan range of m/z 150−2000. Analytical and semi-preparative HPLC were performed on an UltiMate 3000 HPLC system (Thermo Fisher Scientific).

Cyanobacterial Material: Generation of Medium Extract. *Nostoc* sp. CBT1153 (CCY0508) was classified as *Nostoc* based on its morphology and is deposited in the culture collection of the Cyano Biotech GmbH, Germany. The strain was cultivated in BG11 medium[59] at 28 °C, illuminated continuously by Sylvania GROLUX fluorescent lamps (50−200 μmol photons m^{-2} s^{-1}), and aerated with 0.5−5% CO_2 in sterile filtrated air in 20 L polycarbonate carboys. To minimize cell death and lysis, the cultures were harvested weekly and diluted with fresh medium (semi-continuous cultivation to avoid entering into the stationary phase). Frequent microscopic examination of the cultures did not show significant amounts of sheath fragments that would indicate dead or lysed cells. XAD-16 adsorption resin was present during the whole cultivation duration to adsorb organic compounds present in the cultivation medium, and the adsorbed compounds were subsequently extracted with MeOH. Sufficient amounts of cyanobacteria biomass and medium extract for further processing were obtained after a cultivation duration of about 10 weeks. After separation of the biomass from the medium by centrifugation, the biomass was lyophilized. The dried biomass was resuspended in 50% MeOH (v/v), treated with an ultrasonication rod (Bandelin), and extracted on a shaker for 30 min at room temperature. After centrifugation, the biomass was subsequently extracted using 80% MeOH (v/v). The solutions were combined and dried *in vacuo* to yield the biomass extract.

Bioassay-Guided Fractionation and Isolation of Compound 1 and Its Derivatives. The medium extract was dissolved in MeOH and fractionated by HPLC using a Luna C18 column (250 × 10 mm, 5 μm, 100 Å, Phenomenex) and a gradient of 30−75% MeCN in H_2O (0.1% formic acid each) at 4.5 mL/min over 23 min. Fractions were collected every 0.5 min, resulting in five fractions inhibiting rhodesain. These fractions contained all of the major compounds detectable in the extract. A total of 140 mg of medium extract was dissolved in 1.4 mL of MeCN and subjected to semi-preparative HPLC using a Luna C18 column (250 × 10 mm, 5 μm, 100 Å, Phenomenex) and a gradient of 40−46% MeCN in H_2O (0.1% formic acid each) at 4.5 mL/min over 30 min, yielding compounds **2** (0.5 mg, t_R of 4.7 min), **A** (<0.1 mg, t_R of 6.2 min), **3** (9.5 mg, t_R of 8.8 min), **B** (0.1 mg, t_R of 9.7 min), **4** (4.3, t_R of 12.0 min), **5** (9.4 mg, t_R of 13.1 min), **C** (3.6 mg, t_R of 16.7 min), **1** (40.5 mg, t_R of 17.5 min), and **D** (<0.1 mg, t_R of 21.1 min). The compounds were found to be not optically active.

Nostotrebin 6 (1): yellow amorphous powder; UV (MeCN) λ_{max} (log ε), 226 (4.75) nm; IR (ATR) ν_{max}, 3393, 1734, 1686, 1610, 1510, 1437, 1337, 1224, 1171, 821 cm^{-1}; ^{1}H and ^{13}C NMR data, Table 2; HRESIMS, m/z 799.2514 [M + H]$^+$ (calculated for $C_{50}H_{39}O_{10}$, 799.2538).

Nostotrebinol 3 (2): yellow amorphous powder; UV (MeCN) λ_{max} (log ε), 225 (4.02), 277 (3.61) nm; IR (ATR) ν_{max}, 3196, 2917, 1701, 1594, 1513, 1445, 1241, 1172, 1022, 998, 825 cm^{-1}; ^{1}H and ^{13}C NMR data, Table 1; HRESIMS, m/z 415.1182 [M − H]$^-$ (calculated for $C_{25}H_{19}O_6$, 415.1182).

Nostolactone 4 (3): yellow amorphous powder; UV (MeCN) λ_{max} (log ε), 226 (4.28), 279 (3.92), 359 (4.33) nm; IR (ATR) ν_{max}, 3342, 1722, 1601, 1513, 1445, 1372, 1229, 1173, 1104, 974, 823 cm^{-1}; ^{1}H and ^{13}C NMR data, Table 1; HRESIMS, m/z 417.1319 [M + H]$^+$ (calculated for $C_{25}H_{21}O_6$, 417.1333).

Nostotrebin 7 (4): orange amorphous powder; UV (MeCN) λ_{max} (log ε), 225 (4.49), 275 (3.99) nm; IR (ATR) ν_{max}, 3172, 2918, 1735, 1691, 1612, 1513, 1447, 1375, 1242, 1023, 824 cm^{-1}; ^{1}H and ^{13}C NMR data, Table 2; HRESIMS, m/z 815.2462 [M + H]$^+$ (calculated for $C_{50}H_{39}O_{11}$, 815.2487).

Nostotrebinlactone 7 (5): yellow amorphous powder; UV (MeCN) λ_{max} (log ε), 227 (4.59), 278 (4.05), 357 (4.32) nm; IR (ATR) ν_{max}, 3350, 1273, 1690, 1599, 1512, 1441, 1350, 1241, 1173, 832 cm^{-1}; ^{1}H and ^{13}C NMR data, Table 2; HRESIMS, m/z 815.2462 [M + H]$^+$ (calculated for $C_{50}H_{39}O_{11}$, 815.2487).

Quantification by Evaporative Light Scattering Detection (ELSD). To avoid weighing inaccuracies, the concentrations of test compound solutions for bioactivity testing were quantified using HPLC coupled with ELSD (Sedex 85, Sedere) according to Adnani et al.[60] Quercetin (>99%, Carl Roth) was used as a standard substance to establish the calibration curve (injection of 0.5 to 50 μL of a 20 ng/μL solution in 90% MeCN in H_2O). Solutions were injected in triplicate on a Kinetex C18 column (100 × 3.1 mm, 5 μm, 100 Å, Phenomenex), eluted with 90% MeCN in H_2O (0.1% formic acid each) at 0.85 mL/min over 2.5 min. ELSD response areas were averaged, and log(ELSD response area) was plotted against log(amount) to generate a linear calibration curve. Solutions of the compounds in 90% MeCN in H_2O were injected in triplicate under identical conditions. ELSD response areas were averaged, and the corresponding compound concentration was calculated using the quercetin calibration curve.

Rhodesain Assay: General Procedure. Rhodesain was recombinantly expressed as described previously.[61] The hydrolysis of Cbz-Phe-Arg-AMC by rhodesain was detected by a kinetic measurement over 10 min in intervals of 30 s with a Tecan infinite M200 pro plate reader according to Breuning et al.[46] (excitation wavelength, 380 nm; excitation bandwidth, 9 nm; detection wavelength, 460 nm; detection bandwidth, 20 nm; and z position, 18 400 μm). The assay was performed in white 96-well plates (Lumitrac 600 white 96-well microplates, Greiner Bio-One). As the assay buffer, 50 mM sodium acetate at pH 5.5 with 5 mM ethylenediaminetetraacetic acid (EDTA), 200 mM NaCl, and 0.005% Brij 35 was used. The following solution was applied as the enzyme buffer: 50 mM sodium acetate at pH 5.5 containing rhodesain, 5 mM EDTA, 200 mM NaCl, and 5 mM DTT. Substrate (10 mM final concentration) and inhibitor stock solutions were prepared in dimethyl sulfoxide (DMSO) and diluted with assay buffer to a final DMSO concentration of 5%. DMSO alone (5% final concentration) served as the negative control. The determination of the inner filter effect is described in the Supporting Information.

Studies on the Rhodesain Inhibition Mechanism. For more detailed studies on the inhibition mechanism of the compounds on rhodesain, the assays were adjusted as follows: To study a time-dependent inhibition, enzyme and test compound were incubated 0, 5, and 30 min prior to substrate addition.[48] Subsequently, the standard kinetic measurement over 10 min in intervals of 30 s was performed. To evaluate unspecific electrophilic reactions of the test compounds with the target enzyme, the assay buffer was supplemented with a concentration of 1 and 5 mM DTT (0.125 and 4.75 mM final concentration; see the Supporting Information) and influence on the inhibition was evaluated.[46,49] The formation of aggregates by the test compound and target enzyme was investigated by the addition of Brij 35 to the assay buffer (final concentration of 0.01 and 0.025%; see the Supporting Information).[46,47] The inner filter effect was determined as described by Ludewig et al.[47] IC$_{50}$ was calculated using Graph Pad PRISM 6. Data were fit by nonlinear regression, applying the equation "log(inhibitor) versus response − variable slope (four parameters)".

Cell Culture and Cell Survival Rate. HeLa cells were maintained in RPMI 1640 medium supplemented with 10% fetal bovine serum, which was heat-inactivated at 60 °C for 30 min, and 1% penicillin/streptomycin mixture. Cells were cultured at 37 °C in a humidified atmosphere containing 5% CO_2. For estimation of the cell viability against compound **1** and its derivatives, a serial dilution of the test compounds from 100 to 0.05 μM in RPMI 1640 medium supplemented with 10% fetal bovine serum was prepared in 96-well flat-bottom polystyrene microplates (Sarstedt). Cycloheximide was used as a control. A total of 100 μL of cell culture was added to a 96-well plate

containing the serial dilution of the test compounds, achieving a final cell concentration of 1×10^4 cells/well. A growth control (cells in medium but no inhibitor) and a sterility control (medium only) were added. After 24 h of incubation with test compounds at 37 °C, 10 μL of resazurin solution (1 mg/mL) was added to each well, followed by 24 h of further incubation at 37 °C and 5% CO_2. Fluorescence was measured in a TECAN infinite M200 plate reader at 560 nm excitation and 600 nm emission. The cell viability was estimated in relation to the growth control. All experiments were performed at least in triplicate.

Antimicrobial Activity. The antimicrobial activity of compound **1** and its derivatives against the Gram-positive bacteria *B. subtilis*, *S. aureus*, and *E. faecium* was evaluated by determination of their MIC according to the guidelines of the Clinical and Laboratory Standards Institute (CLSI).[62] Serial 2-fold dilutions of the test compounds from 100 to 0.05 μM in cation-adjusted Mueller−Hinton broth were prepared in 96-well round-bottom polystyrene microplates (Sarstedt). Each well contained 50 μL of test compound solution at twice the desired final concentration and was inoculated with 50 μL of bacterial suspension, yielding a final inoculum of 5×10^5 colony-forming units (CFU)/mL in 100 μL final volume. Microplates were incubated for 16−20 h at 37 °C, and the MIC was determined as the lowest concentration of the test compound that inhibited visible bacterial growth.

■ ASSOCIATED CONTENT

⑤ Supporting Information

The Supporting Information is available free of charge at https://pubs.acs.org/doi/10.1021/acs.jnatprod.9b00885.

UV, IR, MS, MS/MS, ^{1}H, ^{13}C, HSQC, and HMBC spectra of compounds **1−5** and additional information about the rhodesain assays (PDF)

■ AUTHOR INFORMATION

Corresponding Author

Timo H. J. Niedermeyer − *Department of Pharmaceutical Biology/Pharmacognosy, Institute of Pharmacy, University of Halle-Wittenberg, 06120 Halle (Saale), Germany; German Center for Infection Research (DZIF), Partner Site Tübingen, 72076 Tübingen, Germany;* ⓘ orcid.org/0000-0003-1779-7899; Email: timo.niedermeyer@pharmazie.uni-halle.de

Authors

Ronja Kossack − *Department of Pharmaceutical Biology/Pharmacognosy, Institute of Pharmacy, University of Halle-Wittenberg, 06120 Halle (Saale), Germany*

Steffen Breinlinger − *Department of Pharmaceutical Biology/Pharmacognosy, Institute of Pharmacy, University of Halle-Wittenberg, 06120 Halle (Saale), Germany*

Trang Nguyen − *Department of Microbiology/Biotechnology, Interfaculty Institute for Microbiology and Infection Medicine (IMIT), University of Tübingen, 72076 Tübingen, Germany*

Julia Moschny − *Department of Pharmaceutical Biology/Pharmacognosy, Institute of Pharmacy, University of Halle-Wittenberg, 06120 Halle (Saale), Germany*

Jan Straetener − *Department of Microbial Bioactive Compounds, Interfaculty Institute for Microbiology and Infection Medicine (IMIT), University of Tübingen, 72076 Tübingen, Germany; German Center for Infection Research (DZIF), Partner Site Tübingen, 72076 Tübingen, Germany*

Anne Berscheid − *Department of Microbial Bioactive Compounds, Interfaculty Institute for Microbiology and Infection Medicine (IMIT), University of Tübingen, 72076 Tübingen, Germany; German Center for Infection Research (DZIF), Partner Site Tübingen, 72076 Tübingen, Germany*

Heike Brötz-Oesterhelt − *Department of Microbial Bioactive Compounds, Interfaculty Institute for Microbiology and Infection Medicine (IMIT), University of Tübingen, 72076 Tübingen, Germany; German Center for Infection Research (DZIF), Partner Site Tübingen, 72076 Tübingen, Germany*

Heike Enke − *Cyano Biotech GmbH, 12489 Berlin, Germany*

Tanja Schirmeister − *Institute of Pharmacy and Biochemistry, University of Mainz, 55128 Mainz, Germany*

Complete contact information is available at:
https://pubs.acs.org/10.1021/acs.jnatprod.9b00885

Notes

■ ACKNOWLEDGMENTS

■ REFERENCES

(1) Salvador-Reyes, L. A.; Luesch, H. *Nat. Prod. Rep.* **2015**, *32*, 478−503.

(2) Niedermeyer, T. H. *Planta Med.* **2015**, *81*, 1309−1325.

(3) Tan, L. T. *J. Appl. Phycol.* **2010**, *22*, 659−676.

(4) Nunnery, J. K.; Mevers, E.; Gerwick, W. H. *Curr. Opin. Biotechnol.* **2010**, *21*, 787−793.

(5) Niedermeyer, T.; Brönstrup, M. In *Microalgal Biotechnology: Integration and Economy*; Posten, C., Walter, C., Eds.; de Gruyter: Berlin, Germany, 2012; pp 169−200.

(6) Tidgewell, K.; Clark, B. R.; Gerwick, W. H. *Comprehensive Natural Products II*; Elsevier: Amsterdam, Netherlands, 2010; pp 141−188.

(7) Younes, A.; Yasothan, U.; Kirkpatrick, P. *Nat. Rev. Drug Discovery* **2012**, *11*, 19−20.

(8) Flahive, E.; Srirangam, J. The Dolastatins: Novel Antitumor Agents from *Dolabella auricularia*. In *Anticancer Agents from Natural Products*; Kingston, D., Cragg, G., Newman, D., Eds.; CRC Press: Boca Raton, FL, 2005; pp 191−214.

(9) Luesch, H.; Harrigan, G. G.; Goetz, G.; Horgen, F. D. *Curr. Med. Chem.* **2002**, *9*, 1791−1806.

(10) Bouchard, H.; Brun, M.-P.; Commerçon, A.; Zhang, J. Novel conjugates, preparation thereof, and therapeutic use thereof. WO Patent WO/2011/001052, Jan 6, 2011.

(11) Rohr, J. *ACS Chem. Biol.* **2006**, *1*, 747−750.

(12) Hirsch, C. F.; Liesch, J. M.; Salvatore, M. J.; Schwartz, R. E.; Sesin, D. F. Antifungal fermentation product and method. U.S. Patent 4,946,835, Aug 7, 1990.

(13) Llewellyn, L. E. *Nat. Prod. Rep.* **2006**, *23*, 200−222.

(14) Rodriguez-Navarro, A. J.; Lagos, N.; Lagos, M.; Braghetto, I.; Csendes, A.; Hamilton, J.; Figueroa, C.; Truan, D.; Garcia, C.; Rojas, A.; Iglesias, V.; Brunet, L.; Alvarez, F. *Anesthesiology* **2007**, *106*, 339−345.

(15) Halland, N.; Brönstrup, M.; Czech, J.; Czechtizky, W.; Evers, A.; Follmann, M.; Kohlmann, M.; Schiell, M.; Kurz, M.; Schreuder, H. a.; Kallus, C. *J. Med. Chem.* **2015**, *58*, 4839−4844.

(16) Schreuder, H.; Liesum, A.; Lönze, P.; Stump, H.; Hoffmann, H.; Schiell, M.; Kurz, M.; Toti, L.; Bauer, A.; Kallus, C.; Klemke-Jahn, C.; Czech, J.; Kramer, D.; Enke, H.; Niedermeyer, T. H. J.; Morrison, V.; Kumar, V.; Brönstrup, M. *Sci. Rep.* **2016**, *6*, 32958.

(17) Dittmann, E.; Gugger, M.; Sivonen, K.; Fewer, D. P. *Trends Microbiol.* **2015**, *23*, 642−652.

(18) Babu, K. S.; Li, X.-C.; Jacob, M. R.; Zhang, Q.; Khan, S. I.; Ferreira, D.; Clark, A. M. *J. Med. Chem.* **2006**, *49*, 7877−7886.

(19) Wang, S.-Y.; Lan, X.-Y.; Xiao, J.-H.; Yang, J.-C.; Kao, Y.-T.; Chang, S.-T. *Phytother. Res.* **2008**, *22*, 213−216.

(20) Antkowiak, R.; Antkowiak, W. Z.; Banczyk, I.; Mikolajczyk, L. *Can. J. Chem.* **2003**, *81*, 118−124.

(21) Wijeratne, E. M. K.; Turbyville, T. J.; Zhang, Z.; Bigelow, D.; Pierson, L. S.; van Etten, H. D.; Whitesell, L.; Canfield, L. M.; Gunatilaka, A. A. L. *J. Nat. Prod.* **2003**, *66*, 1567−1573.

(22) Hayashi, M.; Kim, Y.-P.; Takamatsu, S.; Enomoto, A.; Shinose, M.; Takahashi, Y.; Tanaka, H.; Komiyama, K.; Omura, S. *J. Antibiot.* **1996**, *49*, 1091−1095.

(23) Noble, M.; Noble, D.; Fletton, R. A. *J. Antibiot.* **1978**, *31*, 15−18.

(24) Sevcikova, Z.; Pour, M.; Novak, D.; Ulrichova, J.; Vacek, J. *Mini-Rev. Med. Chem.* **2014**, *14*, 322−331.

(25) Clemo, N. G.; Gedge, D. R.; Pattenden, G. *J. Chem. Soc., Perkin Trans. 1* **1981**, 1448.

(26) Li, X.-C.; Ferreira, D.; Jacob, M. R.; Zhang, Q.; Khan, S. I.; ElSohly, H. N.; Nagle, D. G.; Smillie, T. J.; Khan, I. A.; Walker, L. A.; Clark, A. M. *J. Am. Chem. Soc.* **2004**, *126*, 6872−6873.

(27) Zelik, P.; Lukesova, A.; Voloshko, L. N.; Stys, D.; Kopecky, J. J. *J. Enzyme Inhib. Med. Chem.* **2009**, *24*, 531−536.

(28) Zelik, P.; Lukesova, A.; Cejka, J.; Budesinsky, M.; Havlicek, V.; Cegan, A.; Kopecky, J. *J. Enzyme Inhib. Med. Chem.* **2010**, *25*, 414−420.

(29) Vacek, J.; Hrbáč, J.; Kopecký, J.; Vostálová, J. *Molecules* **2011**, *16*, 4254−4263.

(30) Cheel, J.; Bogdanová, K.; Ignatova, S.; Garrard, I.; Hewitson, P.; Kolář, M.; Kopecký, J.; Hrouzek, P.; Vacek, J. *Algal Res.* **2016**, *18*, 244−249.

(31) Radau, G. *Curr. Enzyme Inhib.* **2005**, *1*, 295−307.

(32) Chlipala, G.; Mo, S.; Carcache de Blanco, E. J.; Ito, A.; Bazarek, S.; Orjala, J. *Pharm. Biol.* **2009**, *47*, 53−60.

(33) Miller, B.; Friedman, A. J.; Choi, H.; Hogan, J.; McCammon, J. A.; Hook, V.; Gerwick, W. H. J. *J. Nat. Prod.* **2014**, *77*, 92−99.

(34) Mazur-marzec, H.; Fidor, A.; Cegłowska, M.; Wieczerzak, E.; Kropidłowska, M.; Goua, M.; Macaskill, J.; Edwards, C. *Mar. Drugs* **2018**, *16*, 220.

(35) Liu, L.; Jokela, J.; Wahlsten, M.; Nowruzi, B.; Permi, P.; Zhang, Y. Z.; Xhaard, H.; Fewer, D. P.; Sivonen, K. *J. Nat. Prod.* **2014**, *77*, 1784−1790.

(36) Jokela, J.; Heinilä, L. M. P.; Shishido, T. K.; Wahlsten, M.; Fewer, D. P.; Fiore, M. F.; Wang, H.; Haapaniemi, E.; Permi, P.; Sivonen, K. *Front. Microbiol.* **2017**, *8*, 1963.

(37) Ettari, R.; Tamborini, L.; Angelo, I. C.; Micale, N.; Pinto, A.; de Micheli, C.; Conti, P. *J. Med. Chem.* **2013**, *56*, 5637−5658.

(38) Lonsdale-Eccles, J. D.; Grab, D. J. *Trends Parasitol.* **2002**, *18*, 17−19.

(39) Overath, P.; Chaudhri, M.; Steverding, D.; Ziegelbauer, K. *Parasitol. Today* **1994**, *10*, 53−58.

(40) Volk, R.-B.; Girreser, U.; Al-Refai, M.; Laatsch, H. *Nat. Prod. Res.* **2009**, *23*, 607−612.

(41) Jaki, B.; Orjala, J.; Sticher, O. *J. Nat. Prod.* **1999**, *62*, 502−503.

(42) Caicedo, N. H.; Kumirska, J.; Neumann, J.; Stolte, S.; Thöming, J. *Mar. Biotechnol.* **2012**, *14*, 436−445.

(43) Hirata, K.; Takashina, J.; Nakagami, H.; Ueyama, S.; Murakami, K.; Kanamori, T.; Miyamoto, K. *Biosci., Biotechnol., Biochem.* **1996**, *60*, 1905−1906.

(44) Baell, J. B.; Holloway, G. A. *J. Med. Chem.* **2010**, *53*, 2719−2740.

(45) Baell, J.; Walters, M. A. *Nature* **2014**, *513*, 481−483.

(46) Breuning, A.; Degel, B.; Schulz, F.; Buchold, C.; Stempka, M.; Machon, U.; Heppner, S.; Gelhaus, C.; Leippe, M.; Leyh, M.; Kisker, C.; Rath, J.; Stich, A.; Gut, J.; Rosenthal, P. J.; Schmuck, C.; Schirmeister, T. *J. Med. Chem.* **2010**, *53*, 1951−1963.

(47) Ludewig, S.; Kossner, M.; Schiller, M.; Baumann, K.; Schirmeister, T. *Curr. Top. Med. Chem.* **2010**, *10*, 368−382.

(48) Han, H.; Yang, Y.; Olesen, S. H.; Becker, A.; Betzi, S.; Schönbrunn, E. *Biochemistry* **2010**, *49*, 4276−4282.

(49) Blanchard, J. E.; Elowe, N. H.; Huitema, C.; Fortin, P. D.; Cechetto, J. D.; Eltis, L. D.; Brown, E. D. *Chem. Biol.* **2004**, *11*, 1445−1453.

(50) Wang, I.-K.; Lin-Shiau, S.-Y.; Lin, J.-K. *Eur. J. Cancer* **1999**, *35*, 1517−1525.

(51) Shimoi, K.; Masuda, S.; Furugori, M.; Esaki, S.; Kinae, N. *Carcinogenesis* **1994**, *15*, 2669−2672.

(52) Son, S.; Lewis, B. A. *J. Agric. Food Chem.* **2002**, *50*, 468−472.

(53) Li, K.; Li, X.-M.; Ji, N.-Y.; Wang, B.-G. *J. Nat. Prod.* **2008**, *71*, 28−30.

(54) Masella, R.; Cantafora, A.; Modesti, D.; Cardilli, A.; Gennaro, L.; Bocca, A.; Coni, E. *Redox Rep.* **1999**, *4*, 113−121.

(55) Sroka, Z.; Cisowski, W. *Food Chem. Toxicol.* **2003**, *41*, 753−758.

(56) Riveira, M. J.; Tekwani, B. L.; Labadie, G. R.; Mischne, M. P. *MedChemComm* **2012**, *3*, 1294−1298.

(57) Chen, L.; Liu, B.; Deng, J.-J.; Zhang, J.-S.; Li, W.; Ahmed, A.; Yin, S.; Tang, G.-H. *RSC Adv.* **2018**, *8*, 17898−17904.

(58) Simeonov, A.; Michaelian, K. *Biol. Phys.* **2017**, 1−38.

(59) Andersen, R. A. *Algal Culturing Techniques*; Elsevier Academic Press: Burlington, MA, 2005.

(60) Adnani, N.; Michel, C. R.; Bugni, T. S. J. *J. Nat. Prod.* **2012**, *75*, 802−806.

(61) Caffrey, C. R.; Hansell, E.; Lucas, K. D.; Brinen, L. S.; Alvarez Hernandez, A.; Cheng, J.; Gwaltney, S. L.; Roush, W. R.; Stierhof, Y.-D.; Bogyo, M.; Steverding, D.; Mckerrow, J. H. *Mol. Biochem. Parasitol.* **2001**, *118*, 61−73.

(62) Clinical and Laboratory Standards Institute (CLSI). *Methods for Dilution Antimicrobial Susceptibility Tests for Bacteria that Grow Aerobically: Approved Standard*, 10th ed.; CLSI: Wayne, PA, 2015; Vol. *35*.

[3]: Hunting the eagle killer: A cyanobacterial neurotoxin causes vacuolar myelinopathy

This article has been selected as cover story for the March 26th issue of the journal. AAAS decided to publish it immediately Open Access.

RESEARCH ARTICLE SUMMARY

WILDLIFE DISEASE

Hunting the eagle killer: A cyanobacterial neurotoxin causes vacuolar myelinopathy

Steffen Breinlinger*, Tabitha J. Phillips*, Brigette N. Haram, Jan Mareš, José A. Martínez Yerena, Pavel Hrouzek, Roman Sobotka, W. Matthew Henderson, Peter Schmieder, Susan M. Williams, James D. Lauderdale, H. Dayton Wilde, Wesley Gerrin, Andreja Kust, John W. Washington, Christoph Wagner, Benedikt Geier, Manuel Liebeke, Heike Enke, Timo H. J. Niedermeyer†‡, Susan B. Wilde†‡

INTRODUCTION: Vacuolar myelinopathy (VM) is a neurological disease characterized by widespread vacuolization in the white matter of the brain. First diagnosed in 1994 in bald eagles, it has since spread throughout the southeastern United States. In addition to avian species such as waterfowl and birds of prey, VM has also been found to affect amphibians, reptiles, and fish. Despite intense research efforts, the cause of this mysterious disease has been elusive. Neither contagious agents nor xenobiotics were detected in deceased animals, but field and laboratory studies demonstrated that VM can be transferred through the food chain from herbivorous fish and wildlife to birds of prey.

RATIONALE: Occurrence of VM has been linked to a cyanobacterium (*Aetokthonos hydrillicola*) growing on an invasive plant (*Hydrilla verticillata*) in man-made water bodies. Cyanobacteria are known to produce potent toxins, so we hypothesized that a neurotoxin produced by the epiphytic cyanobacterium causes VM.

RESULTS: Field studies in the southeastern United States confirmed that *H. verticillata* was colonized with *A. hydrillicola* in more than half of the watersheds. Wildlife VM deaths occurred only in reservoirs with dense *H. verticillata* and *A. hydrillicola* populations. Laboratory bioassays confirmed the neurotoxicity of crude extracts of *A. hydrillicola–H. verticillata*

biomass collected during VM outbreaks, but neurotoxicity was not detected in samples from VM-free sites. Laboratory cultures of the cyanobacterium, however, did not elicit VM. *A. hydrillicola* growing on *H. verticillata* collected at VM-positive reservoirs was then analyzed by mass spectrometry imaging, which revealed that cyanobacterial colonies were co-localized with a brominated metabolite. Sup-

plementation of an *A. hydrillicola* laboratory culture with potassium bromide resulted in pronounced biosynthesis of this metabolite. *H. verticillata* hyperaccumulates bromide from the environment, potentially supplying the cyanobacterium with this biosynthesis precursor. Isolation and structure elucidation of the metabolite revealed a structurally unusual pentabrominated biindole alkaloid, which we called aetokthonotoxin (AETX). Genome sequencing of *A. hydrillicola* allowed the identification of the AETX biosynthetic gene cluster. Biochemical characterization of a halogenase detected in the cluster demonstrated that it brominates tryptophan with the expected substitution pattern. AETX is highly toxic to the nematode *Caenorhabditis elegans* [median lethal concentration (LC_{50}) 40 nM] and zebrafish (*Danio rerio*; LC_{50} 275 nM). Leghorn chickens (*Gallus gallus*) gavaged with AETX developed brain lesions characteristic of VM, whereas no lesions were observed in control chickens. VM diagnosis in treated chickens was verified using transmission electron microscopy of brain tissue.

CONCLUSION: We confirmed that AETX is the causative agent of VM. AETX biosynthesis relies on the availability of bromide. Seasonal environmental conditions promoting toxin production of *A. hydrillicola* are watershed specific. The consequences of elevated bromide from geologic and anthropogenic sources (e.g., water treatment and power plants) on VM should be further investigated. Notably, integrated chemical plant management plans to control *H. verticillata* should avoid the use of bromide-containing chemicals (e.g., diquat dibromide). AETX is lipophilic with the potential for bioaccumulation during transfer through food webs, so mammals may also be at risk. Increased monitoring and public awareness should be implemented for *A. hydrillicola* and AETX to protect both wildlife and human health. ∎

S READ THE FULL ARTICLE AT
https://doi.org/10.1126/science.aax9050

From the cyanobacterium to the bald eagle— toxin transmission through the food chain.
A. hydrillicola, growing in colonies on aquatic vegetation, produces the neurotoxin AETX. Waterbirds, tadpoles, aquatic turtles, snails, and fish consume this contaminated vegetation and develop VM. Predators develop VM when they consume animals that have been grazing on *A. hydrillicola*–covered plants.

A cyanobacterial neurotoxin causes Vacuolar Myelinopathy

Authors:

Steffen Breinlinger[1,†], Tabitha J. Phillips[2,†], Brigette N. Haram[2], Jan Mareš[3,4,5], José A. Martínez Yerena[3,5], Pavel Hrouzek[4,5], Roman Sobotka[4,5], W. Matthew Henderson[6], Peter Schmieder[7], Susan M. Williams[8], James D. Lauderdale[9], H. Dayton Wilde[10], Wesley Gerrin[2], Andreja Kust[3], John W. Washington[6], Christoph Wagner[11], Benedikt Geier[12], Manuel Liebeke[12], Heike Enke[13], Timo H. J. Niedermeyer[1,‡,*], Susan B. Wilde[2,‡,*]

Affiliations:

[1]Institute of Pharmacy, Martin-Luther-University Halle-Wittenberg, Halle (Saale), Germany.

[2]Warnell School of Forestry and Natural Resources, University of Georgia, Athens, GA USA.

[3]Biology Centre of the Czech Academy of Sciences, Institute of Hydrobiology, České Budějovice, Czech Republic.

[4]Centre Algatech, Institute of Microbiology of the Czech Academy of Sciences, Třeboň, Czech Republic.

[5]Faculty of Science, University of South Bohemia, České Budějovice, Czech Republic.

[6]Office of Research and Development, Center for Environmental Measurement and Modeling, U.S. Environmental Protection Agency, Athens, Georgia, USA.

[7]Leibniz-Forschungsinstitut für Molekulare Pharmakologie (FMP), Berlin, Germany.

[8]Department of Population Health, Poultry Diagnostic and Research Center, College of Veterinary Medicine, University of Georgia, Athens, GA, USA.

[9]Department of Cellular Biology, University of Georgia, Athens, GA, USA.

[10]Horticulture Department, University of Georgia, Athens, GA, USA.

[11]Institute of Chemistry, Martin-Luther-University Halle-Wittenberg, Halle (Saale), Germany

[12]Max Planck Institute for Marine Microbiology (MPIMM), Bremen, Germany.

[13]Cyano Biotech GmbH, Berlin, Germany.

* Correspondence to: swilde@uga.edu (S.B.W.); timo.niedermeyer@pharmazie.uni-halle.de (T.H.J.N.)

†, ‡ These authors contributed equally to this work.

Abstract

Vacuolar Myelinopathy is a fatal neurologic disease initially discovered during a mysterious mass mortality of the iconic bald eagle in Arkansas, US. The cause for this wildlife disease eluded scientists for decades while its occurrence has continued to spread throughout freshwater reservoirs in the southeastern United States. Recent studies demonstrated that Vacuolar Myelinopathy is induced by consumption of the epiphytic cyanobacterial species *Aetokthonos hydrillicola* growing on aquatic vegetation, primarily invasive *Hydrilla verticillata*. Here, we describe the identification, biosynthetic gene cluster, and biological activity of aetokthonotoxin, a pentabrominated biindole alkaloid that is produced by the cyanobacterium *A. hydrillicola*. We identified this cyanobacterial neurotoxin as the causal agent of Vacuolar Myelinopathy, and discuss environmental factors, especially bromide availability, promoting toxin production.

One Sentence Summary

A mysterious brain lesion disease, fatal to wildlife, is caused by a toxin produced by a cyanobacterium growing on invasive plants.

Introduction

46

Over the winter of 1994-1995, the largest undiagnosed mass mortality of bald eagles (*Haliaeetus leucocephalus*) in the United States occurred at DeGray Lake, Arkansas (*1*). Over 70 dead eagles were found within the next two years. The mysterious mortalities were characterized by a spongiform myelinopathy that had never been documented in wild avian populations (*2, 3*). Investigators of the Arkansas die off began to notice eagles and waterbirds with similar neurological impairment throughout the southeastern states. By 1998, the emerging disease was termed Avian Vacuolar Myelinopathy (AVM) and had been confirmed at 10 sites within 6 states (*1*). AVM has since been documented in numerous avian species across the Southeastern United States during the fall and winter, most notably in waterbirds such as American coots (*Fulica americana*), Ringnecked ducks (*Aythya collaris*), mallards (*Anas platyrhynchos*), Canada geese (*Branta canadensis*), and in various birds of prey (*3–7*). All documented AVM cases were recovered on or near man-made waterbodies with abundant aquatic vegetation that senesces during the late fall and winter months (*3–7*). The abundance of fish and avian prey associated with these aquatic plants attracts overwintering and nesting bald eagles and other birds of prey (*8–10*). AVM afflicted wildlife are prone to injury and become easy prey for predators, as clinical signs include severe loss of motor functions (Movie S1 of affected American coots) (*2, 10*). While neurological impairment is a visual indication of disease, AVM diagnosis relies upon histological confirmation of widespread vacuolization of the myelinated axons (intramyelenic edema) in the white matter of the brain and spinal cord (*1*).

Early sentinel field trials documented neuropathy and vacuolar lesions in wild coots and mallards within five days of release into a lake with an ongoing AVM epizootic (*4–6*). Initial chemical analysis of sediment and dead birds recovered from reservoirs where AVM cases were documented revealed no xenobiotic compounds known to induce intramyelenic edema in mammals and birds, e.g. hexachlorophene, triethyltin, or bromethalin (*1, 11, 12*). Early lab feeding trials using plants, water and sediment collected from disease sites failed to induce neuropathy and vacuolar lesions seen in wild birds (*13, 14*). Additionally, no contagious transfer, pathogens inducing myelinopathy or neuroinflammation were documented in wild or experimental AVM affected animals (*12, 13*). These early studies suggested an unknown, seasonal environmental neurotoxin could be responsible (*14, 15*).

The search for the elusive source of this disease then focused on environmental conditions in AVM positive waterbodies, which revealed that all supported invasive submerged aquatic vegetation, primarily *Hydrilla verticillata*, with a previously unidentified epiphytic cyanobacterium, *Aetokthonos hydrillicola*, colonizing up to 95% of the plant leaves *(16–18)*. Field and laboratory studies demonstrated that AVM could be transferred up the food chain. It is induced in herbivorous waterbirds after ingestion of *H. verticillata* colonized by *A. hydrillicola*, and in birds of prey consuming affected waterfowl (*9, 16, 19, 20*). Not only does AVM present an emerging threat to the Southeast's avian species (*5, 6*), but subsequent field and laboratory *H. verticillata/A. hydrillicola* feeding trials confirmed neuropathy and mortality in a wide variety of taxa including amphibians, reptiles, and fish as well as secondary disease transfer through the food chain. Thus, the disease is now referred to as Vacuolar Myelinopathy (VM) (*21–24*).

Cyanobacteria have long been associated with the production of toxins and other specialized metabolites (*25–29*). Thus, we hypothesized that a neurotoxin produced by the epiphytic cyanobacterium *A. hydrillicola* is the causative agent of VM. Here, we present our evidence that VM is indeed caused by a cyanobacterial neurotoxin with intriguing structural features. In addition to discovering the neurotoxin, we have identified its biosynthetic gene cluster, and present toxicity data on model birds, fish, nematodes, and crustaceans. Finally, we discuss environmental factors promoting toxin production.

Results

Aetokthonos hydrillicola distribution. Sampling of submerged aquatic vegetation in lakes, reservoirs, and other waterbodies throughout the Southeastern United States revealed a complex and wide-spread pattern of *A. hydrillicola* distribution (*16–18*). As of fall 2019, we documented *H. verticillata* colonized with *A. hydrillicola* in 31 out of 69 sampled watersheds (Fig. 1, Tab. S1). Waterbodies include large (>10,000 hectares) hydropower/water supply reservoirs, county water source reservoirs, suburban recreational lakes, and farm ponds. Given the difficulty of documenting animals dying from VM and the extensive spread of invasive *H. verticillata*, our current map of *A. hydrillicola* distribution is certainly underestimating the prevalence of the cyanobacterium and its threat to endemic wildlife, fish, and freshwater resources.
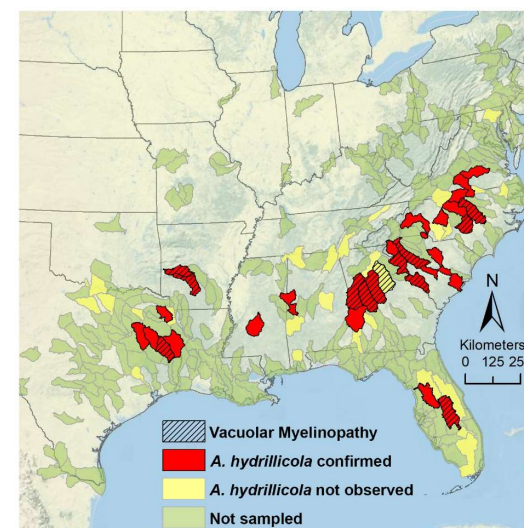
Fig. 1. Vacuolar Myelinopathy occurs in watersheds where *Aetokthonos hydrillicola* colonizes *Hydrilla verticillata*. Watersheds (Hydrologic Unit – HUC 8) where Vacuolar Myelinopathy has been diagnosed [black crosshatching]. Watersheds where *H. verticillata* has been confirmed to be colonized with *A. hydrillicola* [red]. Watersheds where *A. hydrillicola* has not yet been observed on *H. verticillata* [yellow]. Watershed not yet screened for *A. hydrillicola*, but where *H. verticillata* occurs [green]. Basemap copyright: 2013, National Geographic Society.

Discovery and production of the putative toxin. In 2011, we collected *H. verticillata* with epiphytic *A. hydrillicola* from J. Strom Thurmond Reservoir (Georgia/South Carolina, USA) to isolate the cyanobacterial strain for mass cultivation and subsequent isolation of the putative cyanotoxin. Due to challenges in establishing culture conditions for this epiphytic colonizer, it took two years to generate sufficient *A. hydrillicola* biomass for a first feeding trial. The identity of the strain was confirmed as *A. hydrillicola* by 16S rRNA sequencing. However, chickens gavaged with this *A. hydrillicola* biomass did not develop VM, which failed to support that *A. hydrillicola* was producing a VM-inducing toxin.

Hypothesizing that the cyanobacterium produces the hypothetic toxin only when growing on *H. verticillata*, but not in laboratory culture, we collected additional samples of *A. hydrillicola* growing on *H. verticillata* at confirmed VM sites. The cyanobacterial colonies on the *H. verticillata* leaves were analyzed by atmospheric-pressure matrix-assisted laser desorption/ionization mass spectrometry imaging (AP-MALDI-MSI) in order to detect cyanobacteria-specific metabolites *in situ*. Using AP-MALDI-MSI, we could co-localize the cyanobacterial colonies with a metabolite with the sum formula $C_{17}H_6Br_5N_3$ (Fig. 2A-D), that was not detectable in laboratory cultures by HPLC-MS. Neither commercial (Dictionary of Natural Products 28.2, SciFinder) nor in-house natural product databases revealed an entry for this elemental composition, suggesting it to be a novel natural product. The fact that the metabolite contains five bromine atoms is of special interest, as polyhalogenated synthetic compounds, such as bromethalin or hexachlorophene, are known to induce VM-like brain lesions in birds and mammals (*1, 5, 11, 30*).
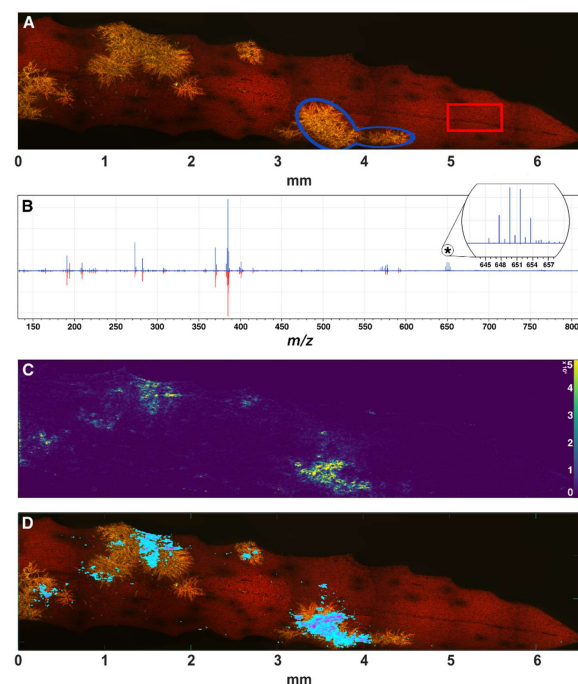
Fig. 2. AP-MALDI-MSI of *A. hydrillicola* colonies growing on *H. verticillata* reveals a cyanobacterium-specific metabolite. (**A**) Micrograph of *A. hydrillicola* colonies on *H. verticillata* leaf. Autofluorescence (excitation 395 – 440 nm, emission 470 nm) was used to acquire the image. Regions of interest for evaluation of the subsequent MSI experiments are shown in red (leaf without cyanobacterium) and blue (cyanobacteria colony on the leaf). (**B**) Comparison of mean mass spectra of the two regions of interest. Enlarged region showing the characteristic isotope pattern of the pentabrominated metabolite at *m/z* 645 ([M-H]⁻). This molecule is exclusively found to be associated with the cyanobacterial colony. (**C**) AP-MALDI image showing the spatial distribution of the distinct feature *m/z* 649.6382 ± 2 ppm ([$C_{17}H_6^{79}Br_3^{81}Br_2N_3$ - H]⁻). Intensity is scaled from 0 (violet) to 5 x 10⁴ (yellow). (**D**) Overlay of micrograph and *m/z* feature 649.6382 ± 2 ppm.

The presence of bromine in the putative toxin presented a potential explanation for why our laboratory cultures of the cyanobacterium did not cause VM. Our standard cultivation medium, BG11, does not contain any bromide, critical for the biosynthesis of the toxin. Indeed, supplementation of the cultivation medium with potassium bromide resulted in the pronounced biosynthesis of this pentabrominated metabolite. We found a non-linear relation between bromide concentration in the medium and production of the pentabrominated metabolite by the cyanobacterium. We determined the optimum bromide concentration for productivity to be between 0.1 and 0.5 mM KBr (Fig. S1).

Although a minor production can readily be detected by HPLC-MS once the medium is supplemented with bromide (data not shown), we observed a significant increase in production under stress conditions. A drop in temperature (from cultivation at 28 °C to 21 °C) or enhanced culture movement (shear stress) trigger metabolite production to an extent (> 100-fold) that it becomes easily detectable by HPLC-UV (Fig. S2-S3).

Hypothesizing that this pentabrominated metabolite was the putative toxin, we screened *A. hydrillicola/H. verticillata* assemblages collected from lakes during VM outbreaks by HPLC-MS, and compared them with biomass from VM free sites (*H. verticillata* not colonized with *A. hydrillicola)*. Indeed, we could detect this metabolite only in biomass collected from VM affected lakes, strengthening our hypothesis (Fig. S4). Furthermore, the compound could be detected in tissues of two deceased wild American coots collected during an AVM outbreak at the J. Strom Thurmond Reservoir (Georgia, US) in November 2014 (Fig. S5), confirming that the compound is absorbed from the gut and accumulates in wild waterfowl. Additionally, we observed a seasonal variation of the toxin concentration in *A. hydrillicola/H. verticillata* biomass collected from J. Strom Thurmond Lake, with the peak concentration detected in November (Fig. S6). This observation agrees with the finding that VM occurrences have been documented in late autumn within reservoirs, coinciding with seasonal water temperature declines and lake turnover.

As the biosynthesis of the pentabrominated metabolite requires bromide, we furthermore investigated bromide availability in *A. hydrillicola* habitats. Total bromine content in *H. verticillata* and sediments, and the bromide concentration in water from VM-positive (containing *H. verticillata* colonized by *A. hydrillicola*) and VM-negative (containing only uncolonized *H. verticillata*) reservoirs was monitored seasonally. Colonized and uncolonized *H. verticillata* leaves contain significantly (p < 0.001) higher concentrations of bromine than sediments (~20-fold) and water (500- to 1000-fold) (Fig. S7). In late summer, Southeastern US reservoirs are stratified, with warm, sunlit, oxygenated water above, and cool, dark, anoxic water trapped below. During late fall, surface water temperatures cool, water layers mix, and *H. verticillata* senesces. We propose that this seasonal shift provides a bromide-enriched local environment, which ultimately triggers *A. hydrillicola*'s production of the elusive toxin.

Isolation and structure elucidation of aetokthonotoxin (AETX). Cultivation of *A. hydrillicola* with bromide supplementation as well as field collections of *A. hydrillicola/H. verticillata* assemblages allowed us to isolate the compound in sufficient amounts for structure elucidation and bioactivity characterization. Due to the proton deficiency of the compound, extensive NMR and infrared spectroscopic as well as high-resolution mass spectrometric analyses were required to elucidate its structure, which was confirmed by X-ray crystallography (Fig. 3; supplementary text, Fig. S13 and Tab. S4-S9). The structure has intriguing chemical features. Most prominent, also from the isotope pattern that is observed in mass spectrometry analyses of the compound, are the five bromo substituents. Brominated organic compounds are often found to be produced by marine organisms, but are also found in plants, fungi, lichen, bacteria, and even humans (*31–33*). Several bromoindoles have been isolated from natural sources (*34*). Tyrian Purple, one of the first brominated indole alkaloids that have been discovered, is not only the most famous example, but also a 2,2'-biindole (*35*). Many brominated organic compounds exhibit strong bioactivity, ranging from antifungal, antimicrobial to antioxidant activity (*36*). Synthetic representatives have lately become infamous as environmental pollutants (*37*): Due to their lipophilicity, they tend to accumulate in sediment and biota, where they can pose a serious threat to ecosystems (*38, 39*). Another intriguing chemical feature is the connection of the two

indole moieties via N1 and C2'; to date, no natural 1,2'-bi-1H-indole has been described. The two indole substructures present in AETX are rare in natural products. The 2,3,5-tribromoindole substructure has only been described from red algae of the genera *Laurencia* and *Nitophyllum (40)*, the mollusk *Aplysia dactylomela* (likely because of its red algal diet) (*41*), and the cyanobacterium *Rivularia firma*, which produces numerous structurally related brominated 1,3'-, 3,3'-, and 3,4'-bi-1H-indoles (*42*). 5,7-Dibromoindole-3-carbonitrile has not yet been found as a natural product substructure. Indole-3-carbonitrile without additional substituents has only once been described as a natural product, isolated from a halophilic bacterium probably belonging to the genus *Bacillus* (*43*). Based on the systematic name of the cyanobacterium, *Aetokthonos hydrillicola* (Greek for "eagle killer residing on *Hydrilla*"), we called this compound aetokthonotoxin (AETX), "poison that kills the eagle" (Greek ἀετός (áetós), eagle; κτείνω (kteínō), to kill; τοξικόν (toxikón), toxin).
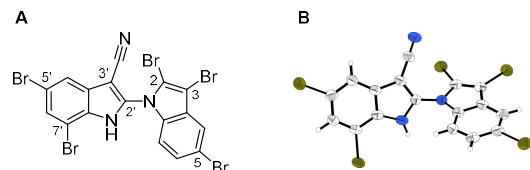

Fig. 3. (A) Structure and (B) X-ray crystallography structure of aetokthonotoxin (AETX).

Aetokthonotoxin biosynthesis. Due to the unique structure of AETX, illustrating several chemical features not yet observed in nature, we investigated its biosynthesis. Biosynthetic machineries of most cyanotoxins are organized in compact gene clusters, which can be linked to the resulting structures by functional annotation. Thus, we sequenced the whole genomes of two independent *A. hydrillicola* strains isolated from J. Strom Thurmond Reservoir in 2011 (confirmed to produce AETX as described above) and 2014, and subsequently performed a bioinformatic analysis. Both sequenced genomes contained an identical gene cluster consisting of six deduced genes (*aetA-F*) whose annotated functions implied their involvement in AETX biosynthesis (Fig. 4A). BLAST searches against all available genomes in the NCBI database did not show the presence of a similar gene cluster sequenced to date (October 2020). The genomic regions adjacent to the candidate gene cluster contained other cyanobacterial genes, and the deduced proteins within the cluster had closest relatives in cyanobacteria (Tab. S10), corroborating its cyanobacterial origin.

The gene *aetE* was predicted to encode a tryptophanase (Fig. S37, Tab. S10), a well-studied enzyme responsible for conversion of tryptophan to indole (*44*). This provides a viable hypothesis explaining the origin of the two indole cores in AETX from tryptophan (or a tryptophan-derived intermediate of the pathway). Two genes, *aetA* and *aetF*, were predicted to encode NAD(P)/FAD-dependent halogenases related to known halogenases involved in the biosynthesis of cyanobacterial metabolites (*45, 46*) (Tab. S10). Bioinformatic analysis of the *A. hydrillicola* genome did not reveal any other homologues to known bacterial tryptophan halogenases organized in a biosynthesis gene cluster besides *aetA* and *aetF* found in the *aet* cluster, further supporting their involvement in AETX biosynthesis. The presence of two distinct halogenases could explain the different substitution patterns of the two indole cores of the AETX molecule, which could be achieved by two or more subsequent (poly)halogenation reactions.
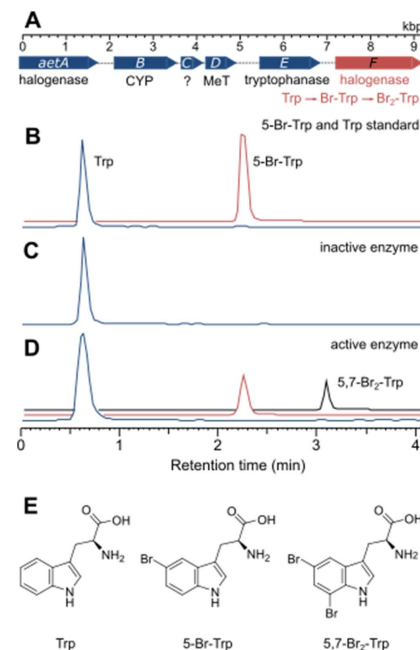

Fig. 4A-E. The halogenase AetF encoded in the aetokthonotoxin gene cluster brominates tryptophan. (**A**) Map of the 9.23 kbp AETX biosynthetic gene cluster consisting of six predicted genes coding for two halogenases, a cytochrome P450 (CYP), a tentative methyl-transferase (MeT), a tryptophanase, and a single unknown protein. (**B-E**) HPLC-MS analysis of authentic standards compared with the reaction mixtures with fresh and heat-inactivated purified His-AetF (N=3). (**B**) L-tryptophan (Trp, t_r 0.73 min) and 5-bromo-DL-tryptophan (5-Br-Trp, t_r 2.26 min) standards. (**C**) Heat-inactivated His-AetF does not brominate L-tryptophan. (**D**) Functional His-tagged AetF brominates L-tryptophan to 5-bromotryptophan and 5,7-dibromotryptophan (5,7-Br$_2$-Trp, t_r 3.03 min), proving the tryptophan brominase activity of AetF *in vitro*. (**E**) Structures of the detected tryptophan variants (L-tryptophan, 5-bromotryptophan, 5,7-dibromotryptophan).

To test this hypothesis and provide initial mechanistic evidence for the role of the *aet* gene cluster in AETX biosynthesis, we assessed the activity of the putative halogenase AetF in in vitro experiments. Assays containing recombinant AetF and L-tryptophan as substrate showed the formation of two brominated products (Fig. 4B-E). The high yield of recombinant AetF from *E. coli* (Fig. S36) allowed conducting a larger-scale in vitro assay with yields of both brominated products sufficient for isolation. Subsequent NMR analysis of the products unambiguously confirmed that AetF is capable of bromination of tryptophan at positions 5 and 7, exactly matching the substitution pattern observed in one of the AETX indole substructures (Fig. S39-47). Additional in vitro assays showed that indole is not a substrate of the enzyme, but 5,7-dibromoindole was obtained when 5-bromoindole was provided to AetF (Fig. S38). Based on these data, we conclude that tryptophan is the primary substrate for AetF, as the enzyme is capable of introducing bromine into unsubstituted tryptophan. The additional AetF bromination activity on 5-bromoindole could result from its steric similarity to 5-bromotryptophan, which we found to be an intermediate of the stepwise bromination of tryptophan. Further in vitro

assays with AetA and structural analysis of its products are needed to fully elucidate the chronology of the individual halogenation reactions. The functions of the remaining predicted genes have yet to be experimentally confirmed. Hypothetically, 5-bromotryptophan produced by AetF (or a later more complex intermediate) could be used for subsequent additional bromination by AetA to generate the 2,3,5-tribrominated indole substructure. Concerning the possible function of AetB, it is noteworthy that cytochrome P450-like proteins have been previously found to play a crucial role in carbonitrile formation in natural products (*47*).

Bioactivity characterization of aetokthonotoxin. Initial HPLC microfractionation of a *A. hydrillicola/H. verticillata* assemblage extract revealed that the microfraction containing the pentabrominated compound is toxic to water fleas (*Ceriodaphnia dubia*), nematodes (*Caenorhabditis elegans*), and larval zebrafish (*Danio rerio*). This again strengthened our hypothesis that this compound might be the toxin responsible for causing VM. After preparative isolation of AETX, we determined the lethal dose for 50 % of the population (LC_{50}) of the purified compound for *C. elegans* (40 nM) and larval *D. rerio* (275 nM) (Fig. S48, Tab. S12-S14). At sublethal concentrations (> 10 nM), an inhibitory effect of AETX on reproduction could be observed for *C. elegans*. Exposure to purified AETX induced neurologic seizure-like behavior in larval zebrafish (Movie S2), consistent with behavior seen when larva were exposed to AETX containing *H. verticillata/A. hydrillicola* biomass extract confirmed to cause VM lesions in the chicken bioassay. Neurologic behavior observed in zebrafish include: twitching, gulping, full body convulsions, loss of equilibrium, bunching toward the edge of the treatment dishes, rapid pectoral fin movements, and lack of escape response when stimulated with a probe.

Aetokthonotoxin causes Vacuolar Myelinopathy. To test whether AETX was the cause of VM, we used an avian bioassay (*3, 9, 15, 19, 21*). Specific pathogen-free leghorn chickens (*Gallus gallus*) were gavaged with either a suspension of purified AETX (15 mg kg^{-1} body weight), an AETX containing *H. verticillata/A. hydrillicola* extract as positive control (HTX; 4 mg AETX kg^{-1} body weight), or solvent control (10 % DMSO in deionized water). All birds appeared normal on physical and neurologic exams prior to the start of the study. During the short duration of the study, chickens did not exhibit pronounced clinical signs of VM in any treatment group (4 doses over 8 days). However, histologic results revealed that chickens in HTX (N=3) and purified AETX treatment (N=3) groups developed extensive vacuolization throughout the white matter of the brainstem, optic tectum, and cerebellum, while no lesions were documented in carrier solvent control chickens (N=2) (Fig. 5A). Transmission electron microscopy of the optic tectum of birds from both the HTX and AETX group revealed numerous vacuoles delimited by myelin laminae that had split at the intraperiod line, confirming the diagnosis of VM (Fig. 5B). Thus, we could confirm that AETX is indeed the causative agent of VM.
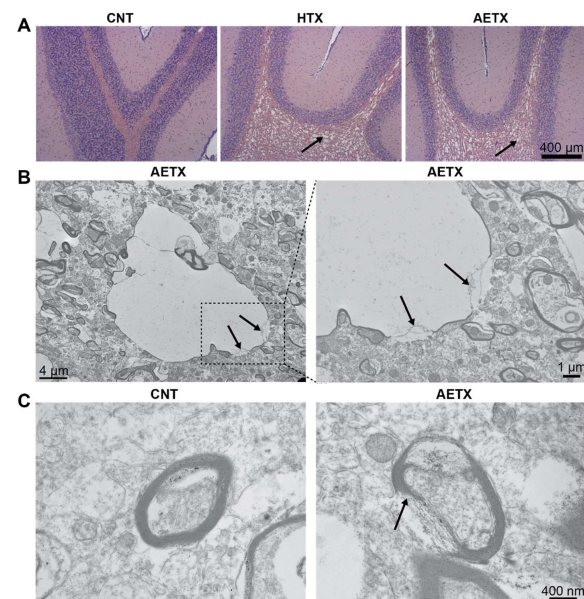
Fig. 5. Light and transmission electron microscopy of brain tissue from chickens exposed to aetokthonotoxin and controls confirms aetokthonotoxin is causing VM. (**A**) Histologic sections of cerebellum with hemotoxilin and eosin stain for solvent control (CNT), aetokthonotoxin containing *H. verticillata* extract (HTX), and pure aetokthonotoxin treatments (AETX). Chickens exposed to HTX and AETX treatments had wide-spread vacuolization of the white matter myelin tracts compared to controls (black arrows). (**B**) Numerous vacuoles delimited by myelin laminae that had split at the intraperiod line (arrows) were observed, confirming the diagnosis of Vacuolar Myelinopathy in both AETX and HTX (not shown) treatment groups. (**C**) Image of solvent control oligodendrocyte and of oligodendrocyte bursting open due to intramyelenic edema when treated with AETX (arrow). Transmission electron micrographs were taken of the optic tectum of test animals.

Conclusions

50

The causative agent of Vacuolar Myelinopathy has eluded scientists for more than twenty-five years. Our discovery that VM is induced by a pentabrominated biindole alkaloid produced by an epiphytic cyanobacterium sheds new light on the role of cyanobacteria as potentially dangerous toxin producers. While harmful blooms of planktonic algae (HABs) have been shown to extensively alter ecosystems, our findings warrant further research into the potential toxins produced by epiphytic and benthic species. Our in vitro cultivation experiments show that the biosynthesis of AETX depends on bromide availability, and that physical stressors (temperature, agitation) enhance production. We need to understand the complex environmental factors that affect the distribution and toxicity of *A. hydrillicola.* Further investigation is also needed on bioavailability of bromide from natural (geologic origin) and anthropogenic (flame retardants, fungicides, gasoline additives) sources and how they influence AETX production.

Dense infestations of submerged aquatic plants can be managed using chemical, biological, or physical controls. Importantly, herbicides containing bromide as counterions (e.g. diquat dibromide) are currently used to combat the spread of invasive submerged aquatic plants, including *H. verticillata*. Benefits and risks of using any bromide-containing chemical control agents within VM reservoir watersheds need to be reassessed. Biological controls, especially triploid grass carp (*Ctenopharyngodon idella*), can remove excess plants, but fisheries managers are reluctant to stock these fish for vegetation control due to concerns of overstocking and escape. These triploid sterile grass carp have been effective in eliminating *H. verticillata* in VM reservoirs with a history of eagle deaths (eg. DeGray Lake, Arkansas and J. Strom Thurmond, Georgia/South Carolina) (*21, 48*). Physical control of *Hydrilla* is often ineffective due to the ability of *H. verticillata* to reproduce from fragments, tubors and turions released during mechanical harvesting. Site specific, integrated management solutions have emerged from over 50 years of research on invasive plant control by the Florida Fish and Wildlife Conservation Commission, the U.S. Army Corps of Engineers, and the University of Florida (*49*). Controlling *H. verticillata* in VM reservoirs with toxic *A. hydrillicola* is critical to protect aquatic species and their consumers, but presents additional complexity and risks. Future vegetation management should prioritize overall ecosystem health and affordable long-term solutions to control and prevent expansion of *H. verticillata/A. hydrillicola*.

Wildlife are exposed to AETX for a significantly longer time period in their environment than the animals in our short-term bioassays. Raptors breeding on VM reservoirs and juveniles returning to their natal territories extend the disease risk over generations. Considering the lipophilicity of AETX and demonstration of trophic transfer, there is potential for bioaccumulation. The confirmation that additional herbivorous aquatic taxa in VM food webs are susceptible to AETX (birds, fish, amphibians, reptiles, and invertebrates) also increases potential risk to their consumers. As we do not yet fully understand how *A. hydrillicola* and its neurotoxin affect the complex aquatic ecosytems, increased monitoring and public awareness should be implemented for *A. hydrillicola* and AETX. A toxin produced by cyanobacteria colonizing a highly invasive plant, with the capacity to affect diverse animal phyla, should not be underestimated in its potential impact on our environment. Analytical methods described should facilitate expanded monitoring of AETX in aquatic environments and animal tissues. Moreover, there remains a critical need for research on mammalian susceptibility and human health risks from consumption of fish and waterbirds from VM reservoirs.

Supplementary Material:
Materials and Methods
Supplementary Text
Figures S1-S50
Tables S1-S14
Movies S1-S2
References (50-93)
MDAR Reproducibility Checklist

ORCIDs:
Steffen Breinlinger	https://orcid.org/0000-0002-8155-814X
Tabitha J. Phillips	https://orcid.org/0000-0003-4599-1154
Brigette Haram	https://orcid.org/0000-0001-8933-5613
Jan Mareš	https://orcid.org/0000-0002-5745-7023
José A. Martínez Yerena	https://orcid.org/0000-0002-7523-822X
Pavel Hrouzek	https://orcid.org/0000-0002-2061-0266
Roman Sobotka	https://orcid.org/0000-0001-5909-3879
W. Matthew Henderson	https://orcid.org/0000-0002-2800-8536
Peter Schmieder	https://orcid.org/0000-0001-9968-9327
Susan M. Williams	https://orcid.org/0000-0003-3127-5384
James D. Lauderdale	https://orcid.org/0000-0001-7503-0528
H. Dayton Wilde	https://orcid.org/0000-0002-4846-9831
Wesley L. Gerrin	https://orcid.org/0000-0002-1725-9372
Andreja Kust	https://orcid.org/0000-0003-4016-6454
John W. Washington	https://orcid.org/0000-0001-9952-600X
Christoph Wagner	https://orcid.org/0000-0001-6141-351X
Benedikt Geier	https://orcid.org/0000-0002-2942-2624
Manuel Liebeke	https://orcid.org/0000-0002-2339-1409
Heike Enke	---
Timo H.J. Niedermeyer	https://orcid.org/0000-0003-1779-7899
Susan B. Wilde	https://orcid.org/0000-0002-5388-9582

References

1. N. J. Thomas, C. U. Meteyer, L. Sileo, Epizootic Vacuolar Myelinopathy of the Central Nervous System of Bald Eagles (*Haliaeetus leucocephalus*) and American Coots (*Fulica americana*). *Veterinary Pathology*. **35**, 479–487 (1998).
2. R. S. Larsen, F. B. Nutter, T. Augspurger, T. E. Rocke, L. Tomlinson, N. J. Thomas, M. K. Stoskopf, Clinical features of Avian Vacuolar Myelinopathy in American coots. *Journal of the American Veterinary Medical Association*. **221**, 80–85 (2002).
3. J. R. Fischer, L. A. Lewis-Weis, C. M. Tate, J. K. Gaydos, R. W. Gerhold, R. H. Poppenga, Avian Vacuolar Myelinopathy Outbreaks at a Southeastern Reservoir. *Journal of Wildlife Diseases*. **42**, 501–510 (2006).
4. T. E. Rocke, N. J. Thomas, T. Augspurger, K. Miller, Epizootiologic studies of Avian Vacuolar Myelinopathy in waterbirds. *Journal of Wildlife Diseases*. **38**, 678–684 (2002).
5. John R. Fischer, Lynn A. Lewis, Tom Augspurger, and Tonie E. Rocke, Avian Vacuolar Myelinopathy: A Newly Recognized Fatal Neurological Disease of Eagles, Waterfowl and Other Birds. *Transactions of the 67th North American Wildlife and Natural Ressources Conference*.
6. T. Augspurger, J. R. Fischer, N. J. Thomas, L. Sileo, R. E. Brannian, K. J. Miller, T. E. Rocke, Vacuolar Myelinopathy in waterfowl from a North Carolina impoundment. *Journal of Wildlife Diseases*. **39**, 412–417 (2003).
7. J. R. Fischer, L. A. Lewis-Weis, C. M. Tate, Experimental Vacuolar Myelinopathy in red-tailed hawks. *Journal of Wildlife Diseases*. **39**, 400–406 (2003).
8. A.L. Bryan Jr., T.M. Murphy, K.L. Bildstein, I.L. Brisbin, Jr., J.J. Mayer, in *Raptors in Human Landscapes*, D.M. Bird, D.E. Varland, J.J. Negro, Ed. (Academic Press, New York, NY, 1996), pp. 285–298.
9. A. H. Birrenkott, S. B. Wilde, J. J. Hains, J. R. Fischer, T. M. Murphy, C. P. Hope, P. G. Parnell, W. W. Bowerman, Establishing a food-chain link between aquatic plant material and Avian Vacuolar Myelinopathy in mallards (Anas platyrhynchos). *Journal of Wildlife Diseases*. **40**, 485–492 (2004).
10. B. N. Haram, S. B. Wilde, M. J. Chamberlain, K. H. Boyd, Vacuolar Myelinopathy: waterbird risk on a southeastern impoundment co-infested with *Hydrilla verticillata* and *Aetokthonos hydrillicola*. *Biol Invasions*. **22**, 2651–2660 (2020).
11. D. C. Dorman, J. F. Zachary, W. B. Buck, Neuropathologic findings of bromethalin toxicosis in the cat. *Veterinary Pathology*. **29**, 139–144 (1992).
12. N. G. Dodder, B. Strandberg, T. Augspurger, R. A. Hites, Lipophilic organic compounds in lake sediment and American coot *(Fulica americana)* tissues, both affected and unaffected by Avian Vacuolar Myelinopathy. *Science of The Total Environment*. **311**, 81–89 (2003).
13. R. S. Larsen, F. B. Nutter, T. Augspurger, T. E. Rocke, N. J. Thomas, M. K. Stoskopf, Failure to Transmit Avian Vacuolar Myelinopathy to Mallard Ducks. *Journal of Wildlife Diseases*. **39**, 707–711 (2003).
14. T. E. Rocke, N. J. Thomas, C. U. Meteyer, C. F. Quist, J. R. Fischer, T. Augspurger, S. E. Ward, Attempts to identify the source of Avian Vacuolar Myelinopathy for waterbirds. *Journal of Wildlife Diseases*. **41**, 163–170 (2005).
15. L. A. Lewis-Weis, R. W. Gerhold, J. R. Fischer, Attempts to reproduce Vacuolar Myelinopathy in domestic swine and chickens. *Journal of Wildlife Diseases*. **40**, 476–484 (2004).
16. S. B. Wilde, T. M. Murphy, C. P. Hope, S. K. Habrun, J. Kempton, A. Birrenkott, F. Wiley, W. W. Bowerman, A. J. Lewitus, Avian Vacuolar Myelinopathy linked to exotic aquatic plants and a novel cyanobacterial species. *Environmental Toxicology*. **20**, 348–353 (2005).
17. S. B. Wilde, J. R. Johansen, H. D. Wilde, P. Jiang, B. Bartelme, R. S. Haynie, *Aetokthonos hydrillicola gen. et sp. nov.*: Epiphytic cyanobacteria on invasive aquatic plants implicated in Avian Vacuolar Myelinopathy. *Phytotaxa*. **181**, 243–260 (2014).
18. S. K. Williams, J. Kempton, S. B. Wilde, A. Lewitus, A novel epiphytic cyanobacterium associated with reservoirs affected by avian vacuolar myelinopathy. *Harmful Algae*. **6**, 343–353 (2007).
19. F. E. Wiley, S. B. Wilde, A. H. Birrenkott, S. K. Williams, T. M. Murphy, C. P. Hope, W. W. Bowerman, J. R. Fischer, Investigation of the link between Avian Vacuolar Myelinopathy and a novel species of cyanobacteria through laboratory feeding trials. *Journal of Wildlife Diseases*. **43**, 337–344 (2007).
20. F. E. Wiley, M. J. Twiner, T. A. Leighfield, S. B. Wilde, F. M. van Dolah, J. R. Fischer, W. W. Bowerman, An extract of *Hydrilla verticillata* and associated epiphytes induces Avian Vacuolar Myelinopathy in laboratory mallards. *Environmental Toxicology*. **24**, 362–368 (2009).
21. R. S. Haynie, W. W. Bowerman, S. K. Williams, J. R. Morrison, J. M. Grizzle, J. M. Fischer, S. B. Wilde, Triploid grass carp susceptibility and potential for disease transfer when used to control aquatic vegetation in reservoirs with Avian Vacuolar Myelinopathy. *The Journal of Aquatic Animal Health*. **25**, 252–259 (2013).
22. A. D. Mercurio, S. M. Hernandez, J. C. Maerz, M. J. Yabsley, A. E. Ellis, A. L. Coleman, L. M. Shelnutt, J. R. Fischer, S. B. Wilde, Experimental feeding of *Hydrilla verticillata* colonized by stigonematales

23. J. C. Maerz, S. B. Wilde, V. K. Terrell, B. Haram, R. C. Trimmer, C. Nunez, E. Cork, A. Pessier, S. Lannoo, M. J. Lannoo, S. L. Diamond, Seasonal and plant specific vulnerability of amphibian tadpoles to the invasion of a novel cyanobacteria. *Biological Invasions*. **21**, 821–831 (2019).
24. S. R. Dodd, R. S. Haynie, S. M. Williams, S. B. Wilde, Alternate food-chain transfer of the toxin linked to Avian Vacuolar Myelinopathy and implications for the endangered florida snail kite (*Rostrhamus sociabilis*). *Journal of Wildlife Diseases*. **52**, 335–344 (2016).
25. I. Chorus, J. Bartram, *Toxic cyanobacteria in water, A guide to their public health consequences, monitoring, and management* (E & FN Spon, London, New York, 1999).
26. J. K. Nunnery, E. Mevers, W. H. Gerwick, Biologically active secondary metabolites from marine cyanobacteria. *Current Opinion in Biotechnology*. **21**, 787–793 (2010).
27. H. K. Hudnell, *Cyanobacterial Harmful Algal Blooms: State of the Science and Research Needs* (Springer-Verlag, s.l., ed. 1, 2008).
28. K. Tidgewell, B. R. Clark, W. H. Gerwick, in *Comprehensive Natural Products II* (Elsevier, 2010), pp. 141–188.
29. T. Niedermeyer, M. Brönstrup, in *Microalgal biotechnology: integration and economy*, W. Posten, Ed. (de Gruyter, Berlin/Boston, 2012), pp. 169–200.
30. F. van Sant, S. M. Hassan, D. Reavill, R. McManamon, E. W. Howerth, M. Seguel, R. Bauer, K. M. Loftis, C. R. Gregory, P. G. Ciembor, B. W. Ritchie, Evidence of bromethalin toxicosis in feral San Francisco "Telegraph Hill" conures. *PLoS ONE*. **14**, e0213248 (2019).
31. G. W. Gribble, The natural production of organobromine compounds. *Environmental Science and Pollution Research*. **7**, 37–49 (2000).
32. I. Yanagisawa, H. Yoshikawa, A bromine compound isolated from human cerebrospinal fluid. *Biochimica et Biophysica Acta*. **329**, 283–294 (1973).
33. D. J. Faulkner, Marine natural products. *Natural Product Reports*. **18**, 1–49 (2001).
34. G. W. Gribble, Occurrence of halogenated alkaloids. *The Alkaloids. Chemistry and biology*. **71**, 1–165 (2012).
35. P. Friedländer, Über den Farbstoff des antiken Purpurs aus murex brandaris. *Berichte der deutschen chemischen Gesellschaft*. **42**, 765–770 (1909).
36. G. W. Gribble, Biological Activity of Recently Discovered Halogenated Marine Natural Products. *Marine Drugs*. **13**, 4044–4136 (2015).
37. S. Weigel, K. Bester, H. Hühnerfuss, Identification and quantification of pesticides, industrial chemicals, and organobromine compounds of medium to high polarity in the North Sea. *Marine Pollution Bulletin*. **50**, 252–263 (2005).
38. K. T. Fielman, S. A. Woodin, D. E. Lincoln, Polychaete indicator species as a source of natural halogenated organic compounds in marine sediments. *Environmental toxicology and chemistry*. **20**, 738–747 (2001).
39. N. Reineke, S. Biselli, S. Franke, W. Francke, N. Heinzel, H. Hühnerfuss, H. Iznaguen, U. Kammann, N. Theobald, M. Vobach, W. Wosniok, Brominated indoles and phenols in marine sediment and water extracts from the north and baltic seas-concentrations and effects. *Archives of environmental contamination and toxicology*. **51**, 186–196 (2006).
40. K.V. Sridevi, U. Venkatesham, A. VijenderReddy, Y. Venkateswarlu, Chemical constituents of the red alga Nitophyllum marginata. *Biochemical Systematics and Ecology*. **31**, 335–337 (2003).
41. M. P. Rahelivao, M. Gruner, H. Andriamanantoanina, B. Andriamihaja, I. Bauer, H.-J. Knölker, Red Algae (Rhodophyta) from the Coast of Madagascar: Preliminary Bioactivity Studies and Isolation of Natural Products. *Marine Drugs*. **13**, 4197–4216 (2015).
42. R. S. Norton, R. J. Wells, A series of chiral polybrominated biindoles from the marine blue-green alga Rivularia firma. Application of carbon-13 NMR spin-lattice relaxation data and carbon-13-proton coupling constants to structure elucidation. *J. Am. Chem. Soc.* **104**, 3628–3635 (1982).
43. X. Fu, F. J. Schmitz, R. S. Tanner, Chemical constituents of halophilic facultatively anaerobic bacteria, 1. *J. Nat. Prod.* **58**, 1950–1954 (1995).
44. Esmond E. Snell, in *Advances in Enzymology and Related Areas of Molecular Biology* (John Wiley & Sons, Ltd, 2006), pp. 287–333.
45. S. Cadel-Six, C. Dauga, A. M. Castets, R. Rippka, C. Bouchier, N. Tandeau de Marsac, M. Welker, Halogenase genes in nonribosomal peptide synthetase gene clusters of Microcystis (cyanobacteria): sporadic distribution and evolution. *Molecular Biology and Evolution*. **25**, 2031–2041 (2008).
46. N. A. Moss, G. Seiler, T. F. Leão, G. Castro-Falcón, L. Gerwick, C. C. Hughes, W. H. Gerwick, Nature's Combinatorial Biosynthesis Produces Vatiamides A-F. *Angewandte Chemie International Edition*. **58**, 9027–9031 (2019).

cyanobacteria induces Vacuolar Myelinopathy in painted turtles (*Chrysemys picta*). *PLoS ONE*. **9**, e93295 (2014).

47. C. Olano, S. J. Moss, A. F. Braña, R. M. Sheridan, V. Math, A. J. Weston, C. Méndez, P. F. Leadlay, B. Wilkinson, J. A. Salas, Biosynthesis of the angiogenesis inhibitor borrelidin by *Streptomyces parvulus* Tü4055: insights into nitrile formation. *Molecular Microbiology*. **52**, 1745–1756 (2004).

48. K. L. Fouts, N. C. Poudyal, R. Moore, J. Herrin, S. B. Wilde, Informed stakeholder support for managing invasive *Hydrilla verticillata* linked to wildlife deaths in a Southeastern reservoir. *Lake and Reservoir Management*. **33**, 260–269 (2017).

49. M. A. Weber, L. A. Wainger, N. E. Harms, G. M. Nesslage, The economic value of research in managing invasive hydrilla in Florida public lakes. *Lake and Reservoir Management*. **644**, 1–14 (2020).

ACKNOWLEDGEMENTS

Additional Results

Laboratory cultures of *A. hydrillicola* were cultivated with standard BG11 medium supplemented either with KBr (0.42 mM) or with KBr + KI (0.42 mM respectively). Detailed cultivation paramters are described in the supporting information of publication 3.[125] Methanolic biomass extracts of these two cultures were screened for halogenated metabolites using Haloseeker 1.0, a user-friendly software for the post-acquisition processing of full-scan HRESIMS-HPLC-data. It allows for a nontargeted screening of organohalogenated metabolites in complex matrixes by identifying and highlighting the halogenated metabolites based on their distinct isotope patterns.[126] Several hits of brominated metabolites were discovered and further characterized as potential precursors of Aetokthonotoxin based on their exact masses and fragmentation patterns in MS/MS-experiments. In addition, an iodine containing AETX derivative could be identified in the extract of the culture that has been supplemented with KBr and KI. The H/Cl-plots (**Fig. 2.1** and **Fig. 2.4**) show all clusters of the halogenated metabolites that have been identified in the KBr-extract and KBr+KI-extract by Haloseeker respectively. Clusters marked with a circle correspond to Aetokthonotoxin itself, the derivative and potential biosynthetic precursors. **Fig. 2.2**, **Fig. 2.5** and **Fig. 2.6** show the EICs of the monoisotopic masses, the calculated sum formulas and the molecular structures of the potential precursors corresponding to those clusters.

$C_{17}H_6Br_4IN_3$ was calculated as the molecular formula for the [M-H]$^-$ ion with m/z 693.6275 of the Aetokthonotoxin derivative (calcd. 693.6262, Δ1.92 ppm), its retention time on a RP-C18 column is slightly increased as expected due to the increased hydrophobicity of iodine in comparison to bromine. An annotated HRMS^2 spectrum of the derivative is shown in **Fig. 2.10**. A similar fragmentation pattern to AETX can be observed (see **Fig. S14** and **Table S3** of publication 3 for comparison). In a subsequent screening of *A.hydrillicola/H. verticillata* assemblages collected from the wild, the iodine-derivative could als be confirmed (**Fig. 2.9**).

HRESIMS^2 data were acquired on a Q Exactive Plus mass spectrometer (Thermo Fisher Scientific) equipped with a heated ESI interface coupled to an UltiMate 3000 HPLC system (Thermo Fisher Scientific). The following parameters were

used for the data acquisition: pos. mode, ESI spray voltage 4.5kV; neg. mode, ESI spray voltage 2.5 kV, scan range $100 - 1500$ m/z. Chromatographic separations of all extract analyses were carried out on a Phenomenex Kinetex C18 column (2.1 x 50 mm, 2,6 µm particle size) using a standard gradient from 5-100 % (v/v) MeCN in water (+0.1 % formic acid each) in 15 min with a flow rate of 0.6 mL/min. Final conditions were maintained for an additional 5 min. Sampling details of the biomass are provided in the supplementary information of publication 3.[125]
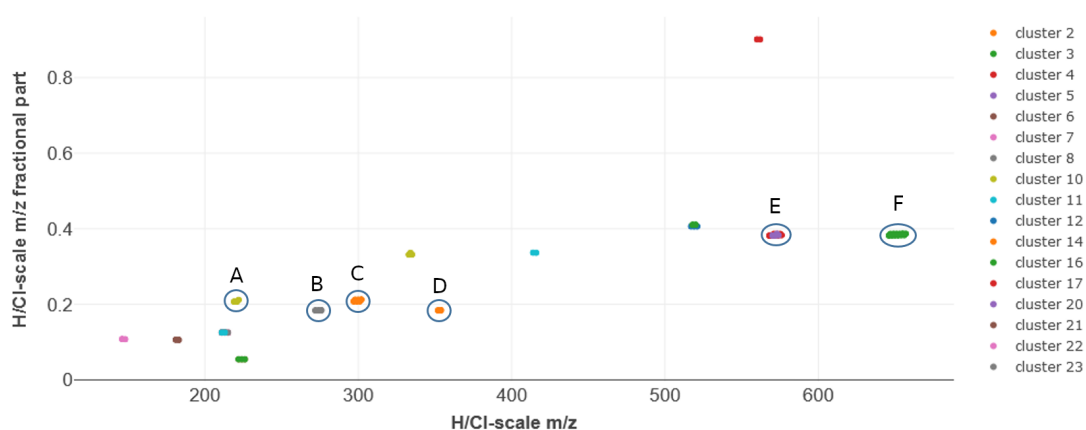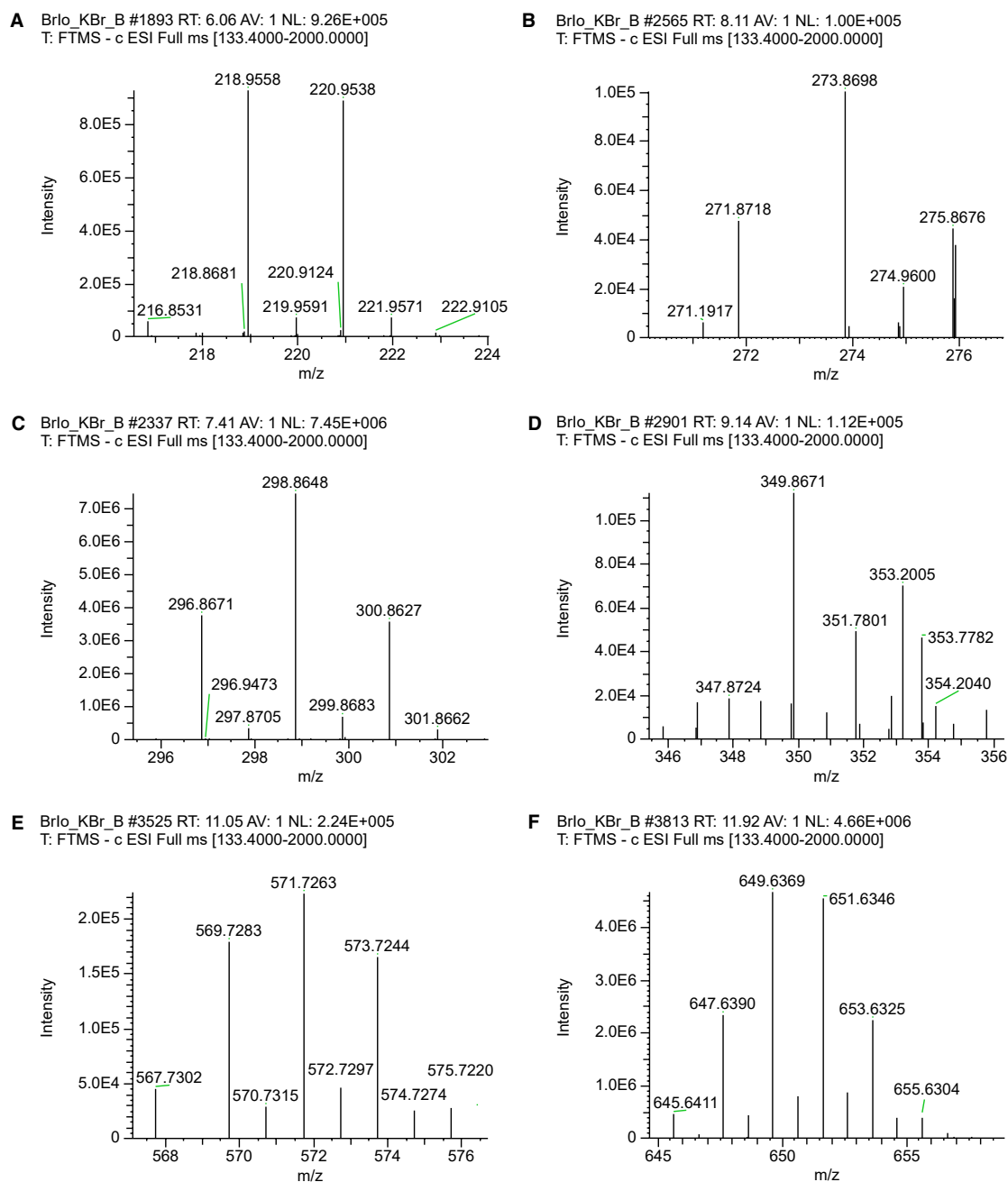

Figure 2.1.: HCl-plot of KBr-extract The plot visualizes the halogenated metabolites that have been identified as clusters which are reflecting the distinct isotope patterns. Clusters A-F corresponding to Aetokthonotoxin (F) and potential biosynthesis precursors are circled.
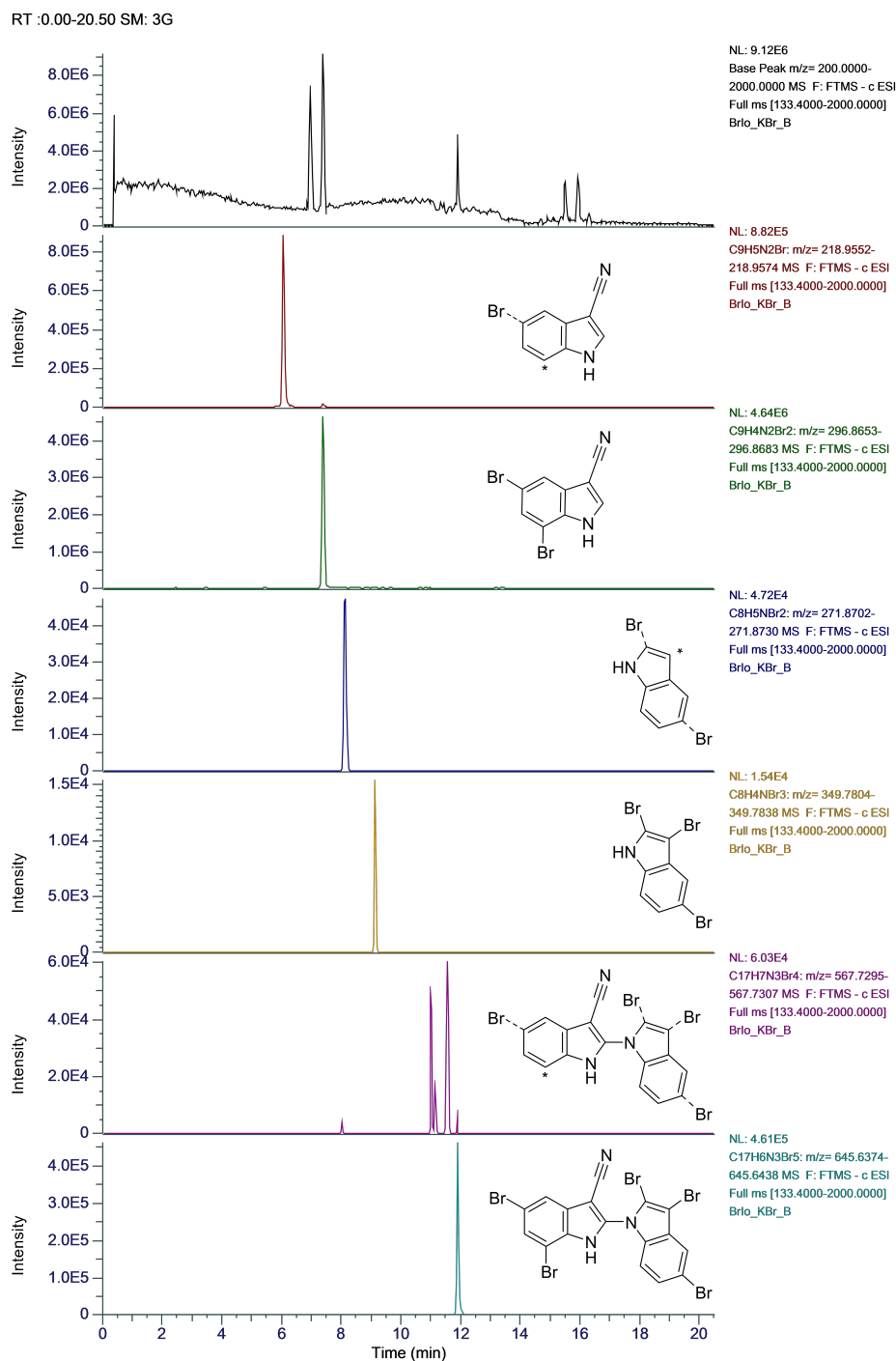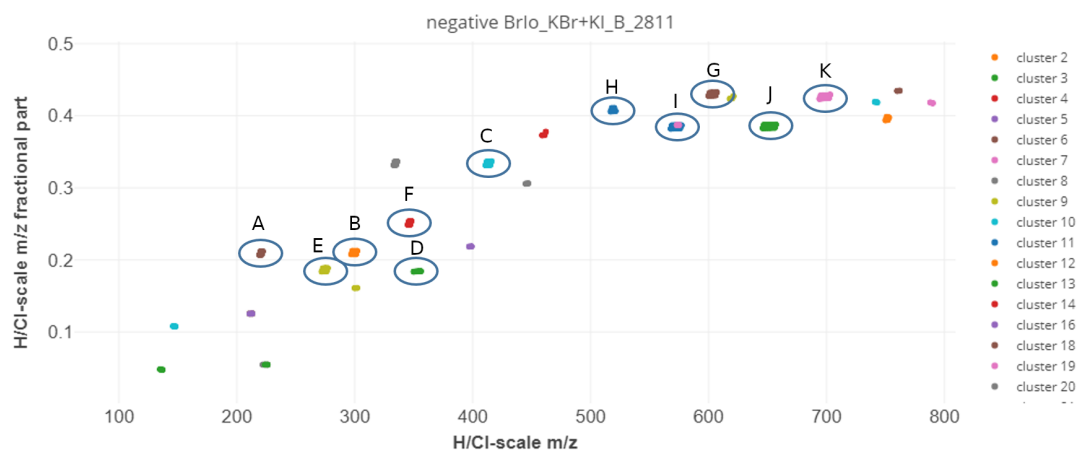
Figure 2.2.: Extracted ion chromatograms of halogenated AETX biosynthesis precursors in the KBr-extract. EICs of the clusters that have been identified by Haloseeker (Fig. 2.1) in a biomass extract of a *A. hydrillicola* culture supplemented with KBr, their calculated sum formulas and predicted structures based on biosynthesis precursor assumption. Because definitive substitution patterns could not be determined by HPLC-MS/MS analysis only, the bromine substituents are depicted via dashed bonds. Most likely alternative positions are marked with asterisks.

55

Figure 2.3.: Mass spectra of halogenated metabolites identified by haloseeker.
The mass spectra (A-F) correspond to the circled clusters in the HCl-plot of the KBr-extract, the complexity of the isotope patterns increases with the number of halogen substituents.

Figure 2.4.: HCl-plot of KBr+KI-extract The plot visualizes the halogenated metabolites that have been identified as clusters which are reflecting the distinct isotope patterns. Clusters (A-K) corresponding to Aetokthonotoxin (J), the iodine-derivative (K) and potential biosynthesis precursors are circled.
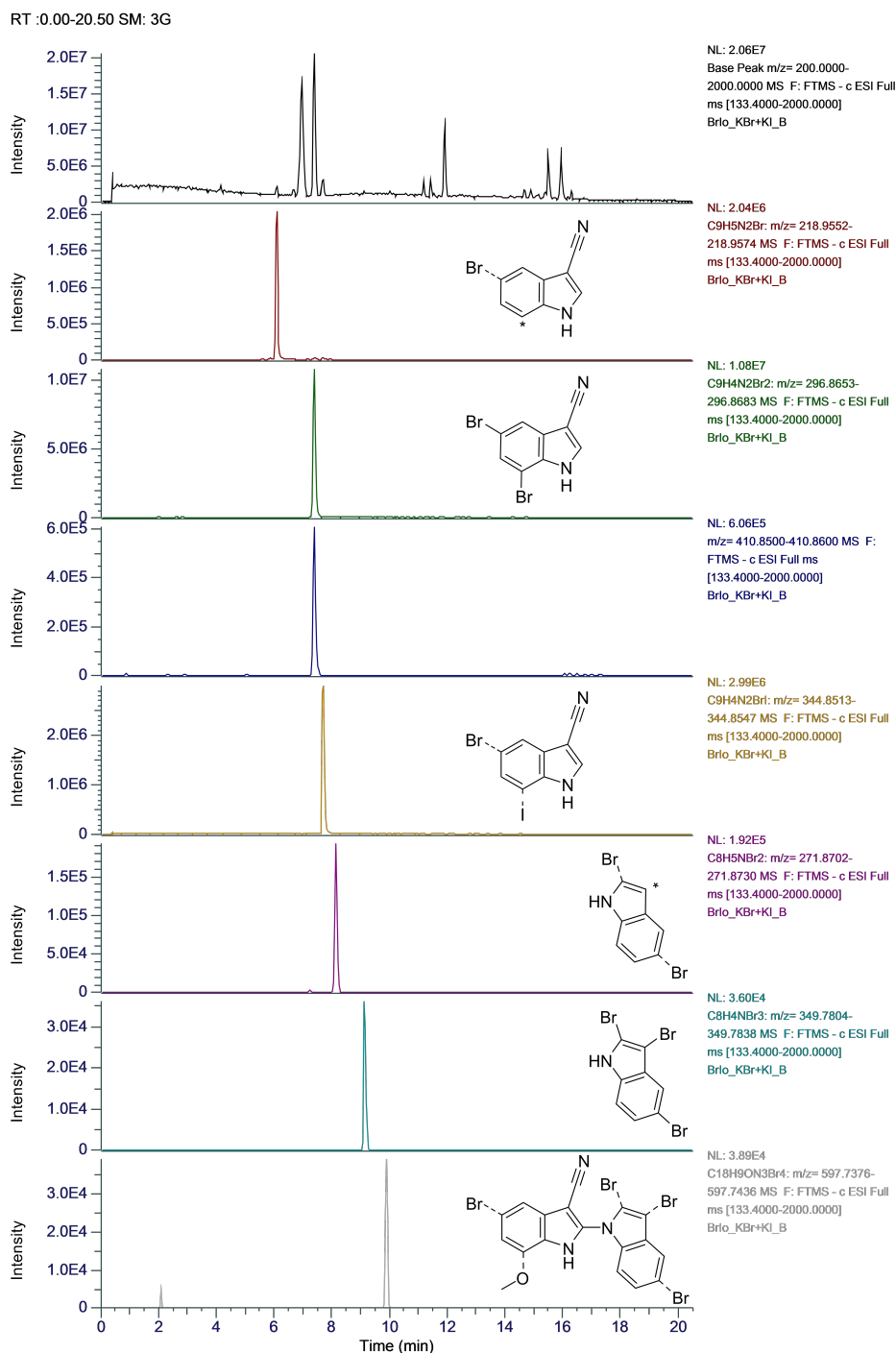
Figure 2.5.: Extracted ion chromatograms of halogenated AETX biosynthesis precursors Clusters that have been identified by Haloseeker (Fig. 2.4) in a biomass extract of a *A. hydrillicola* culture supplemented with KBr + KI, their calculated sum formulas and predicted structures based on biosynthesis precursor assumption. Because definitive substitution patterns could not be determined by HPLC-MS/MS analysis only, the halogen substituents are depicted via dashed bonds. Most likely alternative positions are marked with asterisks.
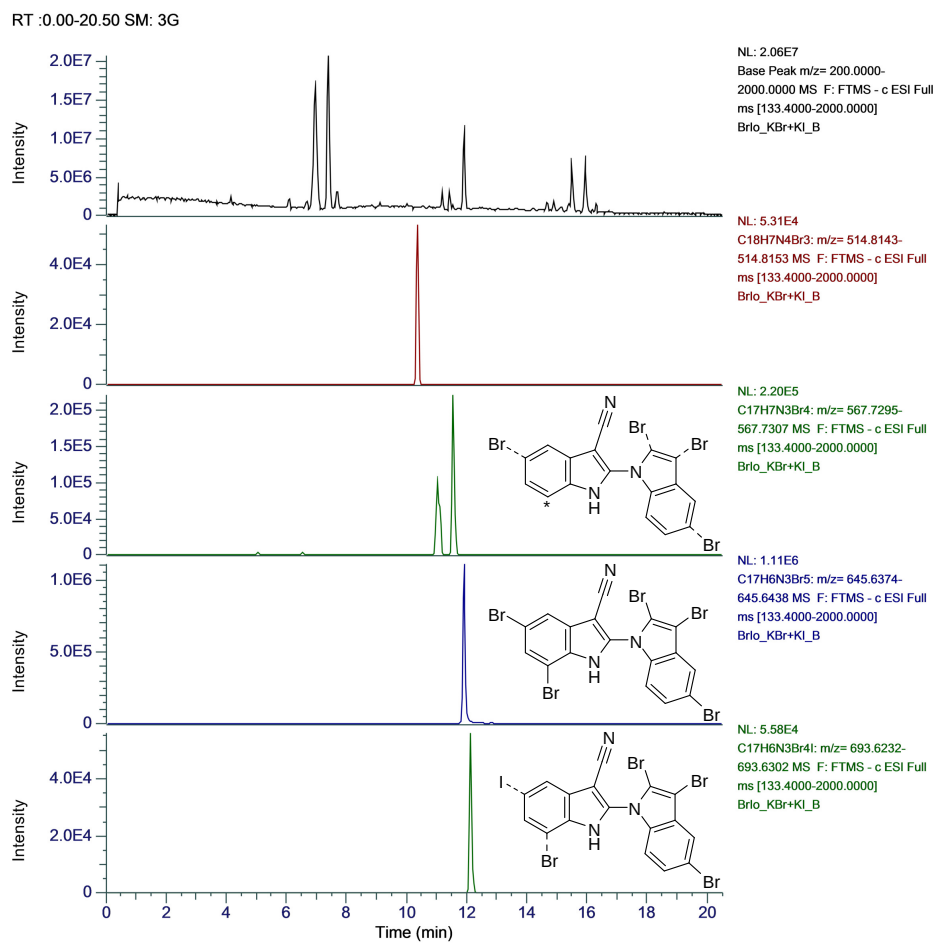
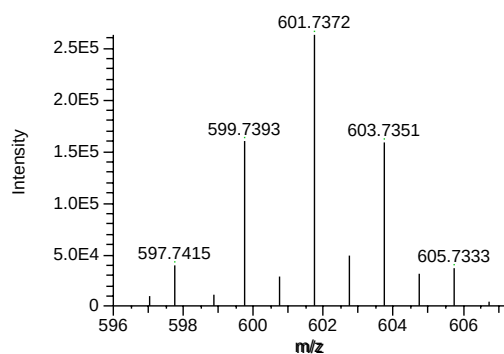**Figure 2.6.: Extracted ion chromatograms of halogenated biosynthesis precursors of Aetokthonotoxin** Continuation of **Fig. 2.5**
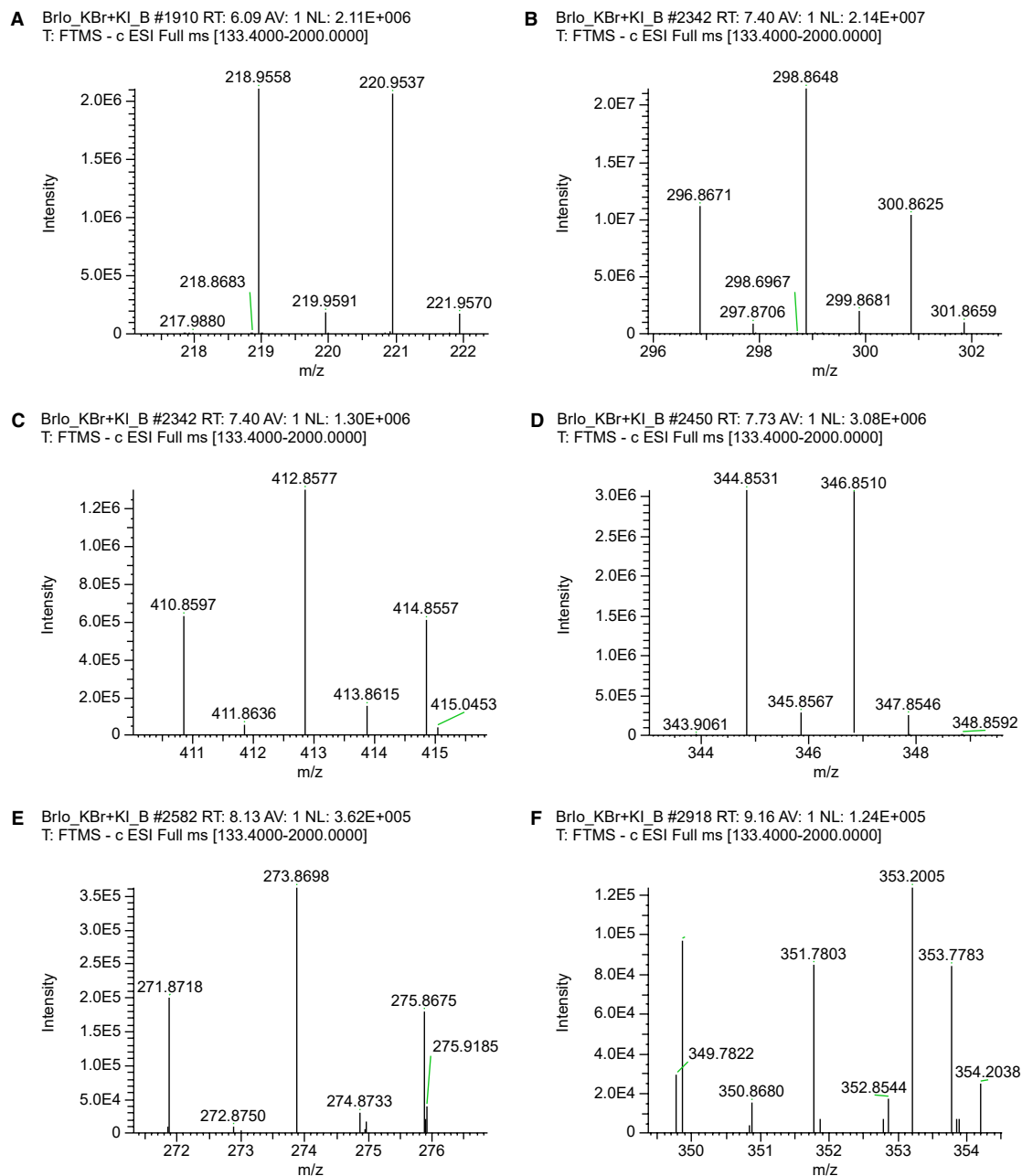
Figure 2.7.: Mass spectra of halogenated metabolites identified by haloseeker.
The mass spectra (A-F) correspond to the circled clusters in the HCl-plot of the KBr+KI-extract, the complexity of the isotope patterns increases with the number of halogen substituents.

G BrIo_KBr+KI_B #3158 RT: 9.90 AV: 1 NL: 2.62E+005
T: FTMS - c ESI Full ms [133.4000-2000.0000]

H BrIo_KBr+KI_B #3314 RT: 10.38 AV: 1 NL: 1.71E+005
T: FTMS - c ESI Full ms [133.4000-2000.0000]
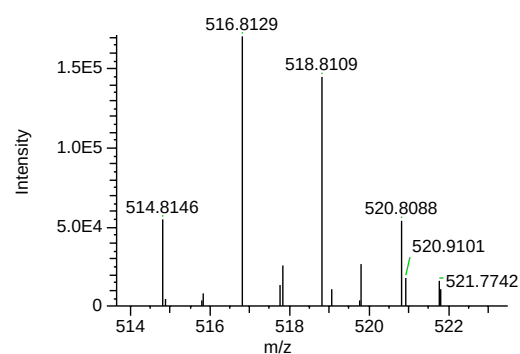
I BrIo_KBr_KI_B #3283 RT: 11.54 AV: 1 NL: 2.15E+004
T: FTMS - c ESI Full ms [133.4000-2000.0000]

J BrIo_KBr+KI_B #3818 RT: 11.91 AV: 1 NL: 1.11E+007
T: FTMS - c ESI Full ms [133.4000-2000.0000]

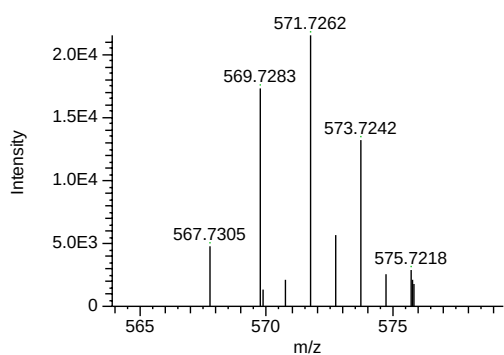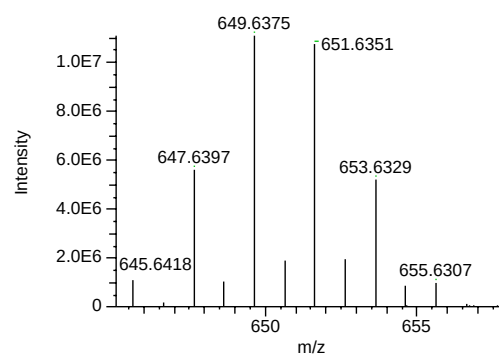**K** BrIo_KBr+KI_B #3890 RT: 12.13 AV: 1 NL: 3.95E+005
T: FTMS - c ESI Full ms [133.4000-2000.0000]
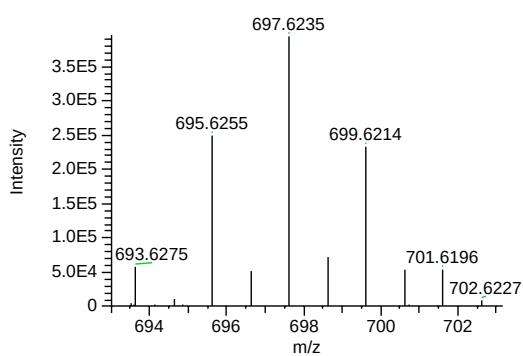
Figure 2.8.: Mass spectra of halogenated metabolites identified by haloseeker.
Mass spectra (G-K), continuation of **Figure 2.7**
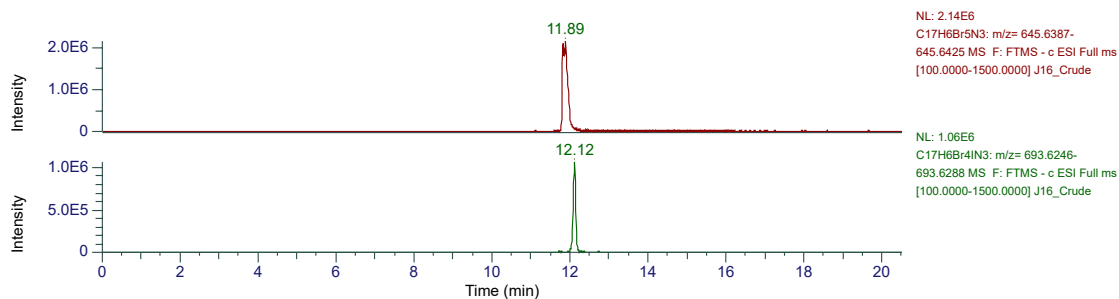
Figure 2.9.: Extracted ion chromatograms of AETX and its iodine-derivative in *A.hydrillicola/H. verticillata* assemblages collected from J. Strom Thurmond reservoir, Georgia. The AETX derivative, in which one of the bromine substituents is replaced by a iodine substituent (first detected in laboratory cultures) is also confirmed in *A. hydrillicola* growing on *H. verticillata* in the wild.
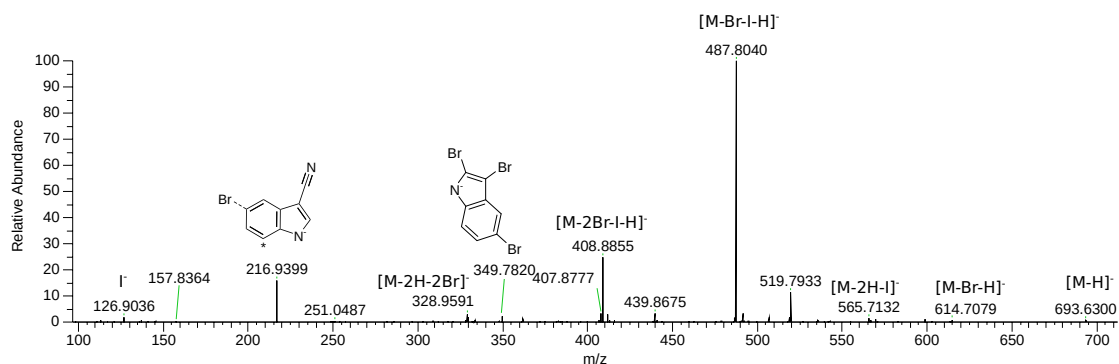
Figure 2.10.: HRMS² spectrum of aetokthonotoxin-iodine derivative (parent ion m/z 693.6281). ESI neg. mode, collision energy 75 eV.

3. Discussion and Conclusion

Nature is often more complex than what we expect it to be. Initial observations lead to first interpretations, to first hypotheses, as we try to grasp the true nature or purpose of this very observation. The story of AETX is so compelling because one can follow this scientific progress by a variety of researchers spanning more than two decades. The investigations into Vacuolar Myelinopathy and its causing agent are a prime example of how scientific discoveries are accomplished: an ever-increasing amount of detail and insight was collected over years by many individual researchers, while initial conclusions were re-evaluated, corrected, and improved until the evidence finally supported an unambiguous response to the 25-year-old question *"What is causing Vacuolar Myelinopathy in wildlife?"*.

The summary figure of publication **3** visualizes this perfectly: every zoom-in adds another layer of complexity, culminating in the discovery of AETX. Still, the current knowledge is only a fraction of the whole picture: the biosynthesis of Aetokthonotoxin is subject to ongoing investigations, as is the ecological role of the toxin and its mechanism of action in affected animals. Until now, it is unknown where *Aetokthonos hydrillicola* comes from, why it chooses mainly one specific invasive plant (*Hydrilla verticillata*) as its habitat or how it overwinters after the dieback of its host plant.

H. verticillata originates from the Indian subcontinent,[127] and was imported to the United States as an aquarium plant in the 1950s. Soon, it entered the inland water system of Florida after plants have been discarded.[128] *H. verticillata* can spread vegetatively through plant fragments and tubers (nutrient storage organs capable of surviving outside of water for several days) quickly forming dense mats.[129] Recreational boats carry plant fragments and promote colonization of new reservoirs. It seems unlikely that *A. hydrillicola* was introduced simultanously with *H. verticillata* since more than 40 years lay between the introduction of *H. verticillata* and the first reported VM cases during the mass mortality event of

3. Discussion and Conclusion

bald eagles at DeGray lake, Arkansas in 1994.[130] *A. hydrillicola* is a unique true branching cyanobacterium that is morphologically most similar to the tropical, also epiphytically growing, species *Fischerella reptans* of the Hapalosiphonaceae family. However, it shows a very distinct 16S rRNA gene sequence to any member of that family.[131] Only few taxa are known to grow epiphytically on aquatic vascular plants.[132] A worldwide screening, especially in regions where *H. verticillata* is native, might shed light on the origin of *A. hydrillicola* and could help to prevent its further spread — for now it has only been detected throughout the southeastern United States (see **publication 3, Fig. 1**).

It seems almost ironic regarding the time we are living in (nicknamed *Anthropocene* after Nobel prize laureate Paul J. Crutzen), that a simple herbicide (diquatdibromide) used to treat the invasive *H. verticillata* might contribute to the concentration increase of an ion (bromine) which allows the epiphytically growing *A. hydrillicola* to produce the fatal neurotoxin AETX. Our preliminary results show that there is an optimal bromide concentration range for AETX production, outside of which the biosynthesis seems to be downregulated. Further controlled cultivation experiments are needed in order to evaluate a correlation between bromide concentration and AETX biosynthesis. AETX is an uncommon pentabrominated biindole alkaloid. Its 9.23 kpb biosynthetic gene cluster has been identified to consist of six predicted genes coding for two halogenases, a cytochrome P450, a tentative methyl-transferase (MeT), a tryptophanase, and a single unknown protein. The two halogenases (aetA and aetF) have been heterologously expressed in *E. coli*. AetF has been successfully characterized, it is capable of sequencially introducing two bromide substituents to the indole scaffold at position 5 and 7. Preliminary results on semi-prufied aetA suggest a similar activity for the second halogenase, as dibrominated tryptrophane and indole products have been found in HPLC-MS analysis. However, until now only low quantities of aetA have been successfully isolated, therefore, no educated guess about the definitive activity of this enzyme, especially regarding the products' substitution patterns, can be made. Further studies with the purified enzyme and isolation and structure elucidation of the products are required.

In the biomass extract of *A. hydrillicola* a compound with the sum formula $C_{17}H_6Br_4IN_3$ has been found. Its retention time and fragmentation pattern in

64

HRMS^2 experiments suggest an AETX derivative that contains an iodine instead of a bromine as a substituent of the carbonitrile-indole subunit (**Fig. 2.10**). Individual assays with aetA and aetF containing an iodide source are necessary to determine whether one of these halogenases additionally accepts iodide as a substrate, and incorperates it selectively, or if another halogenase not part of the AETX gene cluster is responsible for the biosynthesis of this structural variant. Provided that the substitution pattern of the AETX-iodine variant has been elucidated and that one of the halogenases is responsible for the iodination, then these assay results could additionally help in solving the chronology of the individual halogenation reactions for the original biosynthesis of AETX. AetA and aetF are flavin-dependent halogenases — to date only one other flavin-dependant halogenase capable of *in vitro* iodination in the presence of chloride and bromide has been reported from a cyanophage.[133] Screening of the *A. hydrillicola* biomass extract for halogenated metabolites revealed several hits whose masses and chemical formulas correspond to potential biosynthetic precursors of AETX. While single and double brominated versions of the indole-carbonitrile can be oberved, only di- and tribrominated versions of the plain indole subunit seem to be present. This leads to several assumptions: first of all that some of the halogenation reactions happen prior to the fusion of the two indole subunits. Second, *in vivo* the brominated tryptophan does not seem to be a stable intermediate and its apliphatic side chain gets cleaved spontaneously. Additionally, there are four intermediates present with the same molecular mass/chemical formula corresponding to fourfold brominated biindoles differing in retention times. Variations in the substitution patterns of these biindoles are likely responsible for the distinct retention times. If all of these compounds are intermediates of the biosynthetic pathway of AETX, it seems contradicting that the final individual di- and tri-brominated subunits and a fourfold brominated biindole can be observed simultaneously. Maybe some of these intermediates are actually metabolites or derivatives of AETX. Their subsequent isolation and structure elucidation, at best from an *in vitro* experiment, could help in establishing the total biosynthetic pathway of AETX (and its derivatives).

Recently, the successful heterologous expression of a whole cyanobacterial biosynthetic gene cluster has been reported,[134] and although it also would be the most elegant way to elucidate the biosynthesis of AETX, it seems like an impossible task until access of *A. hydrillicola* for genetic modifications will have been developed.

3. Discussion and Conclusion

The toxin concentration in *A. hydrillicola/H. verticillata* is subjected to seasonal variations, in which a peak is found in November. This increased AETX concentration strongly correlates with the documentation of VM occurrences in late autumn. *A. hydrillicola* also becomes acutely toxic in late autumn (when most of the dead animals are found). At this time of the year, *H. verticillata* senesceses, the water temperature of the reservoirs starts to decline and lake turnover takes place. It has been shown, that *H. verticillata* accumulates bromide over the year, which then likely gets released from the cells during the Hydrilla dieback, thus creating a local bromide rich environment for *A. hydrillicola*. Laboratory trials verified these observations: the biosynthesis of AETX only takes place in the presence of a bromide source and under stressful conditions, suboptimal for normal growth, like reduced cultivation temperature and shear stress through vigorous stirring or shaking of the cultures. Why does *A. hydrillicola* produce AETX in the first place, and why does only environmental stress trigger its production? What ecological and/or physiological role might AETX serve for its producer under such pressure for survival? These remain open questions. We did not find AETX being actively secreted into the culture medium, a signal molecule to influence the host plant seems unlikely although there might be cellular connections between *A. hydrillicola* and *H. verticillata* under *in vivo* conditions that could allow for the exchange of signalling molecules, nutrients etc. Qualitative and quantitative transcriptional analysis under different culture conditions could provide insight into the expression levels of the biosynthetic genes involved in AETX biosynthesis, and hence might explain its regulation on the genomic level. A whole transcriptome analysis might even help to answer the question about the ecological and/or physiological role of AETX.

AETX is toxic to a variety of organisms from different animal phyla — until now it has been shown to be toxic to birds, reptiles, fish, water flea, and nematodes. While all these animals possess neuronal systems, they do have a dissimilar brain anatomy. A common mechanism of action therefore might act on a very basic underlying neurophysiological principle that is shared by all these organisms. Promising preliminary studies on the mechanism of action are currently conducted with zebrafish as a model organism (personal conversation with T.J. Phillips). Until now, mammals that have been fed *H. verticillata* colonized with *A. hydrillcola*

have not developed the characteristic lesions for VM.[135,136] This could be related to a different neurophysiology, or it might be a concentration dependent issue related to a low bioavailability at the molecular cellular target of AETX — possibly due to fast metabolic clearance and/or ineffective mammalian blood brain barrier penetration.

A. hydrillicola produces a variety of other toxic metabolites (unpublished results from M. Schwark) that could have synergistic effects with AETX. It has already been shown that AETX travels up the food chain and that its effect is dose-dependent (seasonal fluctuation of toxin concentration and seasonal occurrence of VM align). The combination of a highly invasive plant and an associated cyanobacterium producing a variety of toxic metabolites poses not only a serious threat to wildlife, but also indirectly to humans due to the potential consumption of contaminated animals.

"Blooms Bite the Hand That Feeds Them" is the striking title Paerl and colleagues used to describe how humans and harmful blooms of planktonic algae (HABs) interact in a positive feedback loop. Excessive use of fertilizers in industrial agriculture and climate change promote cyanobacterial HABs with a selection bias for toxic species.[47,137] While this extensive alteration of ecosystems by cyanobacterial HABs is known, our findings point to evidence of a new, emerging danger through toxic epiphytic and benthic species.

The more details we uncover, the more careful and the more holistic we can act towards controlling a further spreading of *H. verticillata* and its toxic occupant. The impact of short-sighted behavior, even unintentionally, in a universe of maximum complexity can lead to unforeseen consequences. The use of Diquatdibromide as an herbicide to control *H. verticillata* is an illuminating example of this very point.

For a researcher with an interest in NPs it is crucial to bear nature's complexity in mind. One of the most common approaches to look for new drug leads is the bioactivity assay guided isolation of novel compounds. While it is a justifiable approach that has led to many successful isolations, and in doing so to life saving new treatment possibilities,[138] only few *in-vitro* detected bioactivities can be transferred into a clinical setting. Initial results and conclusions have to be evaluated with care. Publication **1** "Hapalindoles from the Cyanobacterium *Hapalosiphon*

sp. Inhibit T Cell Proliferation" and publication **2** "Nostotrebin 6 Related Cyclopentenediones and δ-Lactones with Broad Activity Spectrum Isolated from the Cultivation Medium of the Cyanobacterium *Nostoc* sp. CBT1153" enclosed in this thesis demonstrate why this care has to be taken and highlight the advantages and pitfalls of bioactivity guided isolation of novel compounds for drug development purposes.

In publication **1**, we screened 575 cyanobacteria extracts for immunomodulatory effects, resulting in 35 extracts with notable inhibition of T-cell proliferation. The subsequent bioactivity assay guided fractionation of one of the active extracts led to the identification of 5 compounds from the hapalindole family, 3 known hapalindoles and 2 formamide-bearing derivatives reported for the first time from a natural source. Hapalindoles are long known for their broad activity spectrum against bacteria, fungi, algae, insects, vertebrates, and even mammalian cancer cell lines.[139] However, a modulation of human immune cell activity has not been described before. In order to evaluate a therapeutic range for an anti–inflammatory remedy, T-cell proliferation and apoptosis induction by the isolated hapalindoles were compared. Although the Hapalindole family is known for several decades, not much is known about the structure-activity relation regarding their diverse bioactivities. The newly isolated Hapalindole-formamide derivatives showed a weaker anti–proliferative effect compared to their isonitrile and isothiocyanate variants (in line with previously reported results for different bioactivities), strengthening the key role of this functional group. The anti–proliferative effect on human T-cells is more distinct than toxicity on those cells, associating yet another bioactivity with the hapalindoles. Nevertheless, establishing a structure-activity relationship for hapalindole derivatives and/or their individual functional groups, at best exclusively for a specific bioactivity, should be a priority in order to rule out that a substructural motif confers an assay interfering ability. Metal chelation, redox cycling, and protein reactivity are three examples of this interfering ability. Compounds containing such non-specific, reactive substructures register as (false) positive hits in (m)any given assay(s), rendering the results useless and therefore making the tested compounds themselves challenging candidates for future drug development.[140] In 2010, after observing the reappearance of the same compounds registering as positive hits in different screening campaigns, Baell and Holloway created substructure filters for synthetic compound libraries used in HTS for an

automatic exclusion in bioassays. Compounds containing these substructures were termed Pan-Assay Interference Compounds – PAINS.[141] There is increasing evidence that the concept of PAINS can be transferred to NPs, despite NPs unique position in drug discovery and weak resemblance to the compounds from which the PAINS definitions were derived. Some of the functional groups registered as PAINS motifs which are also found in NPs are catechols, quinones, phenolic Mannich bases, hydroxyphenylhydrazones, β-lactams, peroxides, epoxides, disulfides, or enones.[142] From the evolutionary viewpoints of the producer organisms (in terms of the Screening Hypothesis), it makes sense that NPs contain these substructures, and hence display a broad unspecific bioactivity against many targets: This provides a vantage ground for further development of more specific bioactive compounds in case a new habitat, new competitors, or new environmental conditions require novel survival strategies.

Publication **2** describes the Cyclopentenediones and δ-Lactones isolated from the cultivation medium of *Nostoc* sp. CBT1153, which revealed a high activity in an initial screening of 572 cyanobacteria extracts against trypanosomal protease rhodesain. Nostotrebin 6, an already known homodimeric cyclopentenedione and biosynthetically related monomeric, dimeric, and higher oligomeric variants were isolated as the active substances. Due to their polyphenolic nature, the detected bioactivity was interpreted with care as polyphenols are a common PAINS motif. Indeed, Nostotrebin 6 has been attributed diverse bioactivities (cytotoxic and pro-apoptotic on mouse fibroblasts, anti–bacterial against Gram-positive bacteria, Acetylcholinesterase inhibition) in earlier studies.[143–145] In order to either evaluate actual structure-activity relationships for this compound family, or to prove them of being PAINs, a comparative activity testing was performed. The CPD substructure is chemically reactive itself and has been suspected to be responsible for the broad activity spectrum,[146] but this could not be confirmed. In line with previous observations in other polyphenolic NPs, a correlation between the number of free phenolic hydroxy groups per molecule and the bioactivity has been found, probably due to the unspecific polyphenol-like interaction with proteins.[147–151] The physiological role of the nostotrebin compound family has yet to be investigated in detail. As the compounds were found in the cultivation medium it can be presumed that they are actively secreted into the medium — a passive

diffusion with regards to their polyphenolic nature is highly unlikely. Thus, as suggested in previous investigations[145,146], the nostotrebin compound family might serve a protective function for the producing organism against other microbial pathogens. PAINS are a pain for the natural product scientist on the lookout for new treatment possibilities, but for an organism that tries to outcompete its rivals, compounds with a broad unspecific bioactivity might be just the silver bullet it needs for a successful survival strategy. In fact, within the framework of the Screening Hypothesis, a NP that possesses a specific, targeted bioactivity, is an exception, and is only in rare cases preserved in the constantly changing process of evolution.

Bibliography

[1] Wolfender, J.-L.; Nuzillard, J.-M.; van der Hooft, J. J. J.; Renault, J.-H.; Bertrand, S. Accelerating metabolite identification in natural product research: toward an ideal combination of LC-HRMS/MS and NMR profiling, in silico databases and chemometrics. *Analytical Chemistry* **2019**, 704–732.

[2] David, B.; Wolfender, J.-L.; Dias, D. A. The pharmaceutical industry and natural products: historical status and new trends. *Phytochemistry Reviews* **2015**, *14*, 299–315.

[3] Katz, L.; Baltz, R. H. Natural product discovery: Past, present, and future. *Journal of Industrial Microbiology & Biotechnology* **2016**, *43*, 155–176.

[4] Cragg, G. M.; Newman, D. J. Natural products: a continuing source of novel drug leads. *Biochimica et Biophysica Acta* **2013**, *1830*, 3670–3695.

[5] Nunnery, J. K.; Mevers, E.; Gerwick, W. H. Biologically active secondary metabolites from marine cyanobacteria. *Current Opinion in Biotechnology* **2010**, *21*, 787–793.

[6] Bernardini, S.; Tiezzi, A.; Laghezza Masci, V.; Ovidi, E. Natural products for human health: an historical overview of the drug discovery approaches. *Natural Product Research* **2018**, *32*, 1926–1950.

[7] Jones, C. G.; Firn, R. D. On the evolution of plant secondary chemical diversity. *Philosophical Transactions of the Royal Society Biological Sciences* **1991**, *333*, 273–280.

[8] Firn, R. D.; Jones, C. G. Natural products–a simple model to explain chemical diversity. *Natural Product Reports* **2003**, *20*, 382–391.

[9] Firn, R. D.; Jones, C. G. In *Phytochemical Diversity and Redundancy in Ecological Interactions*; Romeo, J. T., Saunders, J. A., Barbosa, P., Eds.; Recent Advances in Phytochemistry; Springer US and Imprint and Springer: Boston, MA, 1996; pp 295–312.

[10] Newman, D. J.; Cragg, G. M. Natural Products as Sources of New Drugs over the Nearly Four Decades from 01/1981 to 09/2019. *Journal of Natural Products* **2020**,

83, 770–803.

[11] Thomford, N. E.; Senthebane, D. A.; Rowe, A.; Munro, D.; Seele, P. et al. Natural Products for Drug Discovery in the 21st Century: Innovations for Novel Drug Discovery. *International Journal of Molecular Sciences* **2018**, *19*, 1578.

[12] Butler, M. S. Natural products to drugs: natural product-derived compounds in clinical trials. *Natural Product Reports* **2008**, *25*, 475–516.

[13] Saniotis, A.; Henneberg, M. An Evolutionary Approach Toward Exploring Altered States of Consciousness, Mind–Body Techniques, and Non-Local Mind. *World Futures* **2011**, *67*, 182–200.

[14] Mishra, B. B.; Tiwari, V. K. Natural products: an evolving role in future drug discovery. *European Journal of Medicinal Chemistry* **2011**, *46*, 4769–4807.

[15] Koehn, F. E.; Carter, G. T. The evolving role of natural products in drug discovery. *Nature Reviews Drug Discovery* **2005**, *4*, 206–220.

[16] Baker, D. D.; Chu, M.; Oza, U.; Rajgarhia, V. The value of natural products to future pharmaceutical discovery. *Natural Product Reports* **2007**, *24*, 1225–1244.

[17] Camp, D.; Davis, R. A.; Evans-Illidge, E. A.; Quinn, R. J. Guiding principles for natural product drug discovery. *Future Medicinal Chemistry* **2012**, *4*, 1067–1084.

[18] DeCorte, B. L. Underexplored Opportunities for Natural Products in Drug Discovery. *Journal of Medicinal Chemistry* **2016**, *59*, 9295–9304.

[19] Williams, D. E.; Andersen, R. J. Biologically active marine natural products and their molecular targets discovered using a chemical genetics approach. *Natural Product Reports* **2020**, *37*, 617–633.

[20] Baltz, R. H. Natural product drug discovery in the genomic era: realities, conjectures, misconceptions, and opportunities. *Journal of Industrial Microbiology & Biotechnology* **2019**, *46*, 281–299.

[21] Harvey, A. L.; Edrada-Ebel, R.; Quinn, R. J. The re-emergence of natural products for drug discovery in the genomics era. *Nature Reviews. Drug Discovery* **2015**, *14*, 111–129.

[22] Brownstein, M. J. A brief history of opiates, opioid peptides, and opioid receptors. *Proceedings of the National Academy of Sciences of the United States of America* **1993**, *90*, 5391–5393.

[23] Dias, D. A.; Urban, S.; Roessner, U. A Historical Overview of Natural Products in Drug Discovery. *Metabolites* **2012**, *2*, 303–336.

[24] Splitstoser, J. C.; Dillehay, T. D.; Wouters, J.; Claro, A. Early pre-Hispanic use of indigo blue in Peru. *Science Advances* **2016**, *2*, e1501623.

[25] Carl, J.; Schwarzer, M.; Klingelhoefer, D.; Ohlendorf, D.; Groneberg, D. A. Curare–a curative poison: a scientometric analysis. *PLoS ONE* **2014**, *9*, e112026.

[26] Miller, M. J.; Albarracin-Jordan, J.; Moore, C.; Capriles, J. M. Chemical evidence for the use of multiple psychotropic plants in a 1,000-year-old ritual bundle from South America. *Proceedings of the National Academy of Sciences of the United States of America* **2019**, *116*, 11207–11212.

[27] Froese, T.; Guzmán, G.; Guzmán-Dávalos, L. On the Origin of the Genus Psilocybe and Its Potential Ritual Use in Ancient Africa and Europe. *Economic Botany* **2016**, *70*, 103–114.

[28] Lietava, J. Medicinal plants in a Middle Paleolithic grave Shanidar IV? *Journal of Ethnopharmacology* **1992**, *35*, 263–266.

[29] Peintner, U.; Pöder, R.; Pümpel, T. The iceman's fungi. *Mycological Research* **1998**, *102*, 1153–1162.

[30] Guglielmino, C. R.; Viganotti, C.; Hewlett, B.; Cavalli-Sforza, L. L. Cultural variation in Africa: role of mechanisms of transmission and adaptation. *Proceedings of the National Academy of Sciences of the United States of America* **1995**, *92*, 7585–7589.

[31] Saslis-Lagoudakis, C. H.; Hawkins, J. A.; Greenhill, S. J.; Pendry, C. A.; Watson, M. F. et al. The evolution of traditional knowledge: environment shapes medicinal plant use in Nepal. *Proceedings of the Royal Society of London. Series B: Biological Sciences* **2014**, *281*, 20132768.

[32] Schopf, J. W.; Packer, B. M. Early Archean (3.3-billion to 3.5-billion-year-old) microfossils from Warrawoona Group, Australia. *Science* **1987**, *237*, 70–73.

[33] Whitton, B. A. *Ecology of Cyanobacteria II*; Springer Netherlands: Dordrecht, 2012.

[34] Martin, W. F.; Garg, S.; Zimorski, V. Endosymbiotic theories for eukaryote origin. *Philosophical transactions of the Royal Society of London. Series B, Biological sciences* **2015**, *370*, 20140330.

[35] Welker, M.; Dittmann, E.; von Döhren, H. Cyanobacteria as a source of natural products. *Methods in Enzymology* **2012**, *517*, 23–46.

[36] Jones, A. C.; Monroe, E. A.; Eisman, E. B.; Gerwick, L.; Sherman, D. H. et al. The unique mechanistic transformations involved in the biosynthesis of modular natural products from marine cyanobacteria. *Natural Product Reports* **2010**, *27*, 1048.

[37] Bergman, B.; Rai, A. N.; Rasmussen, U. In *Associative and Endophytic Nitrogen-*

fixing Bacteria and Cyanobacterial Associations; Elmerich, C., Newton, W. E., Eds.; Nitrogen Fixation; Springer: Dordrecht and Berlin and Heidelberg, 2007; pp 257–301.

[38] Adams, D. G.; Duggan, P. S. Tansley Review No. 107. Heterocyst and akinete differentiation in cyanobacteria. *New Phytologist* **1999**, *144*, 3–33.

[39] Berman-Frank, I.; Lundgren, P.; Falkowski, P. Nitrogen fixation and photosynthetic oxygen evolution in cyanobacteria. *Research in Microbiology* **2003**, *154*, 157–164.

[40] Hudnell, H. K. *Cyanobacterial Harmful Algal Blooms: State of the Science and Research Needs*, 1st ed.; Advances in Experimental Medicine and Biology, 619; Springer-Verlag: s.l., 2008; Vol. 619.

[41] Buratti, F. M.; Manganelli, M.; Vichi, S.; Stefanelli, M.; Scardala, S. et al. Cyanotoxins: producing organisms, occurrence, toxicity, mechanism of action and human health toxicological risk evaluation. *Archives of Toxicology* **2017**, *91*, 1049–1130.

[42] Carmichael, W. W.; Biggs, D. F.; Peterson, M. A. Pharmacology of Anatoxin-a, produced by the freshwater cyanophyte Anabaena flos-aquae NRC-44-1. *Toxicon* **1979**, *17*, 229–236.

[43] Carmichael, W. W.; Boyer, G. L. Health impacts from cyanobacteria harmful algae blooms: Implications for the North American Great Lakes. *Harmful Algae* **2016**, *54*, 194–212.

[44] Corbel, S.; Mougin, C.; Bouaïcha, N. Cyanobacterial toxins: modes of actions, fate in aquatic and soil ecosystems, phytotoxicity and bioaccumulation in agricultural crops. *Chemosphere* **2014**, *96*, 1–15.

[45] Du, X.; Liu, H.; Le Yuan,; Wang, Y.; Ma, Y. et al. The Diversity of Cyanobacterial Toxins on Structural Characterization, Distribution and Identification: A Systematic Review. *Toxins* **2019**, *11*, 530–564.

[46] Dittmann, E.; Fewer, D. P.; Neilan, B. a. Cyanobacterial toxins: biosynthetic routes and evolutionary roots. *FEMS Microbiology Reviews* **2013**, *37*, 23–43.

[47] Paerl, H. W.; Hall, N. S.; Calandrino, E. S. Controlling harmful cyanobacterial blooms in a world experiencing anthropogenic and climatic-induced change. *The Science of the total environment* **2011**, *409*, 1739–1745.

[48] Steffensen, D. A. Economic cost of cyanobacterial blooms. *Advances in Experimental Medicine and Biology* **2008**, *619*, 855–865.

[49] Svirčev, Z. B.; Tokodi, N.; Drobac, D.; Codd, G. A. Cyanobacteria in aquatic ecosystems in Serbia: effects on water quality, human health and biodiversity. *Systematics and Biodiversity* **2014**, *12*, 261–270.

[50] Tidgewell, K.; Clark, B. R.; Gerwick, W. H. In *Comprehensive Natural Products II: Chemistry and Biology*; Mander, L., Liu, H.-W., Eds.; Elsevier: Oxford, 2010; pp 141–188.

[51] Welker, M.; von Dohren, H. Cyanobacterial peptides - nature's own combinatorial biosynthesis. *FEMS Microbiology Reviews* **2006**, *30*, 530–563.

[52] Jones, A. C.; Gu, L.; Sorrels, C. M.; Sherman, D. H.; Gerwick, W. H. New tricks from ancient algae: natural products biosynthesis in marine cyanobacteria. *Current Opinion in Chemical Biology* **2009**, *13*, 216–223.

[53] Demay, J.; Bernard, C.; Reinhardt, A.; Marie, B. Natural Products from Cyanobacteria: Focus on Beneficial Activities. *Marine Drugs* **2019**, *17*, 320–369.

[54] Dittmann, E.; Gugger, M.; Sivonen, K.; Fewer, D. P. Natural Product Biosynthetic Diversity and Comparative Genomics of the Cyanobacteria. *Trends in Microbiology* **2015**, *23*, 642–652.

[55] Shah, S. A. A.; Akhter, N.; Auckloo, B. N.; Khan, I.; Lu, Y. et al. Structural Diversity, Biological Properties and Applications of Natural Products from Cyanobacteria. A Review. *Marine Drugs* **2017**, *15*, 354–384.

[56] Mi, Y.; Zhang, J.; He, S.; Yan, X. New Peptides Isolated from Marine Cyanobacteria, an Overview over the Past Decade. *Marine Drugs* **2017**, *15*, 132–159.

[57] Wang, M.; Zhang, J.; He, S.; Yan, X. A Review Study on Macrolides Isolated from Cyanobacteria. *Marine Drugs* **2017**, *15*.

[58] Chlipala, G. E.; Mo, S.; Orjala, J. Chemodiversity in freshwater and terrestrial cyanobacteria - a source for drug discovery. *Current Drug Targets* **2011**, *12*, 1654–1673.

[59] Sivonen, K.; Leikoski, N.; Fewer, D. P.; Jokela, J. Cyanobactins - ribosomal cyclic peptides produced by cyanobacteria. *Applied Microbiology and Biotechnology* **2010**, *86*, 1213–1225.

[60] van Apeldoorn, M. E.; van Egmond, H. P.; Speijers, G. J. A.; Bakker, G. J. I. Toxins of cyanobacteria. *Molecular Nutrition & Food Research* **2007**, *51*, 7–60.

[61] Pegram, R. A.; Humpage, A. R.; Neilan, B. a.; Runnegar, M. T.; Nichols, T. et al. Cyanotoxins Workgroup Report. *Advances in Experimental Medicine and Biology* **2008**, *619*, 317–381.

[62] Pearson, L.; Mihali, T.; Moffitt, M.; Kellmann, R.; Neilan, B. On the Chemistry, Toxicology and Genetics of the Cyanobacterial Toxins, Microcystin, Nodularin, Saxitoxin and Cylindrospermopsin. *Marine Drugs* **2010**, *8*, 1650–1680.

[63] Marner, F.-J.; Moore, R. E.; Hirotsu, K.; Clardy, J. Majusculamides A and B,

two epimeric lipodipeptides from Lyngbya majuscula Gomont. *Journal of Organic Chemistry* **1977**, *42*, 2815–2819.

[64] Burja, A. M.; Banaigs, B.; Abou-Mansour, E.; Burgess, J. G.; Wright, P. C. Marine cyanobacteria - a prolific source of natural products. *Tetrahedron* **2001**, *57*, 9347–9377.

[65] Dictionary of Natural Products 29.1. 2020; http://dnp.chemnetbase.com/faces/chemical/ChemicalSearch.xhtml.

[66] Niedermeyer, T. H. Anti-infective natural products from cyanobacteria. *Planta Medica* **2015**, *81*, 1309–1325.

[67] Vijayakumar, S.; Menakha, M. Pharmaceutical applications of cyanobacteria—A review. *Journal of Acute Medicine* **2015**, *5*, 15–23.

[68] Gerwick, W. H.; Moore, B. S. Lessons from the past and charting the future of marine natural products drug discovery and chemical biology. *Chemistry & Biology* **2012**, *19*, 85–98.

[69] Raja, R.; Hemaiswarya, S.; Ganesan, V.; Carvalho, I. S. Recent developments in therapeutic applications of Cyanobacteria. *Critical Reviews in Microbiology* **2016**, *42*, 394–405.

[70] Tan, L. T. Pharmaceutical agents from filamentous marine cyanobacteria. *Drug Discovery Today* **2013**, *18*, 863–871.

[71] Singh, R.; Parihar, P.; Singh, M.; Bajguz, A.; Kumar, J. et al. Uncovering Potential Applications of Cyanobacteria and Algal Metabolites in Biology, Agriculture and Medicine: Current Status and Future Prospects. *Frontiers in Microbiology* **2017**, *8*, 515.

[72] Deng, C.; Pan, B.; O'Connor, O. A. Brentuximab vedotin. *Clinical Cancer Research* **2013**, *19*, 22–27.

[73] Luesch, H.; Moore, R. E.; Paul, V. J.; Mooberry, S. L.; Corbett, T. H. Isolation of dolastatin 10 from the marine cyanobacterium Symploca species VP642 and total stereochemistry and biological evaluation of its analogue symplostatin 1. *Journal of Natural Products* **2001**, *64*, 907–910.

[74] Senter, P. D.; Sievers, E. L. The discovery and development of brentuximab vedotin for use in relapsed Hodgkin lymphoma and systemic anaplastic large cell lymphoma. *Nature biotechnology* **2012**, *30*, 631–637.

[75] Dewick, P. M. *Medicinal natural products: A biosynthetic approach*, 3rd ed.; Wiley A John Wiley and Sons Ltd. Publication: Chichester West Sussex United Kingdom, 2009.

[76] Walton, K.; Berry, J. P. Indole Alkaloids of the Stigonematales (Cyanophyta): Chemical Diversity, Biosynthesis and Biological Activity. *Marine Drugs* **2016**, *14*, 73–101.

[77] Castenholz, R. W.; Wilmotte, A.; Herdman, M.; Rippka, R.; Waterbury, J. B. et al. In *Bergey's Manual of Systematic Bacteriology*; Boone, D. R., Castenholz, R. W., Garrity, G. M., Eds.; Springer: New York, March 2012; Vol. 7; pp 473–599.

[78] Dey, P.; Kundu, A.; Kumar, A.; Gupta, M.; Lee, B. M. et al. In *Recent advances in natural products analysis*; Silva, A. S., Nabavi, S. F., Saeedi, M., Nabavi, S. M., Eds.; Elsevier: Amsterdam and Oxford and Cambridge MA, 2020; pp 505–567.

[79] Vasas, G.; Borbely, G.; Nánási, P.; Nánási, P. P. Alkaloids from cyanobacteria with diverse powerful bioactivities. *Mini - Reviews in Medicinal Chemistry* **2010**, *10*, 946–955.

[80] Kochanowska-Karamyan, A. J.; Hamann, M. T. Marine Indole Alkaloids: Potential New Drug Leads for the Control of Depression and Anxiety. *Chemical Reviews* **2010**, *110*, 4489–4497.

[81] Winkelman, M. J. The Mechanisms of Psychedelic Visionary Experiences: Hypotheses from Evolutionary Psychology. *Frontiers in Neuroscience* **2017**, *11*, 539.

[82] Pregenzer, J. F.; Alberts, G. L.; Bock, J. H.; Slightom, J. L.; Bin Im, W. Characterization of ligand binding properties of the 5-HT1D receptors cloned from chimpanzee, gorilla and rhesus monkey in comparison with those from the human and guinea pig receptors. *Neuroscience Letters* **1997**, *235*, 117–120.

[83] Larsen, L. K.; Moore, R. E.; Patterson, G. M. beta-Carbolines from the blue-green alga Dichothrix baueriana. *Journal of Natural Products* **1994**, *57*, 419–421.

[84] Pohl, B.; Luchterhandt, T.; Bracher, F. Total Syntheses of the Chlorinated β–Carboline Alkaloids Bauerine A, B, and C. *Synthetic Communications* **2007**, *37*, 1273–1280.

[85] Inoue, S.; Okada, K.; Tanino, H.; Kakoi, H.; Goto, T. Trace characterization of the fluorescent substances of a dinoflagellate Noctiluca miliaris. *Chemistry Letters* **1980**, *9*, 297–298.

[86] Volk, R.-B. Screening of microalgal culture media for the presence of algicidal compounds and isolation and identification of two bioactive metabolites, excreted by the cyanobacteria Nostoc insulare and Nodularia harveyana. *Journal of Applied Phycology* **2005**, *17*, 339–347.

[87] Volk, R.-B. Antialgal Activity of Several Cyanobacterial Exometabolites. *Journal of Applied Phycology* **2006**, *18*, 145–151.

[88] Nannini, C. J. Novel secondary metabolites from a Madagascar collection of Lyngbya majuscula. Master Thesis, Oregon State Univeristy, Oregon, 2003.

[89] Aimi, N.; Odaka, H.; Sakai, S.; Fujiki, H.; Suganuma, M. et al. Lyngbyatoxins B and C, two new irritants from Lyngbya majuscula. *Journal of Natural Products* **1990**, *53*, 1593–1596.

[90] Taylor, M. S.; Stahl-Timmins, W.; Redshaw, C. H.; Osborne, N. J. Toxic alkaloids in Lyngbya majuscula and related tropical marine cyanobacteria. *Harmful Algae* **2014**, *31*, 1–8.

[91] Becher, P. G.; Beuchat, J.; Gademann, K.; Jüttner, F. Nostocarboline: Isolation and Synthesis of a New Cholinesterase Inhibitor from Nostoc 78-12A. *Journal of Natural Products* **2005**, *68*, 1793–1795.

[92] Rickards, R. W.; Rothschild, J. M.; Willis, A. C.; de Chazal, N. M.; Kirk, J. et al. Calothrixins A and B, Novel Pentacyclic Metabolites from Calothrix Cyanobacteria with Potent Activity Against Malaria Parasites and Human Cancer Cells. *Tetrahedron* **1999**, *55*, 13513–13520.

[93] Norton, R. S.; Wells, R. J. A series of chiral polybrominated biindoles from the marine blue-green alga Rivularia firma. Application of carbon-13 NMR spin-lattice relaxation data and carbon-13-proton coupling constants to structure elucidation. *Journal of the American Chemical Society* **1982**, *104*, 3628–3635.

[94] Hodder, A. R.; Capon, R. J. A New Brominated Biindole from an Australian Cyanobacterium, Rivularia firma. *Journal of Natural Products* **1991**, *54*, 1661–1663.

[95] Kobayashi, A.; Kajiyama, S.-i.; Inawaka, K.; Kanzaki, H.; Kawazu, K. Nostodione A, a Novel Mitotic Spindle Poison from a Blue-Green Alga Nostoc commune. *Zeitschrift für Naturforschung* **1994**, *49*, 464–470.

[96] Garcia-Pichel, F.; Castenholz, R. W. Characterization and biological implications of Scytonemin, a cyanobacterial sheath pigment: Journal of Phycology, 27(3), 395-409. *Journal of Phycology* **1991**, *27*, 395–409.

[97] Stevenson, C. S.; Capper, E. A.; Roshak, A. K.; Marquez, B.; Eichman, C. et al. The identification and characterization of the marine natural product scytonemin as a novel antiproliferative pharmacophore. *The Journal of Pharmacology and Experimental Therapeutics* **2002**, *303*, 858–866.

[98] Balskus, E. P.; Case, R. J.; Walsh, C. T. The biosynthesis of cyanobacterial sunscreen scytonemin in intertidal microbial mat communities. *FEMS Microbiology Ecology* **2011**, *77*, 322–332.

[99] Jones, C. S.; Esquenazi, E.; Dorrestein, P. C.; Gerwick, W. H. Probing the in vivo biosynthesis of scytonemin, a cyanobacterial ultraviolet radiation sunscreen, through small scale stable isotope incubation studies and MALDI-TOF mass spectrometry. *Bioorganic & Medicinal Chemistry* **2011**, *19*, 6620–6627.

[100] Bonjouklian, R.; Smitka, T. A.; Doolin, L. E.; Molloy, R.; Debono, M. et al. Tjipanazoles, new antifungal agents from the blue-green alga Tolypothrix tjipanasensis. *Tetrahedron* **1991**, *47*, 7739–7750.

[101] Slater, M. J.; Cockerill, S.; Baxter, R.; Bonser, R. W.; Gohil, K. et al. Indolocarbazoles: potent, selective inhibitors of human cytomegalovirus replication. *Bioorganic & Medicinal Chemistry* **1999**, *7*, 1067–1074.

[102] Sánchez, C.; Méndez, C.; Salas, J. A. Indolocarbazole natural products: occurrence, biosynthesis, and biological activity. *Natural Product Reports* **2006**, *23*, 1007–1045.

[103] Chilczuk, T.; Schäberle, T. F.; Vahdati, S.; Mettal, U.; El Omari, M. et al. Halogenation–Guided Chemical Screening Provides Insight into Tjipanazole Biosynthesis by the Cyanobacterium Fischerella ambigua. *ChemBioChem* **2020**, *21*, 2170–2177.

[104] Moore, R. E.; Cheuk, C.; Patterson, G. M. L. Hapalindoles: New alkaloids from the blue-green alga Hapalosiphon fontinalis. *Journal of the American Chemical Society* **1984**, *106*, 6456–6457.

[105] Moore, R. E.; Cheuk, C.; Yang, X. Q. G.; Patterson, G. M. L.; Bonjouklian, R. et al. Hapalindoles, antibacterial and antimycotic alkaloids from the cyanophyte Hapalosiphon fontinalis. *Journal of the American Chemical Society* **1987**, *52*, 1036–1043.

[106] Schwartz, R. E.; Hirsch, C. F.; Springer, J. P.; Pettibone, D. J.; Zink, D. L. Unusual cyclopropane-containing hapalindolinones from a cultured cyanobacterium. *Journal of Organic Chemistry* **1987**, *52*, 3704–3706.

[107] Moore, R. E.; Yang, X.-q. G.; Patterson, G. M.; Bonjouklian, R.; Smitka, T. A. Hapalonamides and other oxidized hapalindoles from Hapalosiphon fontinalis. *Phytochemistry* **1989**, *28*, 1565–1567.

[108] Smitka, T. A.; Bonjouklian, R.; Doolin, L.; Jones, N. D.; Deeter, J. B. et al. Ambiguine isonitriles, fungicidal hapalindole-type alkaloids from three genera of blue-green algae belonging to the Stigonemataceae. *Journal of Organic Chemistry* **1992**, *57*, 857–861.

[109] Klein, D.; Daloze, D.; Braekman, J. C.; Hoffmann, L.; Demoulin, V. New Hapalindoles from the Cyanophyte Hapalosiphon laingii. *Journal of Natural Products*

1995, *58*, 1781–1785.

[110] Becher, P. G.; Keller, S.; Jung, G.; Süssmuth, R. D.; Jüttner, F. Insecticidal activity of 12-epi-hapalindole J isonitrile. *Phytochemistry* **2007**, *68*, 2493–2497.

[111] Raveh, A.; Carmeli, S. Antimicrobial Ambiguines from the Cyanobacterium Fischerella sp. Collected in Israel. *Journal of Natural Products* **2007**, *70*, 196–201.

[112] Kim, H.; Lantvit, D.; Hwang, C. H.; Kroll, D. J.; Swanson, S. M. et al. Indole alkaloids from two cultured cyanobacteria, Westiellopsis sp. and Fischerella muscicola. *Bioorganic & Medicinal Chemistry* **2012**, *20*, 5290–5295.

[113] Liu, X.; Hillwig, M. L.; Koharudin, L. M. I.; Gronenborn, A. M. Unified biogenesis of ambiguine, fischerindole, hapalindole and welwitindolinone: identification of a monogeranylated indolenine as a cryptic common biosynthetic intermediate by an unusual magnesium-dependent aromatic prenyltransferase. *Chemical Communications* **2016**, *52*, 1737–1740.

[114] Zhu, Q.; Liu, X. Molecular and genetic basis for early stage structural diversifications in hapalindole-type alkaloid biogenesis. *Chemical Communications* **2017**, *53*, 2826–2829.

[115] Awakawa, T.; Abe, I. Molecular basis for the plasticity of aromatic prenyltransferases in hapalindole biosynthesis. *Beilstein Journal of Organic Chemistry* **2019**, *15*, 1545–1551.

[116] Park, A.; Moore, R. E.; Patterson, G. M. Fischerindole L, a new isonitrile from the terrestrial blue-green alga Fischerella muscicola. *Tetrahedron Letters* **1992**, *33*, 3257–3260.

[117] Mo, S.; Krunic, A.; Santarsiero, B. D.; Franzblau, S. G.; Orjala, J. Hapalindole-related alkaloids from the cultured cyanobacterium Fischerella ambigua. *Phytochemistry* **2010**, *71*, 2116–2123.

[118] Kim, H.; Krunic, A.; Lantvit, D.; Shen, Q.; Kroll, D. J. et al. Nitrile-Containing Fischerindoles from the Cultured Cyanobacterium Fischerella sp. *Tetrahedron* **2012**, *68*, 3205–3209.

[119] Huber,; Moore,; Patterson, Isolation of a nitrile-containing indole alkaloid from the terrestrial blue-green alga Hapalosiphon delicatulus. *Journal of Natural Products* **1998**, *61*, 1304–1306.

[120] Walton, K.; Gantar, M.; Gibbs, P. D. L.; Schmale, M. C.; Berry, J. P. Indole alkaloids from Fischerella inhibit vertebrate development in the zebrafish (Danio rerio) embryo model. *Toxins* **2014**, *6*, 3568–3581.

[121] Becher, P. G.; Jüttner, F. Insecticidal compounds of the biofilm-forming cyanobac-

terium Fischerella sp. (ATCC 43239). *Environmental Toxicology* **2005**, *20*, 363–372.

[122] Stratmann, K.; Moore, R. E.; Bonjouklian, R.; Deeter, J. B.; Patterson, G. M. L. et al. Welwitindolinones, Unusual Alkaloids from the Blue-Green Algae Hapalosiphon welwitschii and Westiella intricata. Relationship to Fischerindoles and Hapalinodoles. *Journal of the American chemical society* **1994**, *116*, 9935–9942.

[123] Hillwig, M. L.; Zhu, Q.; Liu, X. Biosynthesis of ambiguine indole alkaloids in cyanobacterium Fischerella ambigua. *ACS Chemical Biology* **2014**, *9*, 372–377.

[124] Zhu, Q.; Liu, X. Characterization of non-heme iron aliphatic halogenase WelO5* fromHapalosiphon welwitschiiIC-52-3: Identification of a minimal protein sequence motif that confers enzymatic chlorination specificity in the biosynthesis of welwitindolelinones. *Beilstein Journal of Organic Chemistry* **2017**, *13*, 1168–1173.

[125] Breinlinger, S.; Phillips, T. J.; Haram, B. N.; Mareš, J.; Martínez Yerena, J. A. et al. Hunting the eagle killer: A cyanobacterial neurotoxin causes vacuolar myelinopathy. *Science* **2021**, *371*, eaax9050.

[126] Léon, A.; Cariou, R.; Hutinet, S.; Hurel, J.; Guitton, Y. et al. HaloSeeker 1.0: A User-Friendly Software to Highlight Halogenated Chemicals in Nontargeted High-Resolution Mass Spectrometry Data Sets. *Analytical Chemistry* **2019**, *91*, 3500–3507.

[127] Madeira, P. T.; Van, T. K.; Steward, K. K.; Schnell, R. J. Random amplified polymorphic DNA analysis of the phenetic relationships among world-wide accessions of Hydrilla verticillata. *Aquatic Botany* **1997**, *59*, 217–236.

[128] Schmitz, D. C.; Nelson, B. V.; Nall L.E.,; Schardt, J. D. In *Exotic aquatic plants in Florida: a historical perspective and review of the present aquatic plant regulation program*; Center, T. C., Doren, R. F., Hofstetter, R. L., Myers, R. L., Whiteaker, L. D., Eds.; 1991; pp 303–326.

[129] Basiouny, F. M.; Haller, W. T.; Garrard, L. A. Survival of Hydrilla (Hydrilla verticillata) Plants and Propagules After Removal From the Aquatic Habitat. *Weed Science* **1978**, *26*, 502–504.

[130] Thomas, N. J.; Meteyer, C. U.; Sileo, L. Epizootic Vacuolar Myelinopathy of the Central Nervous System of Bald Eagles (Haliaeetus leucocephalus) and American Coots (Fulica americana). *Veterinary Pathology* **1998**, *35*, 479–487.

[131] Wilde, S. B.; Johansen, J. R.; Wilde, H. D.; Jiang, P.; Bartelme, B. et al. Aetokthonos hydrillicola gen. et sp. nov.: Epiphytic cyanobacteria on invasive aquatic plants implicated in Avian Vacuolar Myelinopathy. *Phytotaxa* **2014**, *181*, 243.

[132] Komárek, J.; Pascher, A.; Büdel, B. *Heterocytous Genera*; Süßwasserflora von

Mitteleuropa Cyanoprokaryota; Springer Spektrum: Berlin, 2013; Vol. / Jiří Komárek ; Teil 3.

[133] Gkotsi, D. S.; Ludewig, H.; Sharma, S. V.; Connolly, J. A.; Dhaliwal, J. et al. A marine viral halogenase that iodinates diverse substrates. *Nature Chemistry* **2019**, *11*, 1091–1097.

[134] Taton, A.; Ecker, A.; Diaz, B.; Moss, N. A.; Anderson, B. et al. Heterologous expression of cryptomaldamide in a cyanobacterial host. *Preprint biorxiv.org* **2020**,

[135] Lewis-Weis, L. A.; Gerhold, R. W.; Fischer, J. R. Attempts to reproduce Vacuolar Myelinopathy in domestic swine and chickens. *Journal of Wildlife Diseases* **2004**, *40*, 476–484.

[136] Haram, B. N.; Wilde, S. B.; Chamberlain, M. J.; Boyd, K. H. Vacuolar Myelinopathy: waterbird risk on a southeastern impoundment co-infested with Hydrilla verticillata and Aetokthonos hydrillicola. *Biological Invasions* **2020**, *22*, 2651–2660.

[137] O'Neil, J. M.; Davis, T. W.; Burford, M. A.; Gobler, C. J. The rise of harmful cyanobacteria blooms: The potential roles of eutrophication and climate change. *Harmful Algae* **2012**, *14*, 313–334.

[138] Nothias, L.-F.; Nothias-Esposito, M.; da Silva, R.; Wang, M.; Protsyuk, I. et al. Bioactivity-Based Molecular Networking for the Discovery of Drug Leads in Natural Product Bioassay-Guided Fractionation. *Journal of Natural Products* **2018**, *81*, 758–767.

[139] Bhat, V.; Dave, A.; MacKay, J. A.; Rawal, V. H. The Chemistry of Hapalindoles, Fischerindoles, Ambiguines, and Welwitindolinones. *The Alkaloids: Chemistry and Biology* **2014**, *73*, 65–160.

[140] Baell, J. B.; Nissink, J. W. M. Seven Year Itch: Pan-Assay Interference Compounds (PAINS) in 2017-Utility and Limitations. *ACS Chemical Biology* **2018**, *13*, 36–44.

[141] Baell, J. B.; Holloway, G. A. New substructure filters for removal of pan assay interference compounds (PAINS) from screening libraries and for their exclusion in bioassays. *Journal of Medicinal Chemistry* **2010**, *53*, 2719–2740.

[142] Baell, J. B. Feeling Nature's PAINS: Natural Products, Natural Product Drugs, and Pan Assay Interference Compounds (PAINS). *Journal of Natural Products* **2016**, *79*, 616–628.

[143] Zelik, P.; Lukesova, A.; Cejka, J.; Budesinsky, M.; Havlicek, V. et al. Nostotrebin 6, a Bis(cyclopentenedione) with Cholinesterase Inhibitory Activity Isolated from Nostoc sp. str. Lukesova 27/97. *The Journal of Enzyme Inhibition and Medicinal*

Chemistry **2010**, *25*, 414–420.

[144] Vacek, J.; Hrbáč, J.; Kopecký, J.; Vostálová, J. Cytotoxicity and Pro-Apoptotic Activity of 2,2´-Bis[4,5-bis(4-hydroxybenzyl)-2-(4-hydroxyphenyl)cyclopent-4-en-1,3-dione], a Phenolic Cyclopentenedione Isolated from the Cyanobacterium Strain Nostoc sp. str. Lukešová 27/97. *Molecules* **2011**, *16*, 4254–4263.

[145] Cheel, J.; Bogdanová, K.; Ignatova, S.; Garrard, I.; Hewitson, P. et al. Dimeric Cyanobacterial Cyclopent-4-ene-1,3-dione as Selective Inhibitor of Gram-positive Bacteria Growth: Bio-Production Approach and Preparative Isolation by HPCCC. *Algal Research* **2016**, *18*, 244–249.

[146] Sevcikova, Z.; Pour, M.; Novak, D.; Ulrichova, J.; Vacek, J. Chemical properties and biological activities of cyclopentenediones: a review. *Mini - Reviews in Medicinal Chemistry* **2014**, *14*, 322–331.

[147] Shimoi, K.; Masuda, S.; Furugori, M.; Esaki, S.; Kinae, N. Radioprotective effect of antioxidative flavonoids in Y-Ray irradiated mice. *Carcinogenesis* **1994**, *15*, 2669–2672.

[148] Son, S.; Lewis, B. A. Free radical scavenging and antioxidative activity of caffeic acid amide and ester analogues: structure-activity relationship. *Journal of Agricultural and Food Chemistry* **2002**, *50*, 468–472.

[149] Li, K.; Li, X.-M.; Ji, N.-Y.; Wang, B.-G. Bromophenols from the marine red alga Polysiphonia urceolata with DPPH radical scavenging activity. *Journal of Natural Products* **2008**, *71*, 28–30.

[150] Masella, R.; Cantafora, A.; Modesti, D.; Cardilli, A.; Gennaro, L. et al. Antioxidant activity of 3,4-DHPEA-EA and protocatechuic acid: a comparative assessment with other olive oil biophenols. *Redox Report* **1999**, *4*, 113–121.

[151] Sroka, Z.; Cisowski, W. Hydrogen peroxide scavenging, antioxidant and anti-radical activity of some phenolic acids. *Food and Chemical Toxicology* **2003**, *41*, 753–758.

Appendices

Commentary

Due to the page limit for this thesis, it is sadly not possible to reprint the three Supporting Information files of the manuscripts. Thus, only the Tables of Contents are reprinted in the following. Online sources are given in order to freely access and download the respective documents. For additional insight and details about methods, the reader is encouraged to read these complete versions.

A. Supporting Informations

Online sources:

A.1: https://www.thieme-connect.de/media/plantamedica/202002/supmat/ 10-1055-a-1045-5178-sup__pmd0491.pdf

A.2: https://pubs.acs.org/doi/10.1021/acs.jnatprod.9b00885

A.3: http://science.sciencemag.org/content/suppl/2021/03/24/371.6536. eaax9050.DC1

A.1. Publication 1

Supporting Information

Hapalindoles from the Cyanobacterium *Hapalosiphon* sp. Inhibit T Cell Proliferation

Tomasz Chilczuk[1§], Carmen Steinborn[2§], Steffen Breinlinger[1§], Amy Marisa Zimmermann-Klemd[2], Roman Huber[2], Heike Enke[3], Dan Enke[3], Timo Horst Johannes Niedermeyer[1Δ], Carsten Gründemann[2Δ]

Affiliation

[1] Department of Pharmaceutical Biology/Pharmacognosy, Institute of Pharmacy, University of Halle-Wittenberg, Halle, Germany

[2] Center for Complementary Medicine, Institute for Infection Prevention and Hospital Epidemiology, Faculty of Medicine, University of Freiburg, Freiburg, Germany

[3] Cyano Biotech GmbH, Berlin, Germany

Correspondence

PD Dr. Carsten Gründemann

Center for Complementary Medicine

Institute for Infection Prevention and Hospital Epidemiology

Faculty of Medicine

Breisacherstrasse 115B

79106 Freiburg

Germany

Phone: +49 (0)761 270-83170

Fax: +49 (0)761 270-83230

carsten.gruendemann@uniklinik-freiburg.de

Prof. Dr. Timo H. J. Niedermeyer

Department of Pharmaceutical Biology/Pharmacognosy

Institute of Pharmacy

Hoher Weg 8

06120 Halle (Saale)

Germany

Phone: +49 (0)345 55-25765

Fax: +49 / (0)345 55-27407

timo.niedermeyer@pharmazie.uni-halle.de

§, Δ These authors contributed equally to this work.

89

A. Supporting Informations

Fig. 1Sa-c. Inhibition of T cell proliferation by *Hapalosiphon* sp. extract fractions.

Fig. 2S. Base peak chromatogram and extracted ion chromatograms.

Fig. 3S. ^{1}H NMR spectrum (400 MHz) of **1** in CDCl$_3$.

Fig. 4S. NOESY NMR spectrum (600 MHz) of **1** in CDCl$_3$.

Fig. 5S. ^{1}H NMR spectrum (400 MHz) of **2** in CDCl$_3$.

Fig. 6S. NOESY NMR spectrum (400 MHz) of **2** in CDCl$_3$.

Fig. 7S. ^{1}H NMR spectrum (400 MHz) of **3** in DMSO-d_6.

Fig. 8S. NOESY NMR spectrum (400 MHz) of **3** in DMSO-d_6

Fig. 9S. ^{1}H NMR spectrum (600 MHz) of **4** in DMSO-d_6.

Fig. 10S. ^{13}C NMR spectrum (150 MHz) of **4** in DMSO-d_6.

Fig. 11S. HSQC-DEPT NMR spectrum (600 MHz) of **4** in DMSO-d_6.

Fig. 12S. HMBC NMR spectrum (600 MHz) of **4** in DMSO-d_6.

Fig. 13S. NOESY NMR spectrum (600 MHz) of **4** in DMSO-d_6.

Fig. 14S. COSY NMR spectrum (600 MHz) of **4** in DMSO-d_6.

Fig. 15S. ^{1}H NMR spectrum (600 MHz) of **5** in DMSO-d_6.

Fig. 16S. HSQC-DEPT NMR spectrum (400 MHz) of **5** in DMSO-d_6.

Fig. 17S. HMBC NMR spectrum (600 MHz) of **5** in DMSO-d_6.

Fig. 18S. NOESY NMR spectrum (600 MHz) of **5** in DMSO-d_6.

Fig. 19S. COSY NMR spectrum (600 MHz) of **5** in DMSO-d_6.

A.2. Publication 2

Supporting Information

Nostotrebin 6 related Cyclopentenediones and

δ-Lactones with Broad Activity Spectrum Isolated

from the Medium Extract of the Cyanobacterium

Nostoc sp. CBT1153

Ronja Kossack[†], Steffen Breinlinger[†], Trang Nguyen[‡], Julia Moschny[†], Jan Straetener[§,▽],

Anne Berscheid[§,▽], Heike Brötz-Oesterhelt[§,▽], Heike Enke[⊥], Tanja Schirmeister[‖], Timo H. J.

Niedermeyer[†,▽]*

[†]Department of Pharmaceutical Biology/Pharmacognosy, Institute of Pharmacy, University of Halle-Wittenberg, 06120 Halle (Saale), Germany

[‡]Department of Microbiology/Biotechnology, Interfaculty Institute for Microbiology and Infection Medicine (IMIT), University of Tübingen, 72076 Tübingen, Germany

[§]Department of Microbial Bioactive Compounds, Interfaculty Institute for Microbiology and Infection Medicine (IMIT), University of Tübingen, 72076 Tübingen, Germany

[⊥]Cyano Biotech GmbH, 12489 Berlin, Germany

[‖]Institute of Pharmacy and Biochemistry, University of Mainz, 55128 Mainz, Germany

[▽] German Center for Infection Research (DZIF), Partner Site Tübingen, Tübingen, Germany

*Corresponding author

1

A. Supporting Informations

2

A.3. Publication 3

Supplementary Materials for

Hunting the eagle killer: A cyanobacterial neurotoxin causes vacuolar myelinopathy

Steffen Breinlinger*, Tabitha J. Phillips*, Brigette N. Haram, Jan Mareš, José A. Martínez Yerena, Pavel Hrouzek, Roman Sobotka, W. Matthew Henderson, Peter Schmieder, Susan M. Williams, James D. Lauderdale, H. Dayton Wilde, Wesley Gerrin, Andreja Kust, John W. Washington, Christoph Wagner, Benedikt Geier, Manuel Liebeke, Heike Enke, Timo H. J. Niedermeyer†‡, Susan B. Wilde†‡

*These authors contributed equally to this work. †These authors contributed equally to this work.
‡Corresponding author. Email: swilde@uga.edu (S.B.W.);
timo.niedermeyer@pharmazie.uni-halle.de (T.H.J.N.)

This PDF file includes:

> Materials and Methods
> Supplementary Text
> Figs. S1 to S50
> Tables S1 to S14
> Captions for Movies S1 and S2
> References

Other Supplementary Material for this manuscript includes the following:
(available at science.sciencemag.org/content/371/6536/eaax9050/suppl/DC1)

> MDAR Reproducibility Checklist (.pdf)
> Movies S1 and S2 (.mp4)

Table of contents

Materials and Methods

Supplementary Text

Table of figures

3

Steffen Breinlinger

Dipl.-Pharm.

Persönliche Angaben

Nachname, Vorname	Breinlinger, Steffen
Geburtsort	Tuttlingen, Baden-Württemberg
Geburtsdatum	10. September 1986
Staatsangehörigkeit	Deutschland

Beruf

Nov. 2015 – Feb. 2020

Wissenschaftlicher Mitarbeiter, *Eberhard Karls Universität Tübingen und Martin-Luther Universität Halle*, Promotion, Tübingen und Halle (Saale).
Doktorarbeit "Investigations into bioactive natural products from cyanobacteria — a search for drug leads and the discovery of a novel cyanotoxin"

Jan. 2015 – Apr. 2017

Vertretungsapotheker, *freiberufliche Tätigkeit*, Baden-Württemberg.

Nov. 2014

Approbation als Apotheker.
3. Staatsexamen - Landesapothekerkammer, Stuttgart.

Feb. 2014 – Sep. 2014

Pharmazeut im Praktikum, *Herdweg Apotheke*, Stuttgart.

Studium

Jun. 2013 – Jan. 2014

Diplomarbeit, *Ruprecht-Karls-Universität*, Institut für Pharmazie und Molekulare Biotechnologie, Heidelberg.
Titel: Antioxidative Naturstoffe aus *Hibiscus sabdariffa* — In-Vitro-Analyse und Versuche in *Caenorhabditis elegans*, Abschlussnote: 1,3

Okt. 2008 – Mär. 2013

Pharmazie, *Albert-Ludwigs-Universität*, Freiburg i.Br.
Staatsexamenstudiengang, Abschluss mit dem 2. Staatsexamen, Note: 2,2

Jun. 2006

Allg. Hochschulreife, *Otto-Hahn-Gymnasium*, Tuttlingen.
Abiturnote: 1,3

Les Planes d'Hostoles, den 11. April 2021

Acknowledgments

Ohne die folgenden Menschen wäre diese Arbeit niemals möglich gewesen, deshalb gilt mein Besonderer Dank:

Anna und meinen Eltern für ihre bedingungslose Unterstützung in allen Lebenslagen.

Meinen Schwestern für Korrekturlesen, Diskussionen, Lunchpakete und aufbauende Worte.

Timo für sein Vertrauen, seine Unterstützung, sein Verständnis, seine immer offene Tür und für all die Freiheiten die man sich als Doktorand wünschen kann.

Andi Kulik für die Tipps und Tricks, Gespräche, Chromatographie-Lektionen und besten Laborkumpel in Tübingen.

Nico, Tomasz, Julia, Ronja und Uli für all die Jahre mit gemeinsamen Kochen, Lachen, Weinen, Streiten, Diskutieren, Reisen, Experimentieren, Verzweifeln und vor allem Spaß haben.

Anja für ihr herzliche Aufnahme in Halle, ihre Ehrlichkeit, Hilfsbereitschaft und alles in allem beste Komplizin sein.

Mulham, Ela, Max und Kei fürs Aushalten meiner Launen in der WG-Küche.

Jan, Pavel und José für das super Zusammenarbeiten und die gemeinsame Forschung.

Brigette und Susan für zwei Wochen Georgia und die Chance eine Schlüsselrolle bei der Rettung des Weißkopfseeadlers spielen zu dürfen.

Und last but not least Kali, dafür dass sie mir ohne es zu wissen die Motivation gegeben hat, diese Arbeit endlich fertig zu stellen.

Eidesstattliche Erklärung

Ich versichere hiermit, dass ich die vorliegende Dissertation selbständig und ohne unzulässige fremde Hilfe angefertigt habe. Ich habe keine anderen als die im Literaturverzeichnis angeführten Quellen genutzt und sämtliche Textstellen, die wörtlich oder sinngemäß aus veröffentlichten oder unveröffentlichten Schriften entnommen wurden, und alle Angaben, die auf mündlichen Auskünften beruhen, als solche kenntlich gemacht. Alle von anderen Personen bereitgestellten Materialien oder erbrachten Dienstleistungen wurden als solche gekennzeichnet. Die vorgelegte Arbeit ist weder im Inland noch im Ausland in gleicher oder ähnlicher Form einer anderen Prüfungsbehörde zum Zweck einer Promotion oder eines anderen Prüfungsverfahrens vorgelegt worden. Ich habe keine früheren erfolglosen Promotionsversuche unternommen.

16. April, 2021   Unterschrift des Antragstellers